



BIOACTIVE CONSTITUENTS FROM *GARCINIA FUSCA* PIERRE STEM BARKS



AUDCHARA SAENKHAM

Graduate School Srinakharinwirot University

2020

สารออกฤทธิ์ทางชีวภาพจากเปลือกต้นส้มโง



ปริญญานิพนธ์นี้เป็นส่วนหนึ่งของการศึกษาตามหลักสูตร

ปรัชญาดุษฎีบัณฑิต สาขาวิชาเคมีประยุกต์

คณะวิทยาศาสตร์ มหาวิทยาลัยศรีนครินทรวิโรฒ

ปีการศึกษา 2563

ลิขสิทธิ์ของมหาวิทยาลัยศรีนครินทรวิโรฒ

BIOACTIVE CONSTITUENTS FROM *GARCINIA FUSCA* PIERRE STEM BARKS



A Dissertation Submitted in Partial Fulfillment of the Requirements
for the Degree of DOCTOR OF PHILOSOPHY
(Applied Chemistry)

Faculty of Science, Srinakharinwirot University

2020

Copyright of Srinakharinwirot University

THE DISSERTATION TITLED

BIOACTIVE CONSTITUENTS FROM *GARCINIA FUSCA* PIERRE STEM BARKS

BY

AUDCHARA SAENKHAM

HAS BEEN APPROVED BY THE GRADUATE SCHOOL IN PARTIAL FULFILLMENT
OF THE REQUIREMENTS FOR THE DOCTOR OF PHILOSOPHY
IN APPLIED CHEMISTRY AT SRINAKHARINWIROT UNIVERSITY

.....
(Assoc. Prof. Dr. Chatchai Ekpanyaskul, MD.)

Dean of Graduate School
.....

ORAL DEFENSE COMMITTEE

..... Major-advisor

(Assoc. Prof. Dr.Sunit Suksamrarn)

..... Co-advisor

(Asst. Prof. Dr.Nuttapon Apiratikul)

..... Chair

(Assoc. Prof. Dr.Boon-ek Yingyongnarongkul)

..... Committee

(Assoc. Prof. Dr.Siritron Samosorn)

Title	BIOACTIVE CONSTITUENTS FROM <i>GARCINIA FUSCA</i> PIERRE STEM BARKS
Author	AUDCHARA SAENKHAM
Degree	DOCTOR OF PHILOSOPHY
Academic Year	2020
Thesis Advisor	Associate Professor Dr. Sunit Suksamrarn
Co Advisor	Assistant Professor Dr. Nuttapon Apiratikul

Three new oxygenated xanthenes, 3-O-methylcowanin (10), 5-prenyl cowaxanthone (13), and norcowanol (19), together with 14 oxygenated xanthenes (1-3, 5-8, 11-12, and 14-18), and the other known metabolites, lakoochin A (4), oleanane triterpene lactone (9), and GB-2 (20) were isolated and purified from the stem barks of *Garcinia fusca* Pierre. Their structures were elucidated on the basis of the spectroscopic data analysis (mainly NMR and MS) and a comparison with the reported data. The geranylated compounds, cowanin (14), cowagarcinone E (16), norcowanin (17), and cowanol (18) exhibited potent inhibitory effects against acetylcholinesterase (AChE) (IC_{50} 0.33–1.09 μ M) and butyrylcholinesterase (BChE) (IC_{50} 0.048–1.84 μ M), which showed a higher activity level than galanthamine, the standard drug. In particular, compound 16 displayed the most potent BChE inhibitor (IC_{50} 0.048 μ M) and was 76-fold more potent than galanthamine. Structure-activity relationship studies indicated that the C-2 prenyl and C-8 geranyl substituents in the tetraoxygenated scaffold were significantly important and had higher level activity levels.

Keyword : *Garcinia fusca*, Oxygenated xanthenes, Acetylcholinesterase inhibitor,
Butyrylcholinesterase inhibitor

ACKNOWLEDGEMENTS

The first and foremost, I would like to express my sincere gratitude to my supervisor, Assoc. Prof. Dr. Sunit Suksamrarn, for her kind and helpful supervision, hearty encouragement and research assistantship support throughout this work.

I would like to thank all my committee members, Asst. Prof. Dr. Nuttapon Apiratikul my co-advisors, Assoc. Prof. Dr. Siritron Samosorn, for their endless kindness, thoughtful advice, valuable time, patient reading and warm encouragement. In addition, I feel grateful to Assoc. Prof. Dr. Boon-ek Yingyongnarongkul, Ramkhamhaeng University, for his useful comments and encouragement.

This work was partially supported by the Center of Excellence for Innovation in Chemistry (PERCH-CIC).

I am grateful to Department of Chemistry, Faculty of Science, Ramkhamhaeng University for recording the mass spectra and optical rotations.

Many special thanks also go to my teachers, friends, colleagues and staff of the Department of Chemistry, Faculty of Science, Srinakharinwirot University for their friendship, kind support and encouragement.

Finally, I wish to express my profound gratitude to my parents and family for their love, unconditional support and encouragement throughout my whole life.

AUDCHARA SAENKHAM

TABLE OF CONTENTS

	Page
ABSTRACT	D
ACKNOWLEDGEMENTS.....	E
TABLE OF CONTENTS.....	F
LIST OF TABLES.....	I
LIST OF FIGURES.....	K
CHAPTER 1 INTRODUCTION	1
Background.....	1
Objectives of the Study.....	2
CHAPTER 2 REVIEW OF LITERATURE.....	3
Xanthonones and related compound	3
Oxygenated xanthonones	4
Xanthone glycosides	5
Prenylated xanthonones.....	6
Xanthonolignoids	7
Bisxanthonones	7
Caged xanthonones	8
Depsidone	9
Biflavonoids	10
Triterpenoids	13
Recent publications of <i>Garcinia</i> phytochemicals and of their biological activities during the years of 2012-2017.	15

CHAPTER 3 EXPERIMENTAL	36
Plant materials	36
General experimental procedures	36
Extraction of the dried stem barks of <i>G. fusca</i>	37
Isolation of compounds from the EtOAc extract of the stem bark of <i>G. fusca</i>	38
Physical and spectral data of compounds 1-20	45
Anti-ChE assay	51
CHAPTER 4 RESULTS AND DISCUSSION	52
1. Structure determination of the three new xanthonones 10, 13, 19; known xanthonones 1-3, 5-8, 11-12, and 14-18, and other metabolites (4), (9) and (20)	55
1.1. 1,3,6,7-tetraoxygenated xanthone skeleton	55
1.1.1. Geranylated xanthonones	55
1.1.1.1. Compound 14 (Cowarin)	55
1.1.1.2. Compound 10 (Fuscaxanthone M or 3-O-methylcowarin)	56
1.1.1.3. Compound 17 (Norcowarin)	58
1.1.1.4. Compound 7 (Fuscaxanthone A)	59
1.1.1.5. Compound 18 (Cowanol)	62
1.1.1.6. Compound 16 (Cowagarcinone E)	63
1.1.1.7. Compound 19 (Norcowanol or fuscaxanthone N)	65
1.1.1.8. Compound 15 (Cowaxanthone)	69
1.1.1.9. Compound 11 (3-O-methylcowaxanthone)	70
1.1.1.10 Compound 13 (5-Prenyl cowaxanthone or fuscaxanthone L)	72
1.2. Prenylated xanthonones	76

1.2.1. Compound 3 (β -mangostin).....	76
1.2.2. Compound 5 (Cowagarcinone B).....	77
1.2.3. Compound 6 (7-O-methylgarcinone E)	79
1.3. Other oxynatedxanthone fremework (1,3,5,-trioxynated, 1,3,5,8- tetraoxynated and 1,3,5,6-tetraoxynated xanthenes)	82
1.3.1. Compound 2 (8-Deoxygartanin)	82
1.3.2. Compound 1 (Gartanin)	83
1.3.3 Compound 8 (Garbogiol)	84
1.3.4. Compound 12 (Rheediaxanthone-A).....	89
1.3. Non-xanthenes	93
1.3.1. Compound 4 (Lakoochin A).....	93
1.3.2 Compound 9 (An oleanane triterpene lactone)	96
1.3.3 Compound 20 (GB-2)	100
2. Cholinesterase inhibitory activities	105
CHAPTER 5 CONCLUSION	108
REFERENCES.....	111
APPENDIX	121
VITA	131

LIST OF TABLES

	Page
TABLES 1 List of isolated compounds from <i>G. fusca</i>	53
TABLES 2 ¹ H-NMR data of cowanin (14), 3-O-methylcowanin (10), norcowanin (17) and fuscaxanthone A (7) in CDCl ₃	60
TABLES 3 ¹³ C-NMR data of cowanin (14), 3-O-methylcowanin (10), norcowanin (17) and fuscaxanthone A (7) in CDCl ₃	61
TABLES 4 ¹ H-NMR data of cowanin (14), cowanol (19), cowagarcinone E (16) and norcowanol (19) in CDCl ₃	67
TABLES 5 ¹³ C-NMR data of cowanin (14), cowanol (19), cowagarcinone E (16) and norcowanol (19) in CDCl ₃	68
TABLES 6 ¹ H-NMR data of cowaxanthone (15), 3-O-cowaxanthone (11) and 5-prenyl cowaxanthone (13) in CDCl ₃	74
TABLES 7 ¹³ C-NMR data of cowaxanthone (15), 3-O-cowaxanthone (11) and 5-prenyl cowaxanthone (13) in CDCl ₃	75
TABLES 8 ¹ H-NMR data of β-mangostin (3), cowagarcinone B (5) and 7-O-methylgarcinone E (6) in CDCl ₃	80
TABLES 9 ¹³ C-NMR data of β-mangostin (3), cowagarcinone B (5) and 7-O-methylgarcinone E (6) in CDCl ₃	81
TABLES 10 ¹ H-NMR data of 8-deoxygartanin (2), gartanin (1) and garbogirol (8) in CDCl ₃	87
TABLES 11 ¹³ C-NMR data of 8-deoxygartanin (2), gartanin (1) and garbogirol (8) in CDCl ₃	88
TABLES 12 Comparison ¹ H- and ¹³ C-NMR data of compound 12 with rheediaxanthone-A in CDCl ₃	92

TABLES 13 Comparison ^1H - and ^{13}C -NMR data of compound 4 with lakoochin A in CDCl_3	95
TABLES 14 Comparison ^1H - and ^{13}C -NMR data of compound 9 with 3β -acetoxy- 12α -hydroxyoleanan- $28,13\beta$ -olide in CDCl_3	98
TABLES 15 Comparison ^1H - and ^{13}C -NMR data of compound 20 with GB-2 in $\text{DMSO}-d_6$	104
TABLES 16 The ChE inhibitory activity (IC_{50}) of compounds (1-8, 10-12 and 14-20)....	105



LIST OF FIGURES

	Page
FIGURES 1 Basic structure of flavonoids	10
FIGURES 2 Structures of biflavonoids	11
FIGURES 3 Types of interflavonyl link of bioflavonoids	12
FIGURES 4 Isolated compounds obtained from the stem barks of <i>G. fusca</i>	54
FIGURES 5 Structure of compound 14	55
FIGURES 6 Structure of compound 10	56
FIGURES 7 Selected HMBC and NOESY correlation of compound 10	57
FIGURES 8 Structure of compound 17	58
FIGURES 9 Structure of compound 7	59
FIGURES 10 Structure of compound 18	62
FIGURES 11 Structure of compound 16	63
FIGURES 12 Selected HMBC and NOESY correlation of compound 16	64
FIGURES 13 Structure of compound 19	65
FIGURES 14 Selected HMBC and NOESY correlation of compound 19	66
FIGURES 15 Structure of compound 15	69
FIGURES 16 Structure of compound 11	70
FIGURES 17 Selected HMBC and NOESY correlation of compound 11	71
FIGURES 18 Structure of compound 13	72
FIGURES 19 Key HMBC and NOESY correlations for compound 13	73
FIGURES 20 Structure of compound 3	76
FIGURES 21 Structure of compound 5	77

FIGURES 22 Selected HMBC and NOESY correlation of compound 5	78
FIGURES 23 Structure of compound 6	79
FIGURES 24 Structure of compound 2	82
FIGURES 25 Structure of compound 1	83
FIGURES 26 Structure of compound 8	84
FIGURES 27 Selected HMBC correlation of compound 8.....	86
FIGURES 28 ORTEP plot of the X-ray crystal structure for compound 8	86
FIGURES 29 Structure of compound 12	89
FIGURES 30 Key COSY and HMBC correlations for compound 12	91
FIGURES 31 Key NOESY correlations for compound 12	91
FIGURES 32 Structure of compound 4	93
FIGURES 33 Selected HMBC and NOESY correlation of compound 4	94
FIGURES 34 Structure of compound 9	96
FIGURES 35 HMBC and NOESY correlations of compound 9.....	97
FIGURES 36 Structure of compound 20	100
FIGURES 37 Key HMBC correlations for compound 20.....	102
FIGURES 38 Key NOESY correlations for compound 20	102
FIGURES 39 Prenylated and geranylated xanthenes from <i>G. fusca</i>	109
FIGURES 40 Other known metabolites from <i>G. fusca</i>	110

CHAPTER 1

INTRODUCTION

Background

Garcinia is a genus of plants belonging to the family Clusiaceae (Guttiferae). There are about 260 species distributed in the tropical and temperate regions of the world (Sosef & Dauby, 2012), particularly in tropical Asia, Africa, and Polynesia (Ngernsaengsaruy & Suddee, 2016). Historically, *Garcinia* plants exhibit a wide range of biological and pharmacological activities and they have been used in culinary, pharmaceutical, and industrial fields (Hemshekhkar et al., 2011). Extracts of *Garcinia* species have been reported to be a major source of prenylated xanthenes, benzophenones, and biflavonoids (Shagufta & Ahmad, 2016). The fruit hull of *G. mangostana* or “mangosteen” has been traditionally used in traditional Thai medicine for healing skin infections and wounds, and for treating diarrhea (Mahabusarakam et al., 1986). It was also used as an anti-inflammatory agent (Balasubramanian & Rajagopalan, 1988). The mangosteen pericarp extracts show a high antioxidant activity, which inhibits the reactive oxygen species (ROS) (Chomnawang et al., 2007). The cytotoxicity of xanthenes against three human cancer cell lines; epidermoid carcinoma of the mouth (KB), breast cancer (BC-1), and small cell lung cancer (NCI-H187) of *G. mangostana* young fruits was also investigated. Xanthenes (e.g., α -, β -, and γ -mangostins, garcinone E, 8-desoxygartanin, and gartanin) isolated from the mangosteen fruit show remarkable biological activities (Suksamrarn et al., 2006). Moreover, xanthenes obtained from the methanolic extract of *G. mangostana* displayed the anticholinesterase activities (Khaw et al., 2014). The leaves and seeds of *G. dulcis* have been traditionally used in curing the lymphatitis, parotitis, struma, and other disease conditions (Linuma et al., 1996). The fruits and leaves of *G. cowa* are used for the improvement of blood circulation, as an expectorant for the treatment of coughs and indigestion, and as a laxative. In addition, the root is used for fever relief and the bark has been used in Thai folk medicine as an antipyretic agent (Panthong et al., 2009). The xanthenes of *G. cowa* fruits possess antibacterial properties (Auranwiwat et al., 2014).

The prenylated xanthenes of *G. esculenta* show cytotoxic activity in human cancer cell lines (Zhang et al., 2014). The bark of *G. hombroniana*, which contain triterpenes, showed the *in vitro* cytotoxicity against MCF-7, DBTRG, U2OS, and PC-3 cell lines (Jamila et al., 2014). Moreover, the triterpenes of *G. cymosa* stem bark were also tested for cytotoxic activity. The root, stem, leaves and fruits of this plant are also traditionally used for the improvement of blood circulation, as an expectorant, as a laxative, and the relief of fever (Poomipamorn & Kumkong, 1997). Previously, the chemical investigation of *G. fusca* stem barks led to the isolation of eight new xanthenes (fuscaxanthenes A-H) and eight known xanthenes, which showed the inhibitory effects on Epstein–Barr virus early antigen induction (Ito, C. et al., 2003). In addition, xanthenes and bioflavonoids isolated from this plant showed antibacterial activity against *Helicobacter pylori* (Nontakham et al., 2014).

Our research group has previously focused on the study of new biological activities of phytochemicals isolated from some *Garcinia* species. For instance, antimycobacterial and cytotoxicity of xanthenes obtained from *G. mangostana* (Suksamrarn et al., 2006; Suksamrarn et al., 2003) and antibacterial activity against *Helicobacter pylori* of xanthenes and biflavonoids given by *G. fusca* (Nontakham et al., 2014). In continuation of previous studies, the stem bark of a *G. fusca* will be further investigated in order to search for new chemical compounds with new biological activities.

Objectives of the Study

1. To isolate, purify, and identify the chemical structures of the isolated compounds from a *G. fusca*, which was collected from the north eastern area.
2. To evaluate the biological activities of the isolated compounds.

CHAPTER 2

REVIEW OF LITERATURE

The *Garcinia* is a large genus, belongs to the Clusiaceae family, and has been received much attention due to their contents of potential bioactive molecules. There are more than 300 *Garcinia* species and they are native to Asia and Africa (Hemshekhkar et al., 2011) and about 29 species are found in Thailand (Ritthiwigrom et al., 2013). Investigation of *Garcinia* plant parts (fruits, fruit rinds, flowers, leaves, twigs, barks and stems, roots and root barks, heartwood, resin, etc.) revealed the isolations, characterizations and bioactivity evaluations, xanthenes, bioflavonoids, benzophenones derivatives, triterpenes and other compounds (Hemshekhkar et al., 2011).

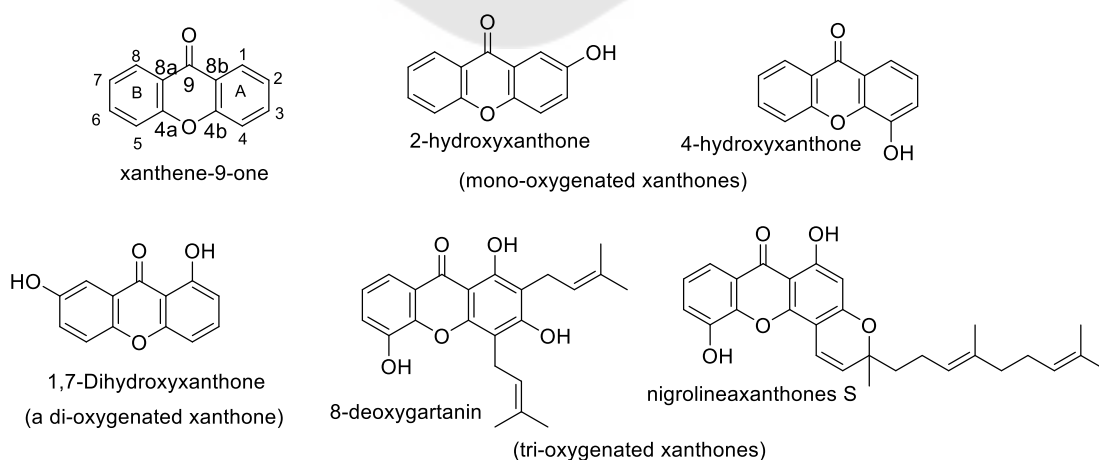
Xanthenes and related compound

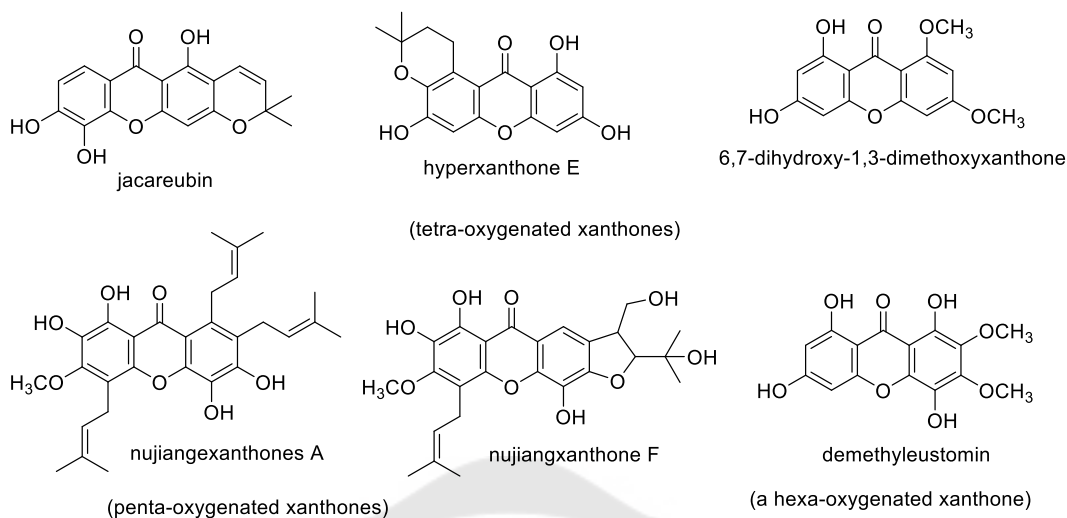
Xanthenes are comprised of rigid tricyclic aromatic rings and xanthene-9-one is the basic skeleton. Xanthenes are natural secondary metabolites commonly found in some higher plant families, fungi, lichens and bacteria (Negi et al., 2013). Xanthenes naturally occur in the families Gentianaceae, Guttiferae, Moraceae, Clusiaceae, and Polygalaceae (Jensen & Schripsema, 2002; Vieira & Kijjoa, 2005). They are widely distributed in nature and exhibit different biological activities depending on their chemical structures and position of substituents on the aromatic rings (Shagufta & Ahmad, 2016). Naturally occurring xanthenes have been extensively discovered since 1959. The first review was published in 1961 by Roberts (Roberts, 1961). Since that time, the number of naturally occurring xanthone compounds has increased to 100 fold (Masters & Brase, 2012). Other reviews were also published in the period up to 2013 by 14 research groups (Al-Hazimi & Miana, 1990; Demirkiran, O., 2007; Denisova-Dyatlova & Glyzin, 1982; El-Seedi et al., 2010; Hostettmann & Hostettmann, 1989; Masters & Brase, 2012; Na, Y., 2009; Negi et al., 2013; Peres & Nagem, 1997; Peres et al., 2000; Pinto et al., 2005; Roberts, 1961; Winter et al., 2013; Yang, Y.-B., 1980). Natural xanthenes can be classified into oxygenated xanthenes, xanthone glycosides, prenylated xanthenes and related

compound, xanthonolignoids, bisxanthenes, caged xanthenes (Negi et al., 2013) and depsidone.

Oxygenated xanthenes

This main group is subdivided according to the degree of oxygenation into seven groups, non-, mono-, di-, tri-, tetra-, penta- and hexaoxygenated xanthenes. Oxygenated xanthenes contain simple substituents such as hydroxyl and methoxy or methyl groups (Negi et al., 2013; Vieira & Kijjoa, 2005). For example, monooxygenated xanthenes, 2-hydroxyxanthone and 4-hydroxyxanthone have been isolated from *Swertia* species (Negi et al., 2013). Di-oxygenated xanthone, 1,7-dihydroxyxanthone was isolated from the pericarp *G. pedunculata* (Vo et al., 2015). 8-Deoxygartanin and nigrolineaxanthenes S have been isolated from *G. speciosa* and *G. nigrolineata*, respectively (Rukachaisirikul, Kamkaew, et al., 2003; Rukachaisirikul, Pailee, et al., 2003). Tetra-oxygenated xanthenes which composed of hydroxyl moiety at C-1,3,5,6, C-1,3,5,7-, and C-1,3,6,7 (Chen et al., 2013). Jacareubin and hyperxanthone E were isolated from the twigs of *G. nujiangensis* (Tang et al., 2015) and *G. esculenta* (Zhang et al., 2014), and 6,7-dihydroxy-1,3-dimethoxyxanthone from *H. geminiflorum* (Chung et al., 1999). Nujiangexanthenes A and nujiangxanthone F were isolated from twigs of *G. nujiangensis* (Tang et al., 2015). Demethyleustomin was isolated from shoots and roots of *Centaurium pulchellum* (Krstić et al., 2003).

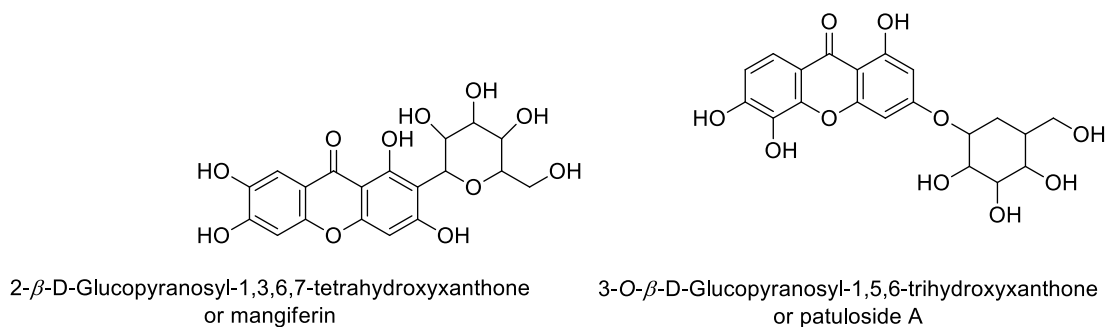




Xanthone glycosides

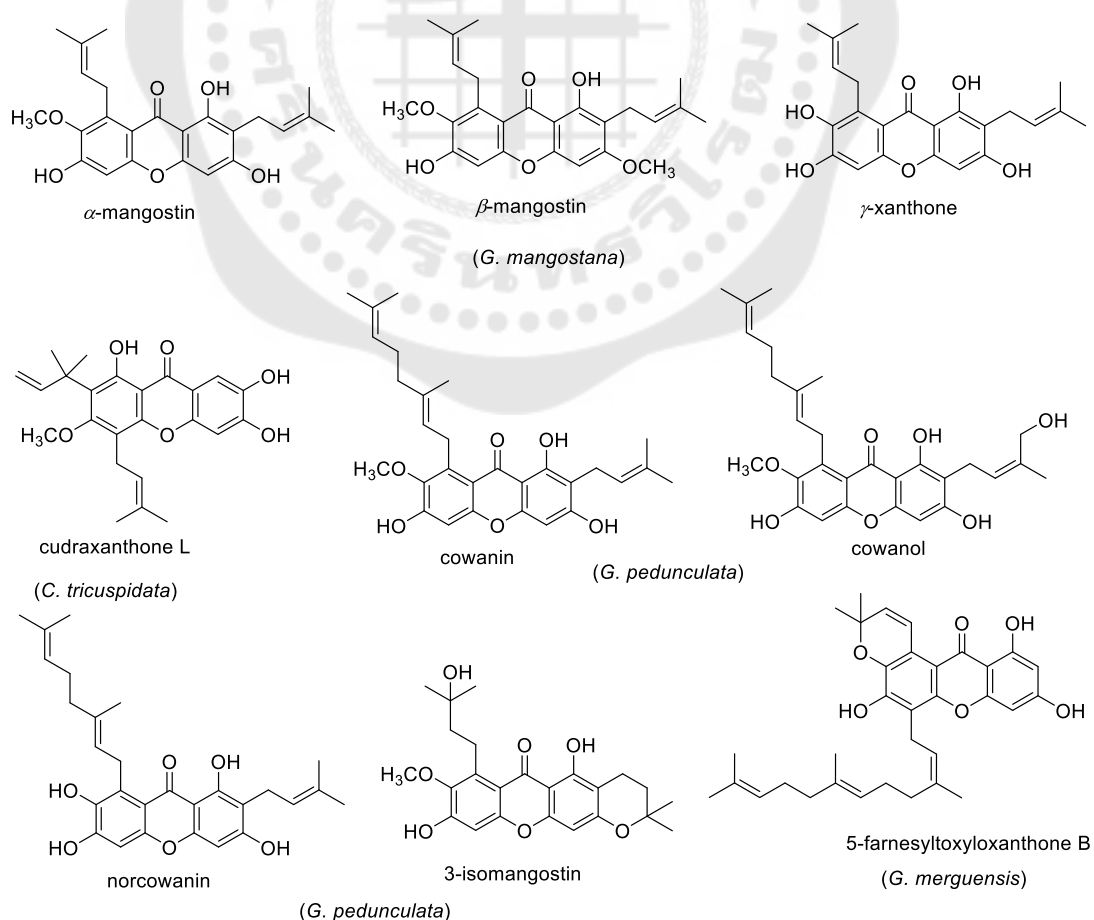
Xanthone glycosides are divided into two types according to the nature of the glycosidic linkages, *O*-glycosides and *C*-glycosides. The *C*-glycosyl xanthenes are a group of compounds which was classified by a sugar moiety attached to the xanthone nucleus through a C-C bond whereas *O*-glycosides bearing C-O glycosidic linkage. Sixty one natural glycosylated xanthenes have been predominantly reported in the families Gentianaceae and Polygalaceae (Demirkiran, O., 2007; Hostettmann & Miura, 1977; Negi et al., 2013). They are rarely founded from fungi. *C*-glycosyl xanthenes are rare xanthenes, their occurrence is very much limited (Negi et al., 2013).

The first *C*-glycoside xanthenes was isolated in 1992 from *Mangifera indica* (Anacardiaceae) (Demirkiran, O., 2007; Mandal et al., 1992). Only one *O*-glycoside xanthenes, patuloside A have been isolated from *Hypericum species* (Chung et al., 1999), while mangiferin isolated from this species was the first *C*-glycoside xanthone.



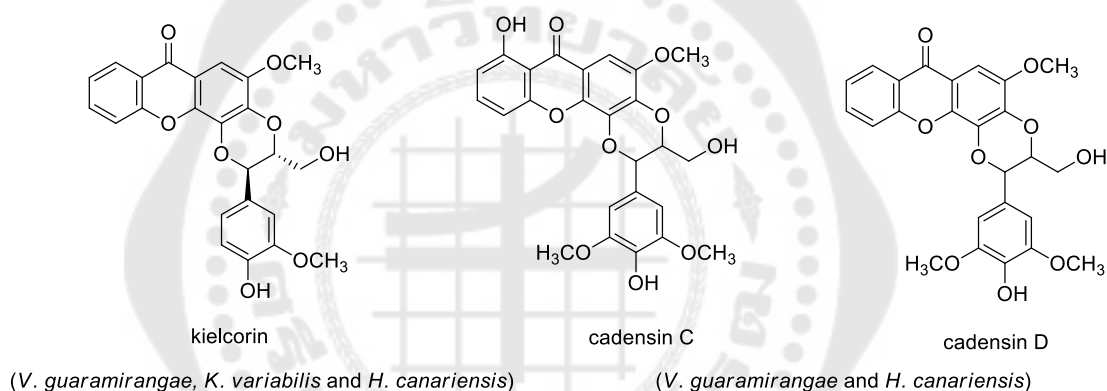
Prenylated xanthones

The family Clusiaceae or Guttiferae appears to produce a large number of xanthones. These compounds are di-, tri-, tetra- and penta-oxygenated xanthones, which aromatic ring system is substituted by prenyl groups such as isoprenyl, 1,1-dimethylprop-2-enyl, geranyl, and farnesyl unit. Cyclisation of these groups with the near-by *O*-hydroxyl groups into furano-(5-membered ring) or pyrano-(6-membered ring) systems are observed. A large number of prenylated tetra-oxygenated xanthones have been found, whereas, prenylated penta-oxygenated xanthones are rare (Demirkiran, O., 2007; Negi et al., 2013). α -Mangostin, β -mangostin and γ -xanthone isolated from the fruit mangosteen (Suksamrarn et al., 2006). Cudraxanthone L isolated from the roots of *C. tricuspidata* (Yoon et al., 2016). Cowanin, cowanol, norcowanin and 3-isomangostin (Vo et al., 2015) isolated from the pericarp of *G. pedunculata*. 5-Farnesyltoxyloxanthone B isolated from *G. merguensis*, is a rare xanthone with a farnesyl group (Kijjoa et al., 2008).



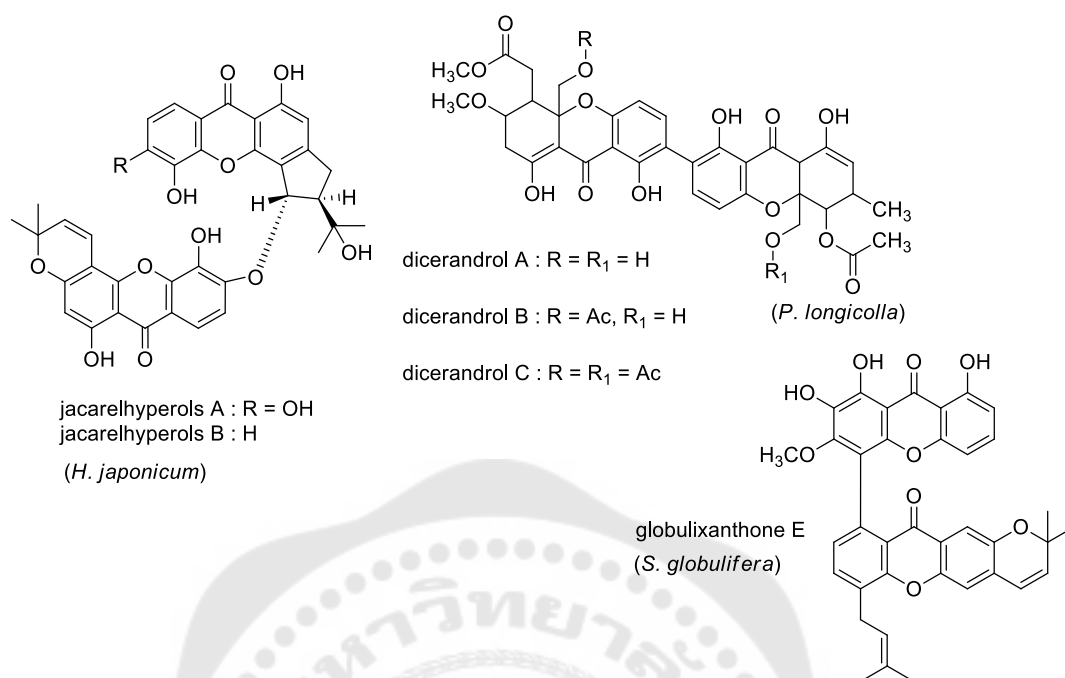
Xanthonolignoids

Xanthonolignoids were first isolated in 1950 from *Kielmeyera coriacea* and *Caraipa densiflora* (Guttiferae). Only a small number of these xanthenes were found in nature (Negi et al., 2013). These compounds are very close is keletal patterns formed from the association of the xanthone nucleus the lignoid pattern (coniferyl alcohol or syringenin) (Demirkiran, O., 2007). Recently, kielcorin was also isolated from *Vismia guaramirangae*, *Kielmeyera variabilis* (Pinheiro et al., 2003), and *Hypericum canariensis*, whereas cadensin C and cadensin D from *Vismia guaramirangae* and *Hypericum canariensis* have been reported (Demirkiran, O., 2007).



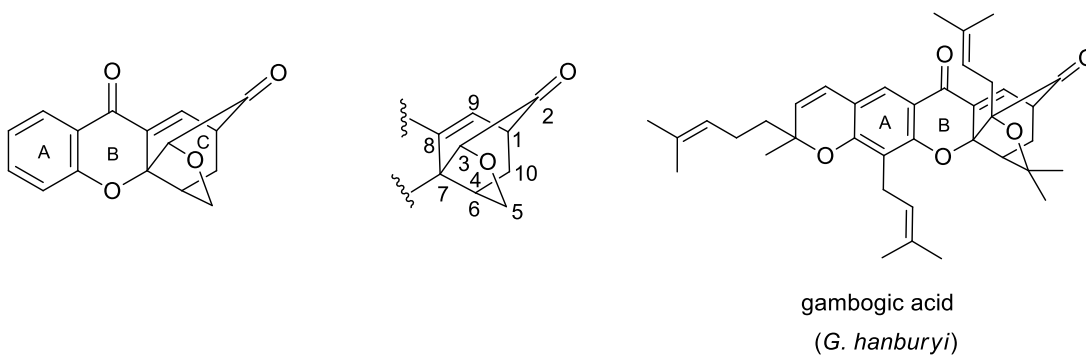
Bisxanthenes

Bisxanthenes are dimeric xanthenes which are formed via a C-C or C-O bond connection from two xanthone monomers. This type of xanthenes is less numerous. According to the report of Negi, five compounds were isolated from higher plants, one from lichen, and six from fungi (Negi et al., 2013). These include jacarelhypoxerols A and B (Ishiguro et al., 2002), from the aerial parts of *Hypericum japonicum* and dimeric xanthone, and globulixanthone E, from the roots of *Symphonia globulifera* (Nkengfack et al., 2002). Three C2-C2' dimeric tetrahydroxyxanthenes dicerandrols A, B, and C, are also isolated from the fungus *Phomopsis longicolla* (Wagenaar & Clardy, 2001).



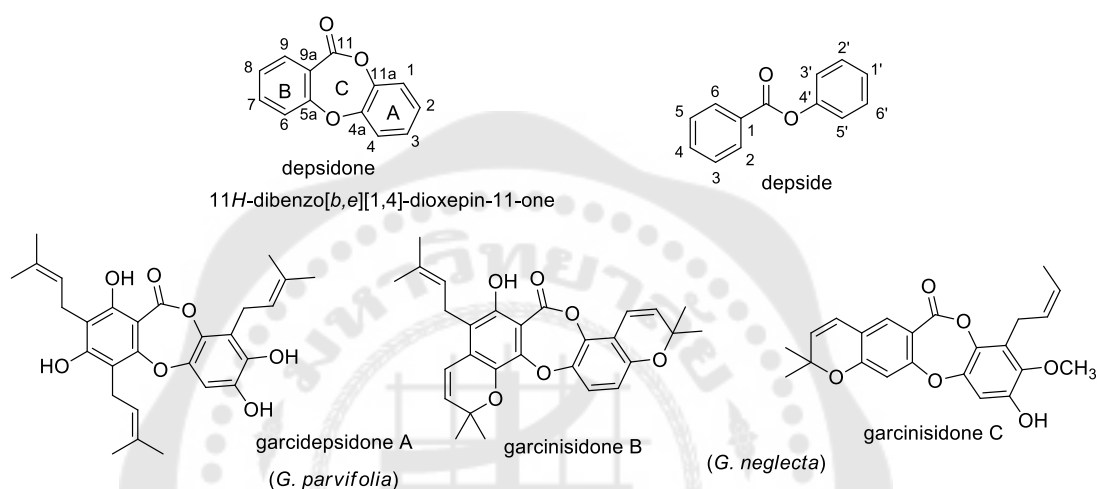
Caged xanthenes

The chemical structure of the caged xanthone is unique, in which the C ring of the xanthone backbone is converted to a cage of 4-oxa-tricyclo[4.3.1.0^{3,7}]dec-8-en-2-one unit (Chantarasriwong et al., 2010). To date, around 100 compounds of caged xanthone have been isolated and *G. hanburyi* is a rich source of this type of compounds. Gambogic acid, the most abundant, and other caged xanthenes isolated from the fruit and resin of *G. hanburyi* exhibited remarkable cytotoxic activity against several mammalian cancer cells and displayed potent anti HIV-1 activities in the reverse transcriptase assay (Hemshkhar et al., 2011).

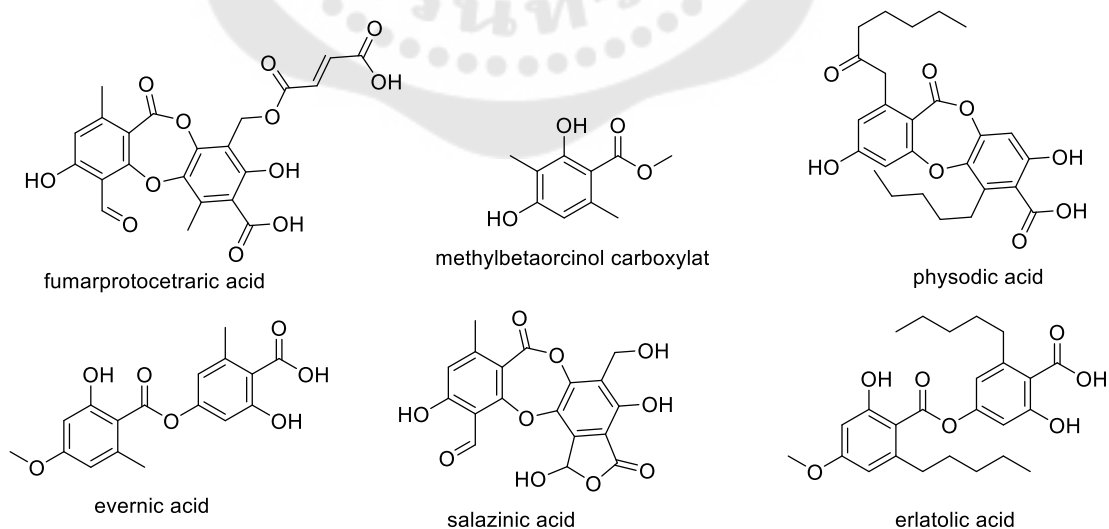


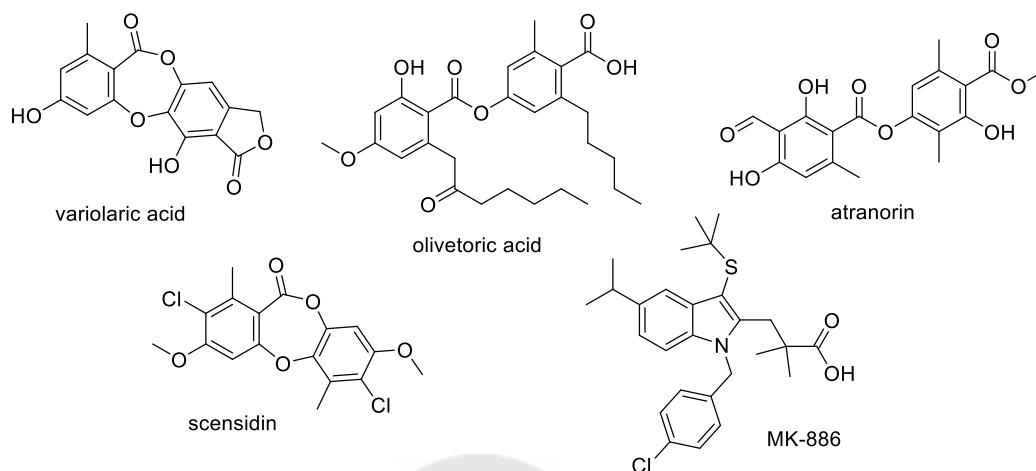
Depsidone

Depsidone is a lactone derivative of xanthone containing a basic structure of 11*H*-dibenzo[*b,e*][1,4]-dioxepin-11-one (Lang et al., 2007). They are found in lichens and endophytic fungus (Hauck et al., 2010; Sukandar et al., 2016). Recent *Garcinia* depsidones have been reported, though to a lesser extent.



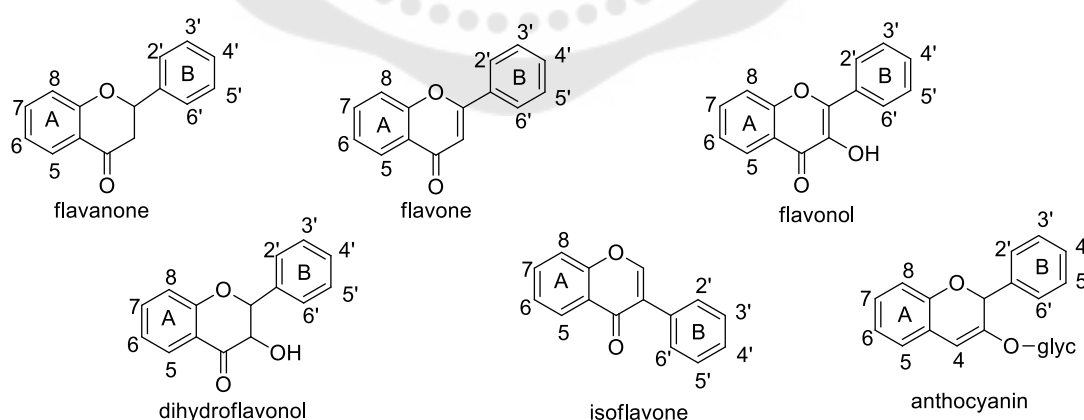
For instance, the general structures of both the depside and depsidone scaffolds with numbering were isolated from lichen.



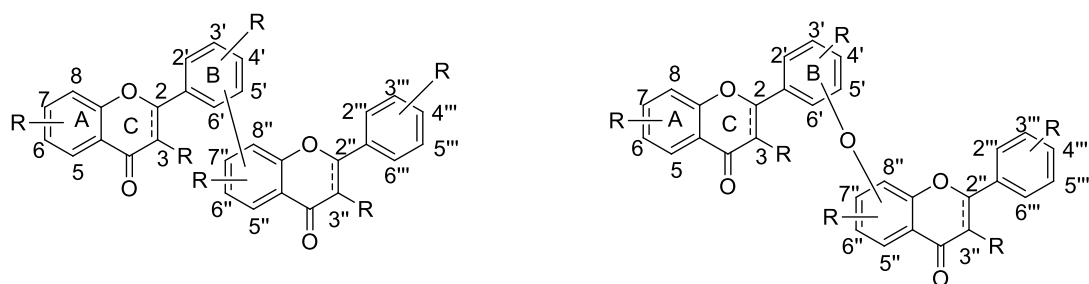


Biflavonoids

Biflavonoids are flavonoid-flavonoid dimers. They can be formed from flavonol, flavone, flavanones, isoflavones, anthocyanin or dihydroflavonol via a C-C or a C-O-C bond (Lee et al., 2008) as shown in Figures 1 and 2. Possible interflavonoyl link in bioflavonoids are the 3-8'', 6-8'', 8-8'', 5'-8'', 3'-6'', 4'-6'' and 5'-4''' linkages as shown in Figure 3. However, the majority is simply 3'-8'' and 3-8'' linked types (Ito, T. et al., 2013). The substituents of hydroxyl and methoxyl groups can be substituted at various positions of the biflavonoid nucleus. *Garcinia* species is a major source of several types of compounds including biflavonoids (Syed et al., 1988).

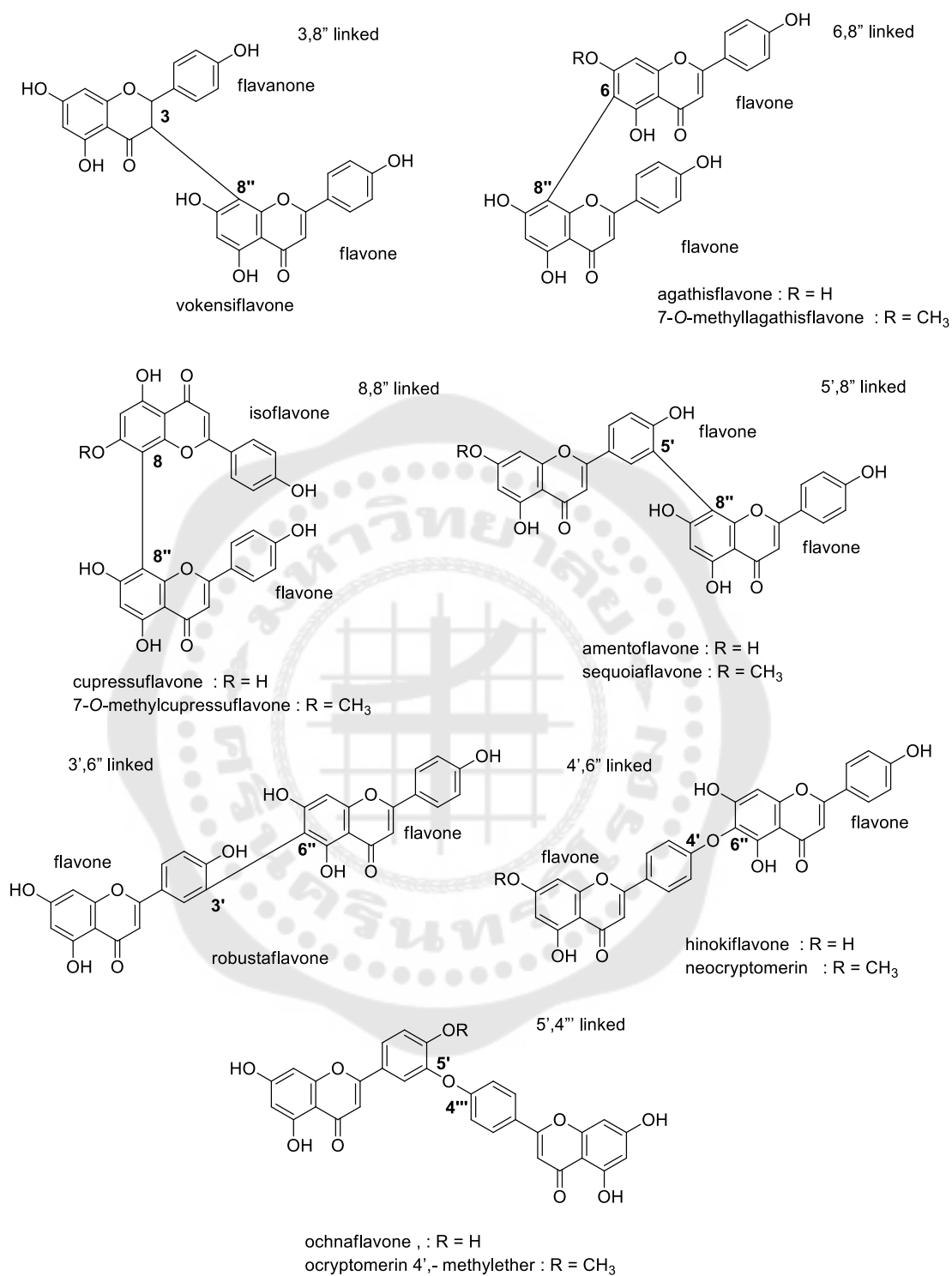


FIGURES 1 Basic structure of flavonoids



FIGURES 2 Structures of biflavonoids

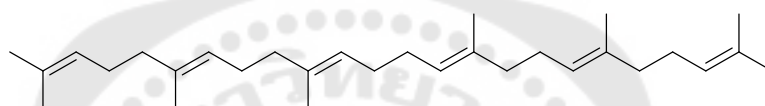




FIGURES 3 Types of interflavonyl link of bioflavonoids

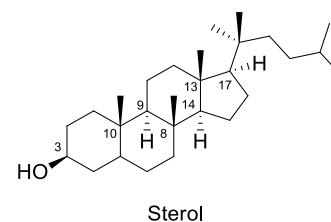
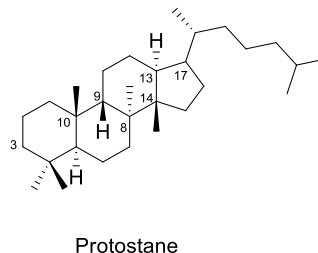
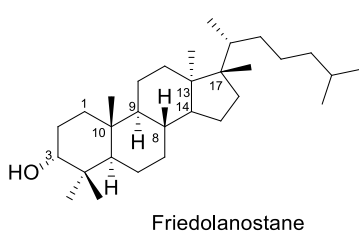
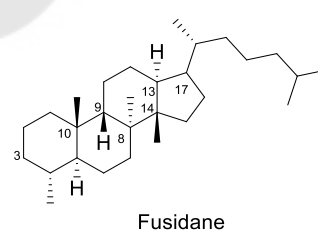
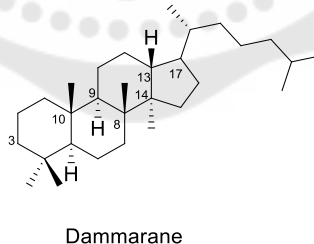
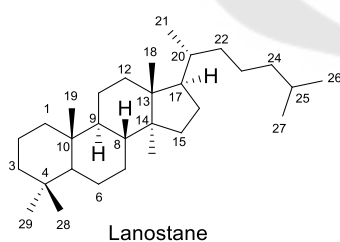
Triterpenoids

Triterpene or triterpenoid is a large group of natural products which derived from cyclization of squalene or related acyclic 30-carbon precursors (Ronco & De Stéfani, 2013). Triterpenes are precursors to steroids in plants and animals. There are two main types, steroidal tetracyclic (of 6-6-6-5 type) and pentacyclic (of 6-6-6-6-5 type and 6-6-6-6-6 type) triterpenes. Triterpene glycosides are also referred as saponins (Xu et al., 2004). Triterpene compounds display a wide range of activities covering, for examples, anti-tumor, anti-inflammatory and immunomodulatory actions (Aldred, 2008).



Structure of squalene

According to their basic core structure, tetracyclic triterpenes may be divided into lanostane, protostane, dammarane, fusidane, friedolanostane and sterols skelatons. Whereas the pentacyclic triterpenes may be grouping into hopane, lupene, ursane, oleanane, gammacerane and serratene types.



Lanostane triterpene or 4,4,14-trimethylcholestane, the stereostructures in positions are 8β -H, 9α -H, 13β -CH₃ and 14α -CH₃.

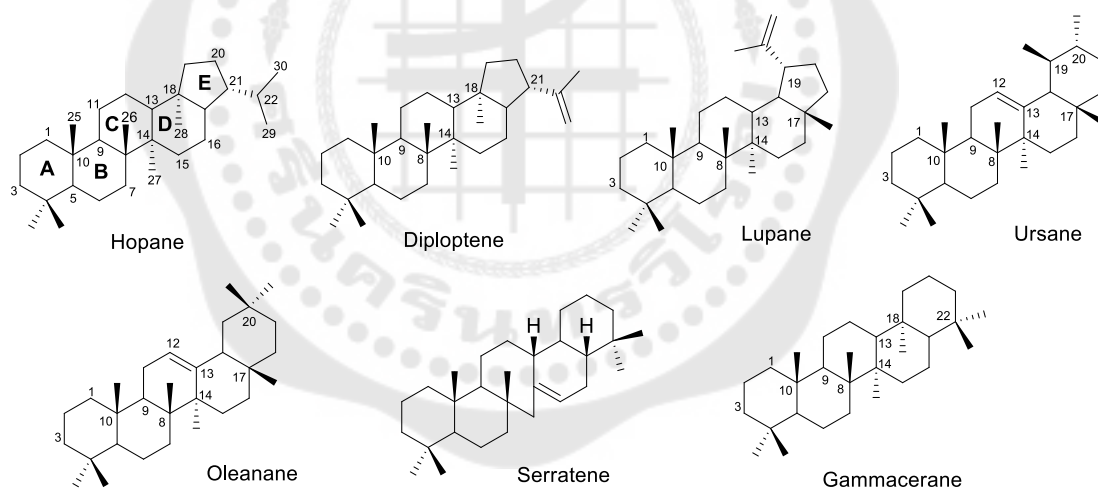
Protostane triterpene, the stereocenters are 8α -CH₃, 9β -H, 13α -H and 14β -CH₃.

Dammarane triterpene is a stereoisomer of the protostane, showing 8β -CH₃, 9α -H, 13β -H and 14α -CH₃.

Fusidane shows characteristic stereostructures difference from tetracyclic protostane by losing one methyl group to be 4α -CH₃.

Friedolanostane backbone displays characteristic stereostructures in positions 8β -H, 9α -H, 13α -CH₃ and 17β -CH₃.

Sterols are an important group among the steroids, form with the cholestane skeleton containing a 3β -hydroxyl group and an aliphatic side chain of C8 or more carbon atoms attached to position C-17 form the group of sterols.



Hopane, a group of hopanoids, is pentacyclic triterpenoid based on the hopane skeleton with a 21α -isopropenyl group at the five-membered ring E (6-6-6-6-5). The simplest C₃₀ hopanoid is diploptene.

Lupane-type triterpene is series of 6-6-6-6-5 pentacyclic, which composed of an isopropenyl (CH₃C=CH₂) moiety at C-19, but difference from hopane at a 17β -CH₃ and 19α -isopropenyl group at ring E.

Ursane-type triterpene is series of 6-6-6-6-pentacyclic, which contain a double bond at C12-C13 and additional of two methyl groups at carbon C-19 and C-20 in the ring E.

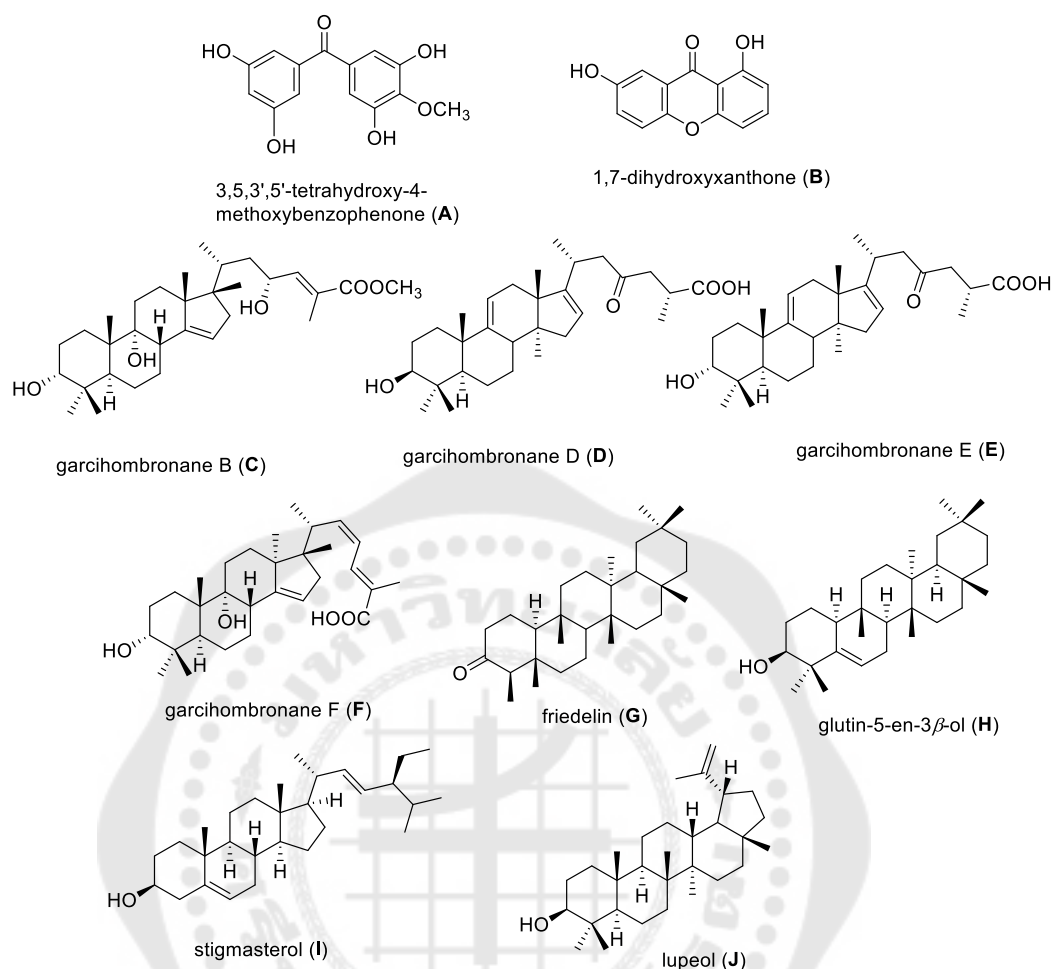
The oleanane-type triterpenes is a series of pentacyclic triterpenes (6-6-6-6-6), which contain a double bond at C12-C13 and additional of two methyl groups at carbon C-20 in the ring E.

The gammacerane skeleton (6-6-6-6-6) is characterized by a six-membered ring E which is substituted by two methyl groups at C-22. Tetrahymanol has been isolated for the first time from the phototrophic bacterium *Rhodospirillum rubrum* (Kleemann et al., 1990)

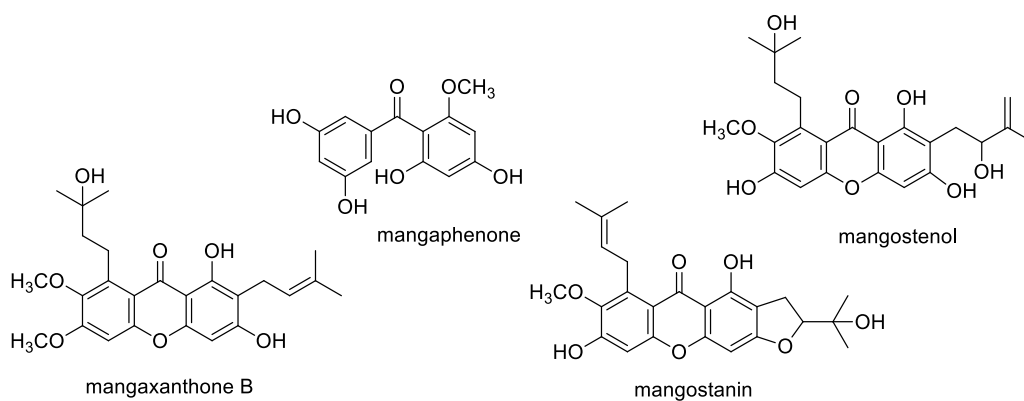
Serratoids are a group of pentacyclic triterpenes with an unusual seven carbons ring (6-6-7-6-6).

Recent publications of *Garcinia* phytochemicals and of their biological activities during the years of 2012-2017.

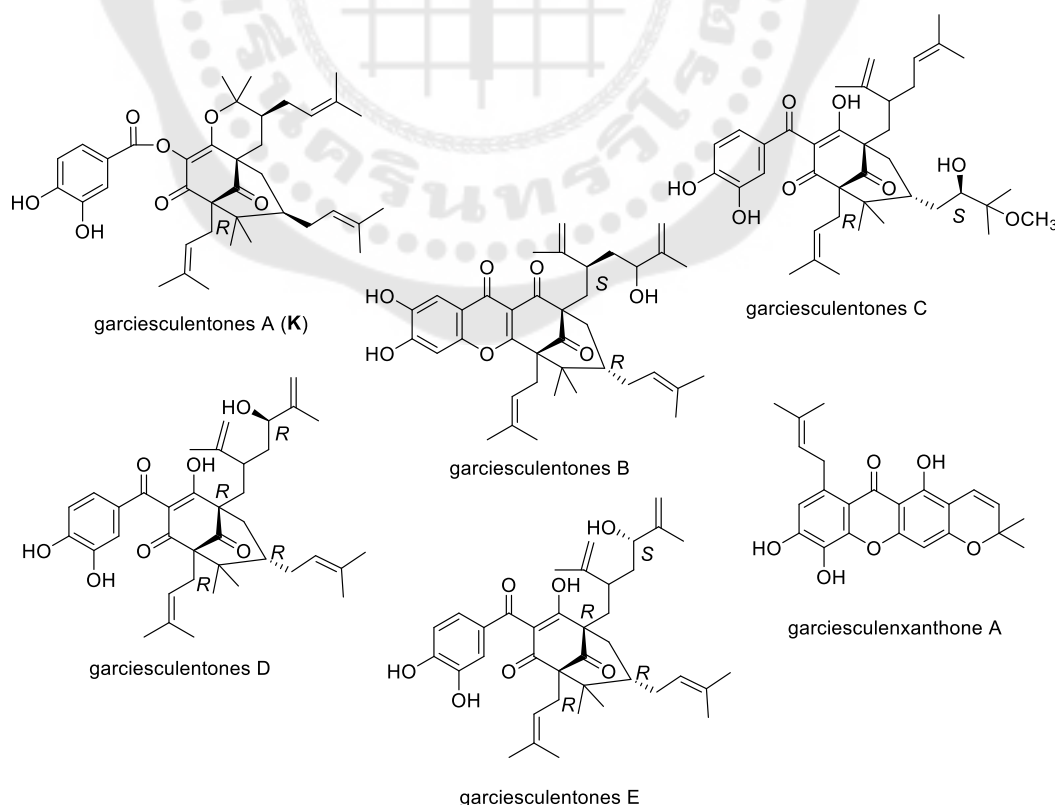
In 2012, Saputri and Jantan reported that the MeOH extract of *G. hombroniana* twigs displayed strong low-density lipoprotein (LDL) antioxidation and antiplatelet aggregation activities. Chemical investigation of MeOH extract fraction gave ten compounds A and B and 8 triterpenes C-J. All compounds were evaluated for their ability to inhibit human LDL oxidation and platelet aggregation *in vitro*. 3,5,3',5'-Tetrahydroxy-4-methoxybenzophenone and 1,7-dihydroxyxanthone showed strong inhibitory activity on LDL oxidation with half-maximal inhibitory concentration (IC₅₀) values of 6.6 and 1.7 μ M, respectively (Saputri & Jantan, 2012).

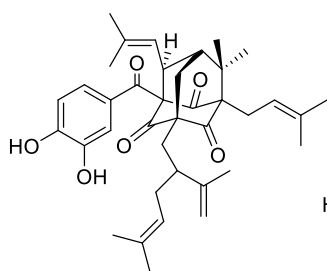


In 2014, See; et al. studied on the investigation of the EtOAc and MeOH extracts of the stem barks from *G. mangostana* resulted in the successive isolation of a new prenylated xanthone, mangaxanthone B, a new benzophenone, mangaphenone, and two known xanthenes, mangostanin and mangostenol (See et al., 2014).

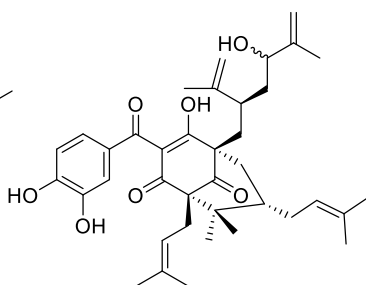


In 2014, Zhang; et al. described that five new xanthenes (garciesculenxanthone A-E), a new public (K), and 15 known xanthenes (garciniagifolone A, garcimultiflorone E, cambogin, guttiferone F, compound L, α -mangostin, garcicowin C, GDPHH-2, 1,3,7-trihydroxy-2-(3-methylbut-2-enyl)-xanthone, griffipavixanthone, 1,3,5,7-tetrahydroxy-8-isoprenylxanthone, γ -xanthone, hyperxanthone E, toxyloxanthone B and compound M were isolated from *G. esculenta*. The isolates were evaluated for their cytotoxicity potency by MTT assay against 3 human cancer cell lines and against normal liver cells. Among tested compounds garciniagifolone A, garcimultiflorone E, cambogin, guttiferone F, compound L and γ -mangostin displayed cytotoxic activity against one or two human cancer cell lines exhibiting IC_{50} values below 10 μM . Only γ -mangostin showed a selective activity toward the cancer cells used demonstrating by no significant cytotoxicity to normal HL-7702 hepatocyte cells. Apart from that, all isolated compounds were tested for their inhibitory activity on IFN- γ plus LPS-induced NO production in RAW264.7 cells. Only garcimultiflorone E, 1,3,5,7-tetrahydroxy-8-isoprenylxanthone, and hyperxanthone E displayed IC_{50} values below 10 μM in this assay (Zhang et al., 2014).

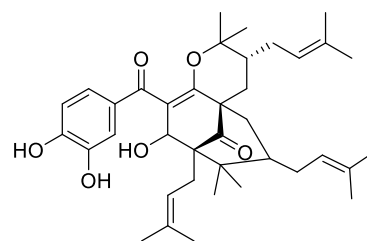




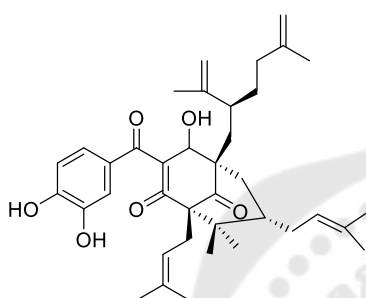
garciniagifolone A



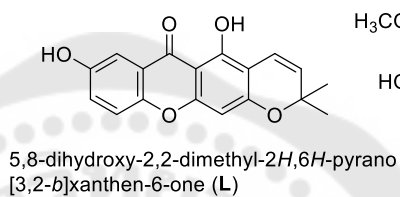
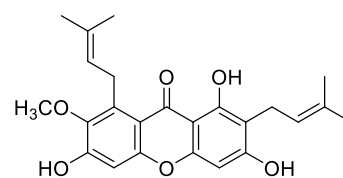
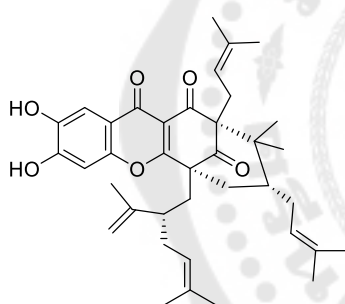
garcimultiflorone E



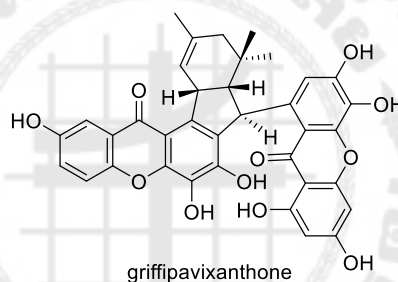
cambogin



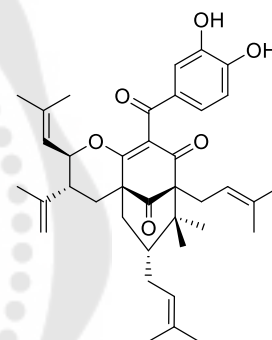
guttiferone F

5,8-dihydroxy-2,2-dimethyl-2H,6H-pyrano
[3,2-b]xanthen-6-one (L) α -mangostin

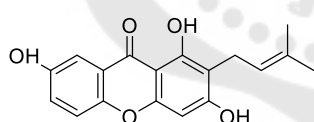
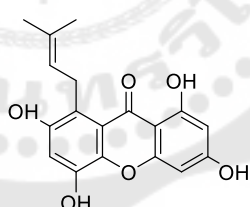
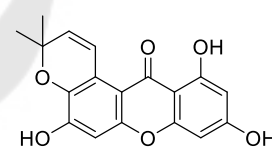
GDPHH-2



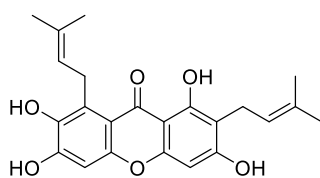
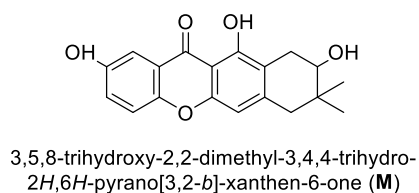
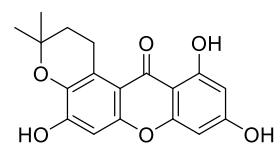
griffipavixanthone



garcicowin C

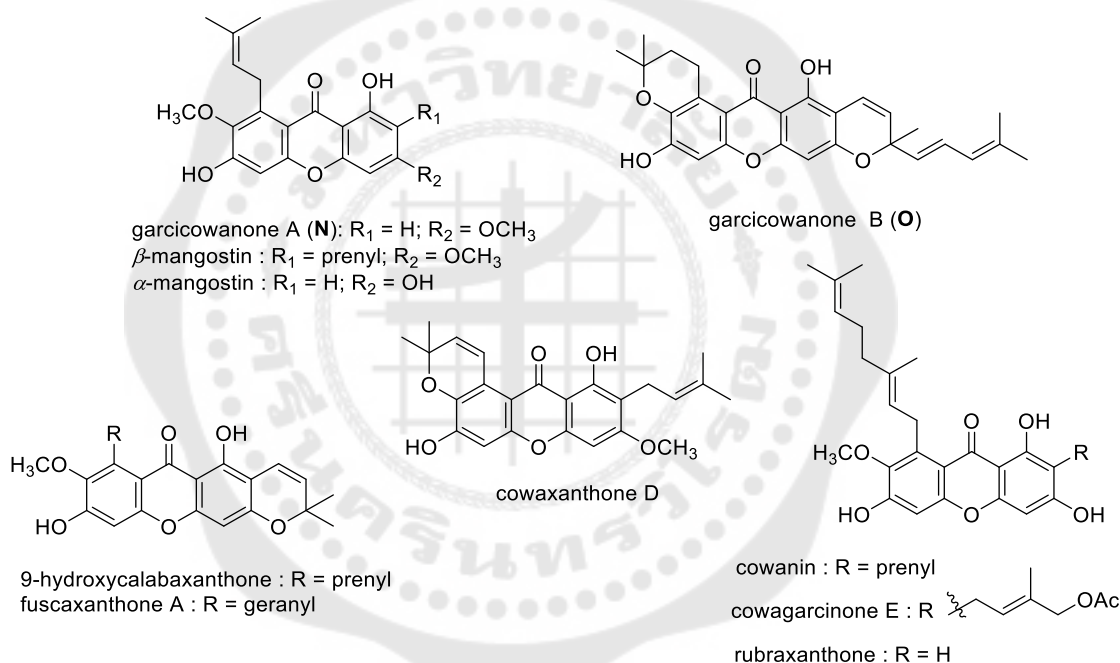
1,3,7-trihydroxy-2-(3-methylbut-
2-enyl)-xanthone1,3,5,7-tetrahydroxy-8-
isoprenylxanthone

toxyloxanthone B

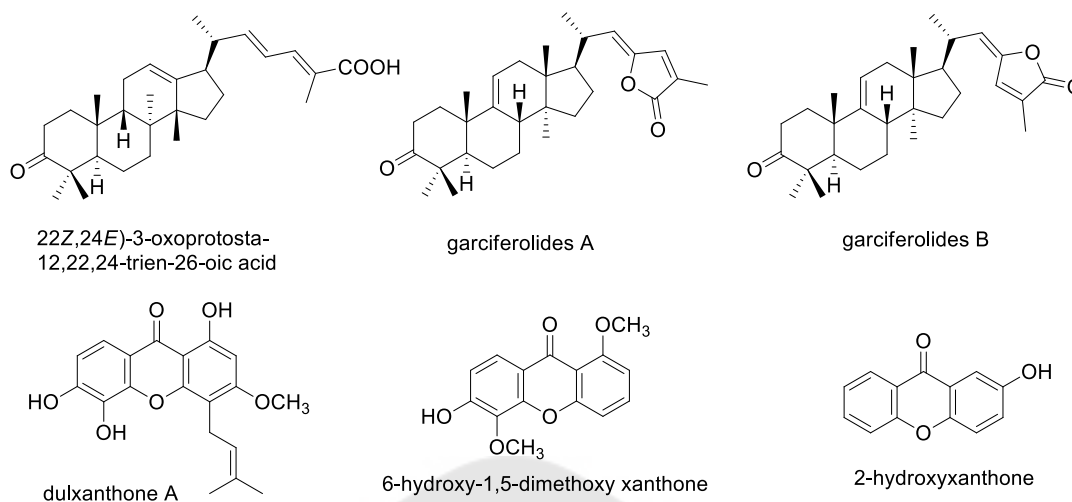
 γ -xanthone3,5,8-trihydroxy-2,2-dimethyl-3,4,4-trihydro-
2H,6H-pyrano[3,2-b]xanthen-6-one (M)

hyperxanthone E

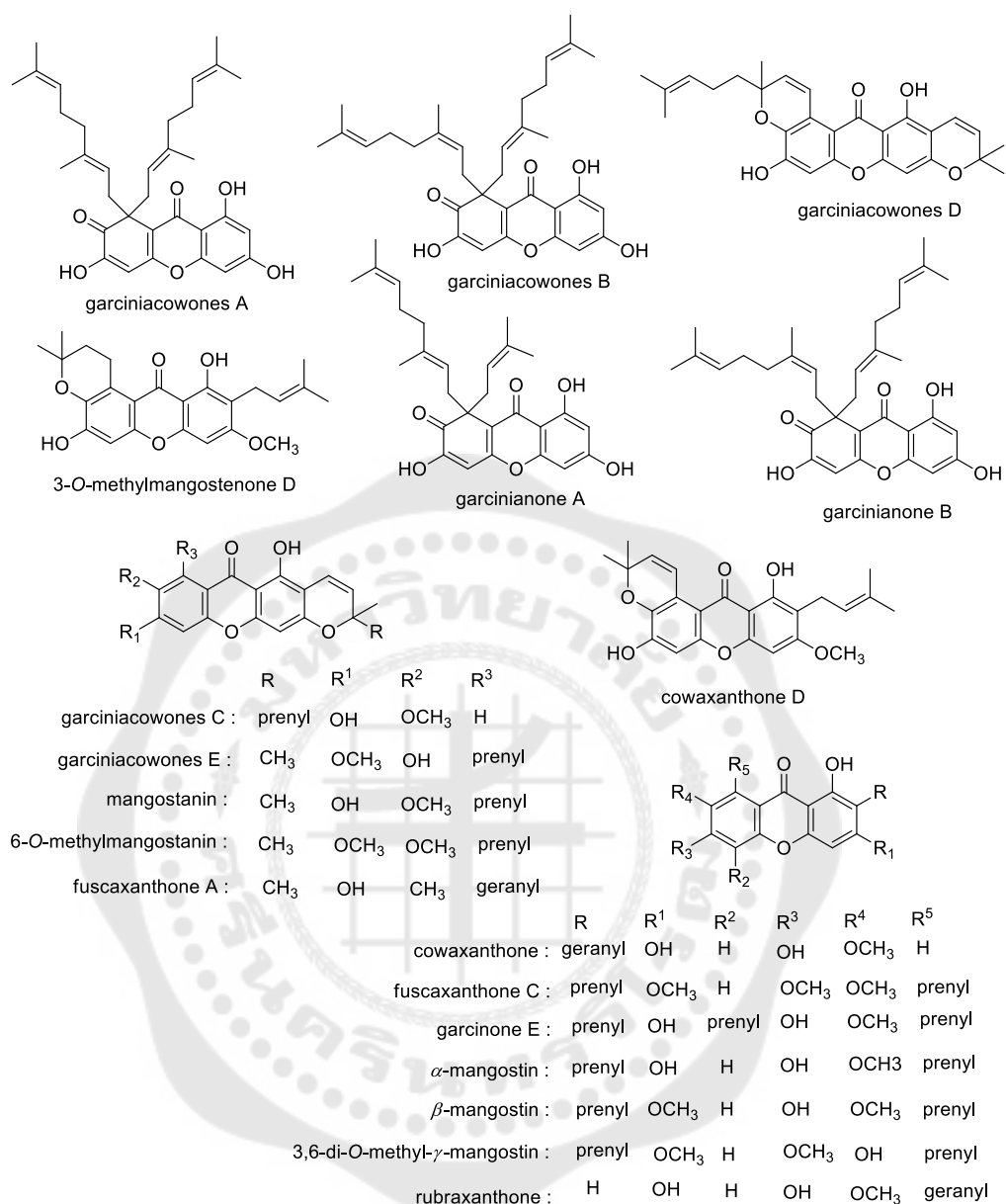
In 2014, Auranwiwat; et al. investigated the acetone extract from the young fruits of *G. cowa*. They enabled to isolate two new xanthenes (garcicowanones A and B), and eight known xanthenes (9-hydroxycalabaxanthone, β -mangostin, fuscaxanthone A, cowaxanthone D, cowanin, α -mangostin, cowagarcinone E, and rubraxanthone). All chemical structures were tested for a series of bacterias. Moreover, the α -mangostin displayed potent activity (MIC 0.25–1 $\mu\text{g/mL}$) against three gram-positive strains. Among them, two compounds (N-O) showed good antibacterial activity against strain *B. cereus* with the same MIC values of 0.25 $\mu\text{g/mL}$ (Auranwiwat et al., 2014).



In 2014, Bui; et al. isolated a new protostane; (22Z,24E)-3-oxoprotosta-12,22,24-trien-26-oic acid, two novel lanostane lactones; garciferolides A and B, and three known compounds; dulxanthone A, 6-hydroxy-1,5-dimethoxyxanthone, and 2-hydroxyxanthone from the barks of *G. ferrea* (Bui et al., 2014).

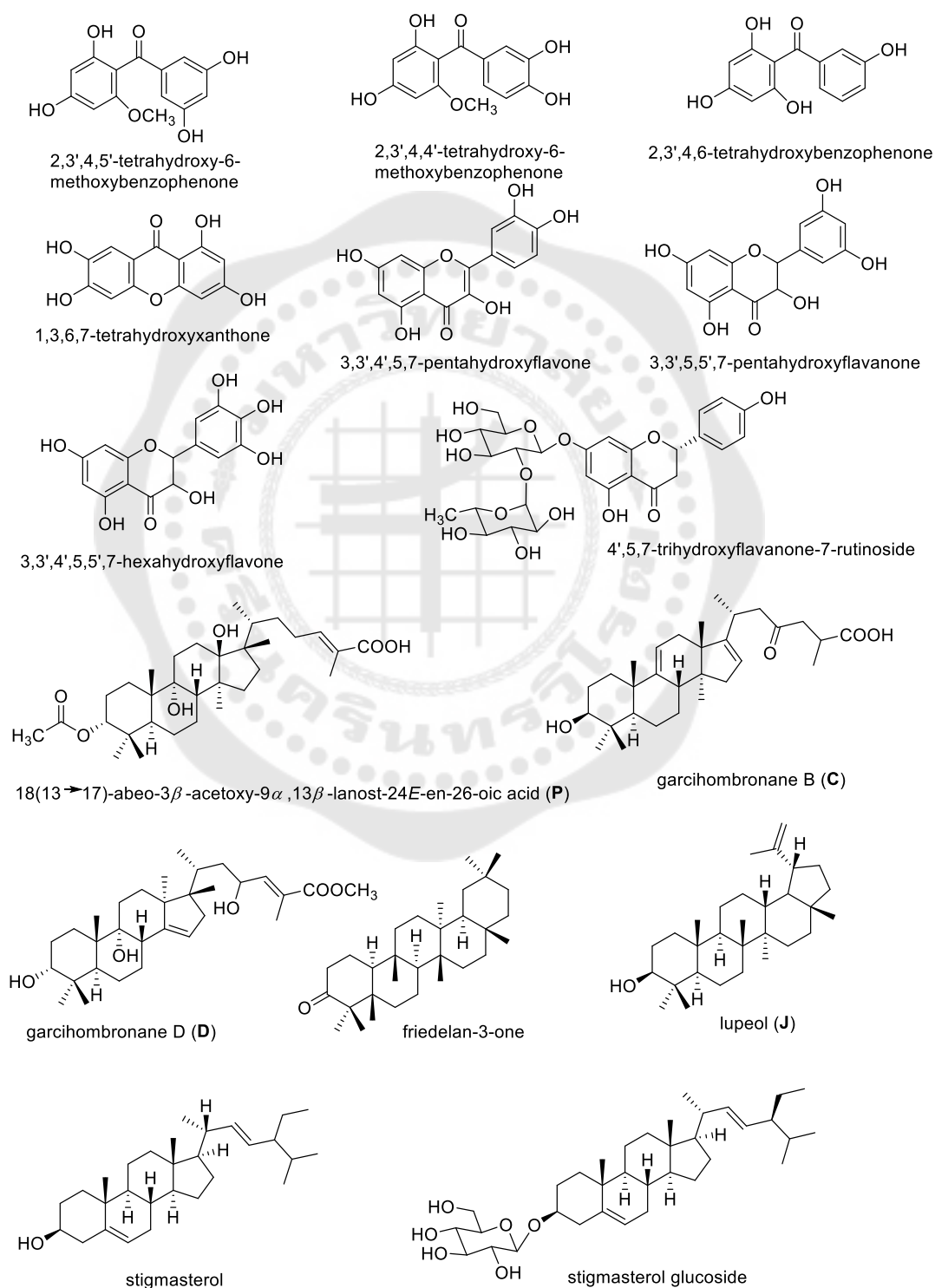


In 2015, Sriyatep; et al. reported 5 new phytochemicals, garciniacowones A-E, together with 14 known compounds, were isolated from the young fruits and fresh flowers of *G. cowa*. The concentrated MeOH extract of the young fruits from *G. cowa* was extracted with CH_2Cl_2 and then EtOAc to give CH_2Cl_2 and EtOAc-soluble fractions, respectively. The CH_2Cl_2 extract was isolated to silica gel CC to yield 3 new xanthenes, garciniacowones A-C, and 4 known xanthenes, cowaxanthone, 3-O-methylmangostenone D, and garcinianone A-B. While the EtOAc extract was further separated obtain two new xanthenes, garciniacowones D-E, a long with 10 known xanthenes, mangostanin, 6-O-methylmangostanin, fuscaxanthone A, fuscaxanthone C, 7-O-methylgarcinone E, cowaxanthone D, α -mangostin, β -mangostin, 3,6-di-O-methyl- γ -mangostin, and rubraxanthone. All compounds were evaluated in vitro for their antimicrobial activity and for their ability to inhibit α -glucosidase. α -Mangostin and β -mangostin showed the most potent α -glucosidase inhibitory activity, with IC_{50} values of 7.8 ± 0.5 and 8.7 ± 0.3 μM , respectively. In addition, garcinianones A-B and rubraxanthone showed antibacterial activity against *Bacillus subtilis* TISTR 088 with identical MIC values of 2 $\mu\text{g/mL}$, while garcinianone A, mangostanin, and rubraxanthone presented antibacterial activity against *B. cereus* TISTR 688 strain with identical MIC values of 4 $\mu\text{g/mL}$ (Sriyatep et al., 2015).

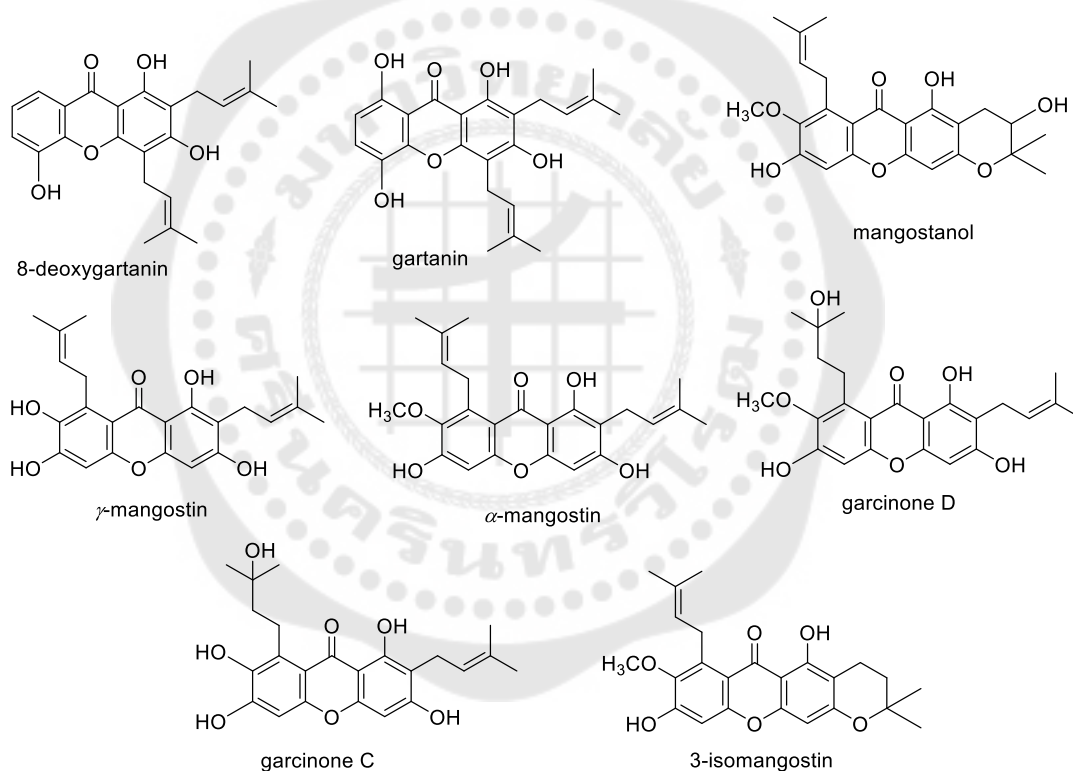


In 2014, Jamila; et al. isolated phytochemicals from EtOAc- and CH₂Cl₂ extracts of *G. hombroniana* to yield two new compounds, 2,3',4,5'-tetrahydroxy-6-methoxybenzophenone and compound **P** and thirteen known compounds, 2,3',4,4'-tetrahydroxy-6-benzophenone, 2,3',4,6-tetrahydroxybenzophenone, 1,3,6,7-tetrahydroxyxanthone, 3,3',4',5,7-pentahydroxyflavone, 3,3',5,5',7-penta-hydroxyflavanone, 3,3',4',5,5',7-hexahydroxyflavone, 4,5,7-trihydroxyflavanone-7-rutinoside, compounds **C** and **D**, friedelan-3-one, compound **J**, stigmasterol and stigmasterol glucoside. The *in vitro* cytotoxicity was evaluated against three cancer cell lines, two new structures 2,3',4,5'-

tetrahydroxy-6-methoxybenzo-phenone and compound **P** exhibited highly cytotoxic effects on DBTRG tumor cell lines with the 50% effective concentrations (EC_{50}) values of 48 and 34 μ M (Jamila et al., 2014).

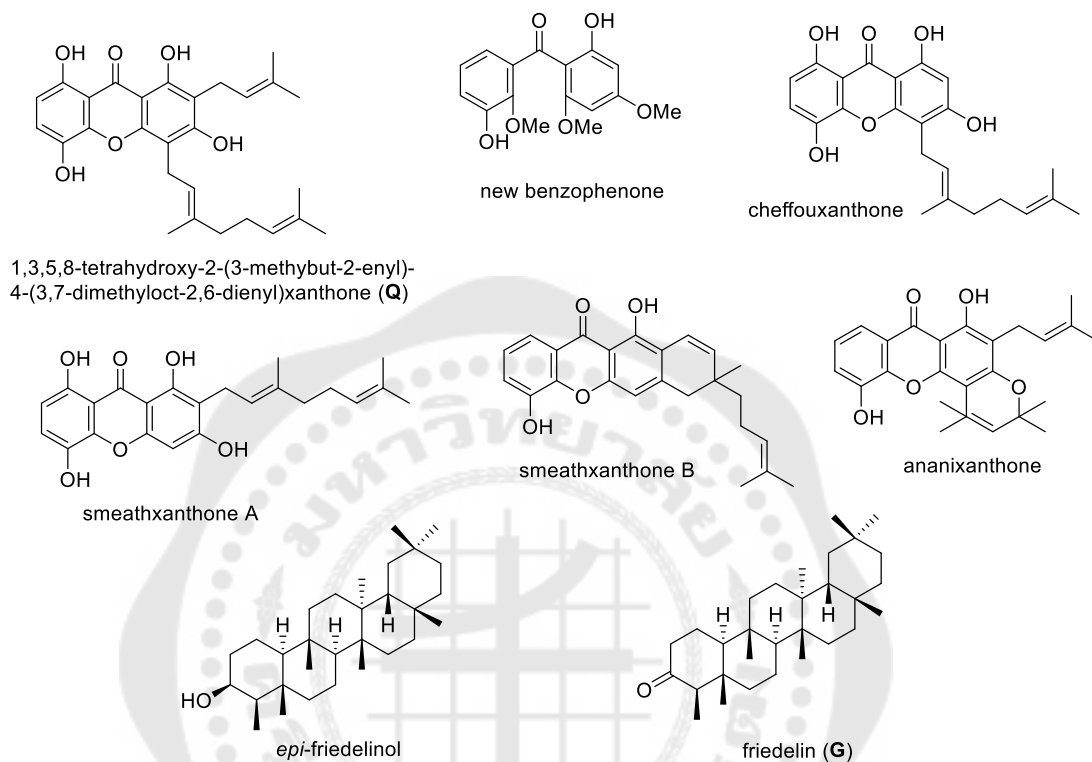


In 2014, Khaw; et al. studied on the isolation of secondary metabolites from MeOH extract of *G. mangostana* fruit hulls. This study described cholinesterases inhibition of the extract and its phytochemical constituents using previous method. Prenylated xanthenes and garcinone C, were the most potent inhibitor of AChE with the same IC_{50} value of 1.24 μM while γ -mangostin was the most potent inhibitor of BChE (IC_{50} 1.78 μM). The molecular docking studies have shown that two 1,3,6,7-tetraoxynated xanthenes (γ -mangostin and garcinone C) interacts differently with the 5 significant regions of both enzyme through protein-ligand interactions, mainly hydrophobic and hydrogen bonding (Khaw et al., 2014).

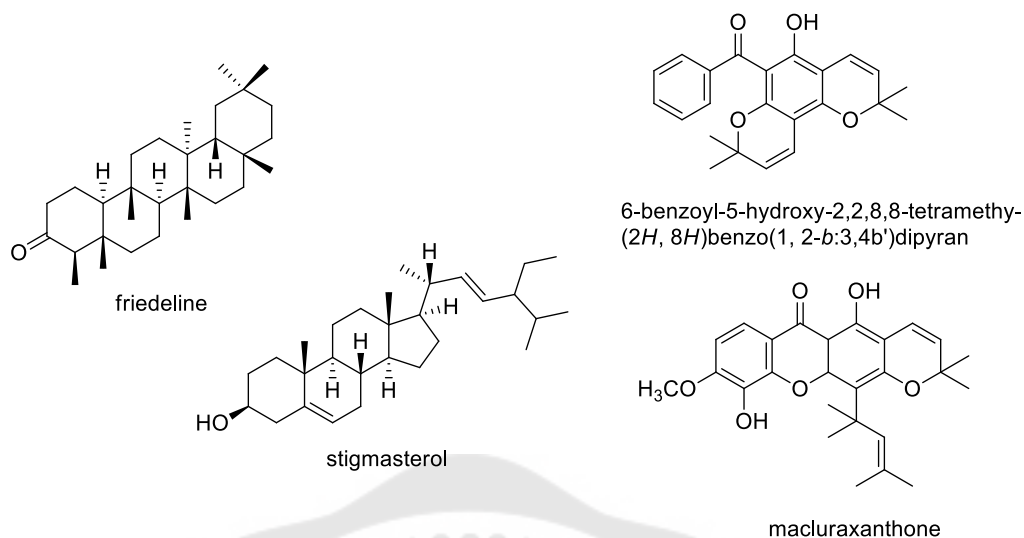


In 2015, Fouotsa; et al. found two new compounds, chemical structure **Q**, and 4 known compounds (cheffouxanthone, smeathxanthone A, smeathxanthone B, ananixanthone, two pentacyclic triterpenes (epifriedelinol and **G**), from the stem barks of *G. smeathmannii*. Two new compounds (xanthone and benzophenone) and cheffouxanthone exhibited the most prominent antibacterial activity against gram-positive *Enterococcus faecalis* with minimal inhibitory concentration values of 8, 8, and 2 $\mu g/mL$,

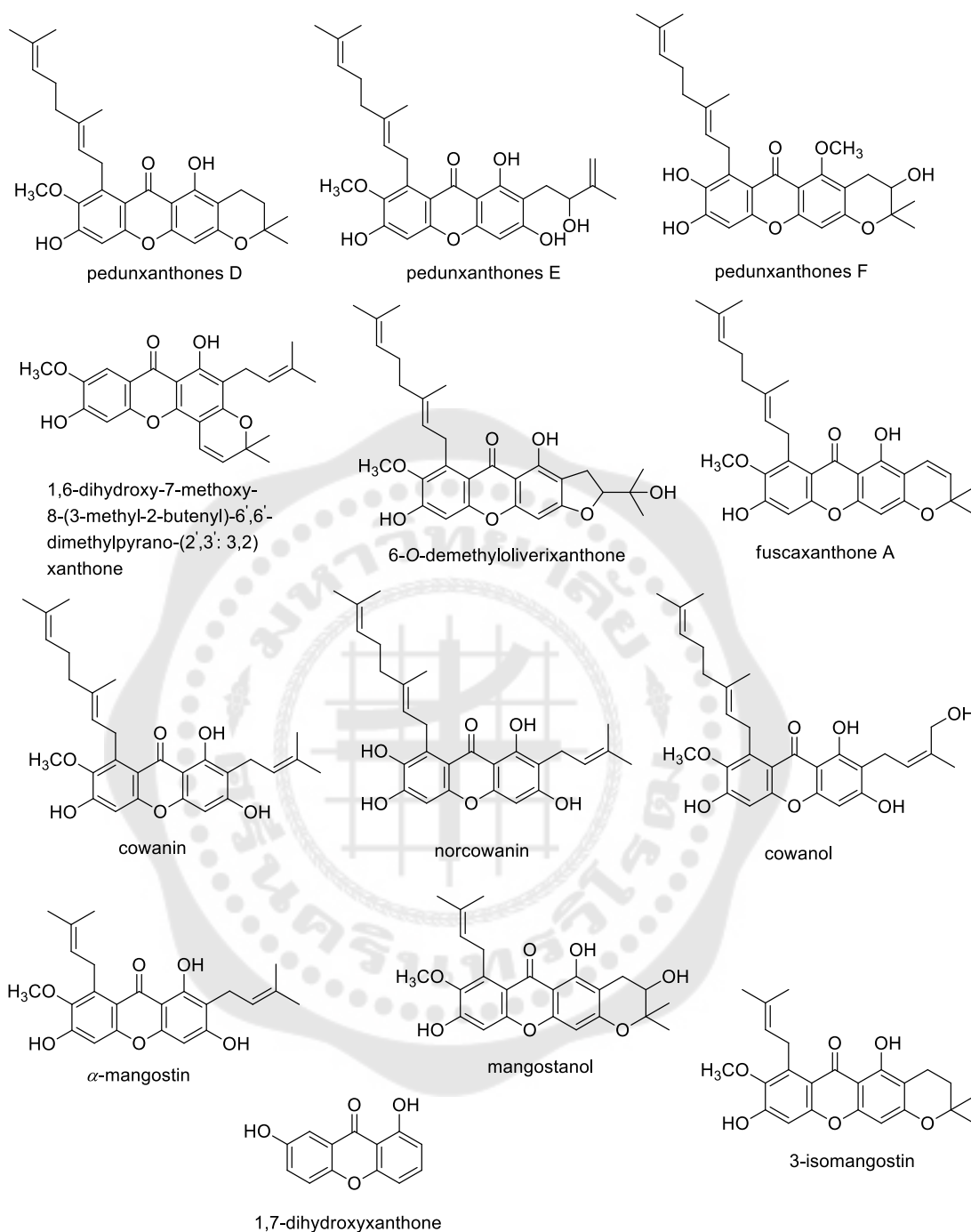
respectively, while new prenylated xanthone, cheffouxanthone, smeathxanthone A, and ananixanthone displayed the capacity to scavenge free radical (Fouotsa et al., 2015).



In 2015, Sangsuwon and Jiratchariyakul studied on the chemical constituents of *G. speciosa* and cytotoxic activity against A549 lung cancer cell lines. The phytochemical study of the leaves and twigs of this plant led to separation of 4 known compounds, friedeline, stigmasterol, 6-benzoyl-5-hydroxy-2,2,8,8-tetramethy-(2*H*, 8*H*)benzo(1, 2-*b*:3,4*b'*) dipyrans, and together with prenylated xanthone, macluraxanthone. The H₂O, MeOH and EtOAc extracts were evaluated for their *in vitro* cytotoxicity against the lung cancer cell lines (A 549) gave ED₅₀ values of 62, 45 and 75 μ g/mL, respectively. The antioxidant activity of macluraxanthone was tested by using DPPH assay and showed IC₅₀ value of 7.65 μ g/mL, and its cytotoxicity displayed ED₅₀ values 15.38 μ g/mL (Sangsuwon & Jiratchariyakul, 2015).

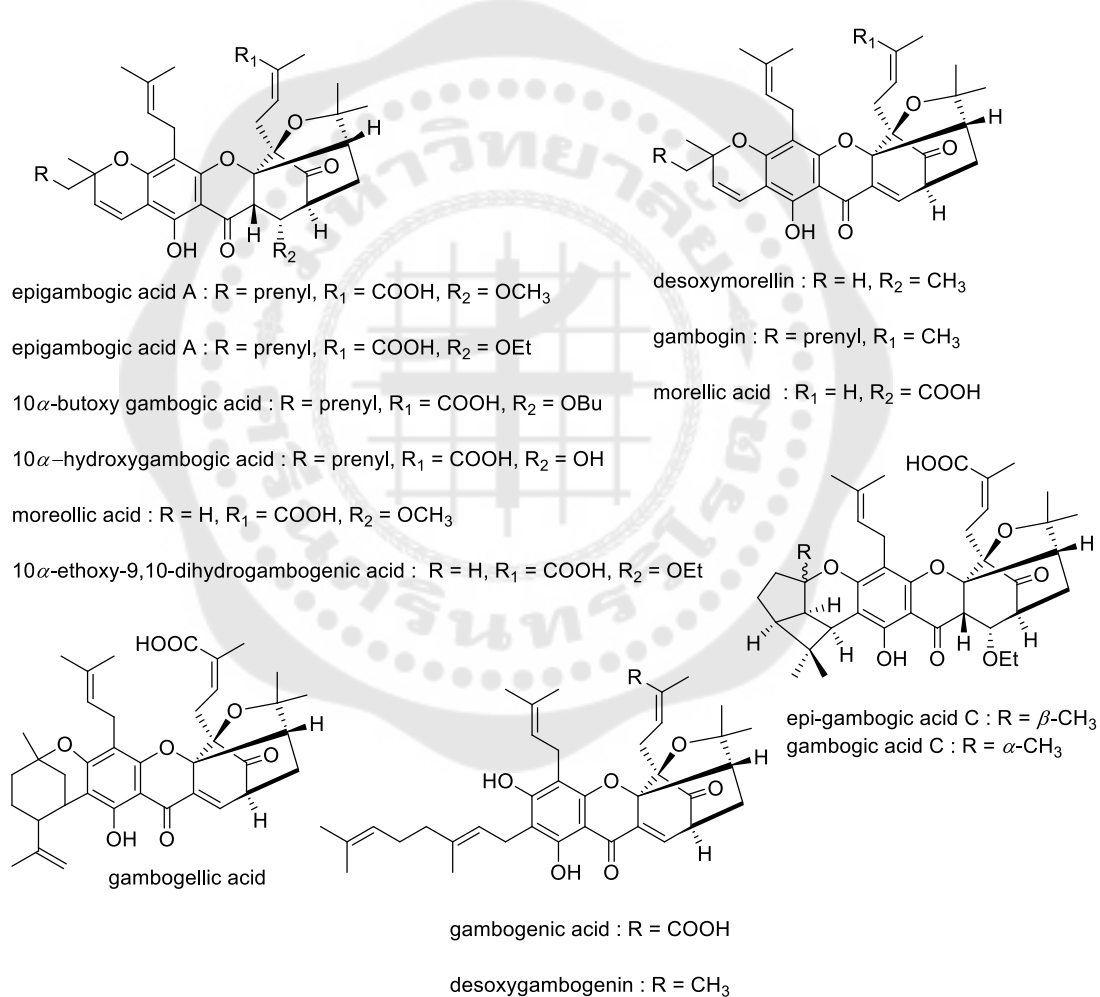


In 2015, Vo; et al. reported three new xanthenes, pedunxanthenes D-F, along with ten known compounds, 1,6-dihydroxy-7-methoxy-8-(3-methyl-2-butenyl)-6',6'-dimethylpyrano-(2',3': 3,2)xanthone, 6-O-demethyloliverixanthone, fuscaxanthone A, cowanin, norcowanin, cowanol, α -mangostin, mangostanol, 3-isomangostin and 1,7-dihydroxyxanthone, from a CHCl_3 extract of *G. pedunculata* pericarps from Viet Nam. Cytotoxicity against HeLa and NCI-H460 cells of the isolated compounds was evaluated; pedunxanthone D was the most active compound with IC_{50} 24.9 ± 0.4 and 26.1 ± 1.5 $\mu\text{g/mL}$, respectively (Vo et al., 2015).

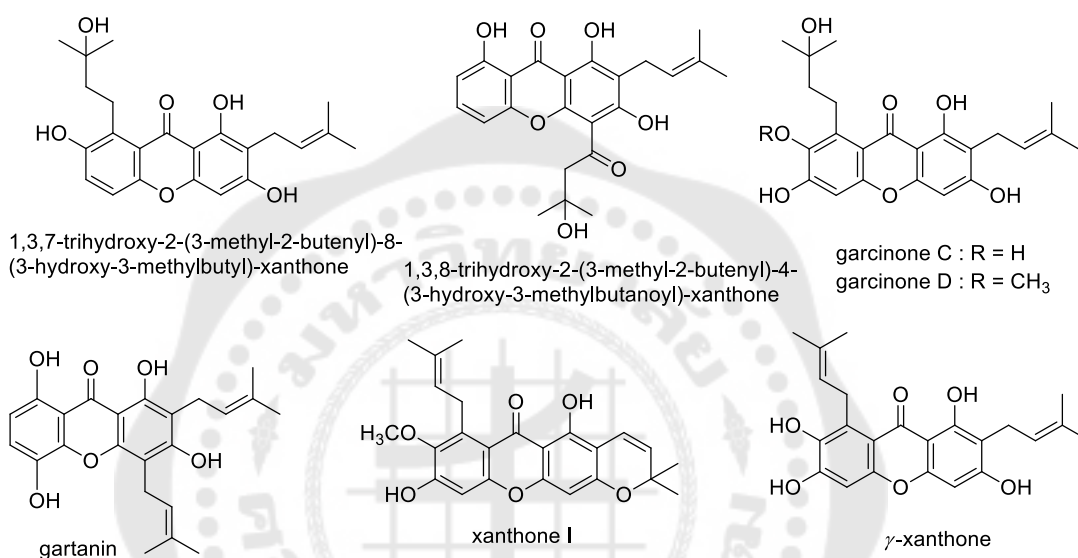


In 2016, Chen; et al. reported five new caged polyprenylated xanthenes, epigambogic acid A, epigambogic acid B, 10 α -butoxy gambogic acid, epi-gambogic acid C and gambogic acid C, and 12 known xanthenes were isolated from the resin of *G. hanburyi*. These known compounds including 10 α -hydroxygambogic acid, moreollic acid, 10 α -ethoxy-9,10-dihydrogambogenic acid, desoxymorellin, gambogin, morellic

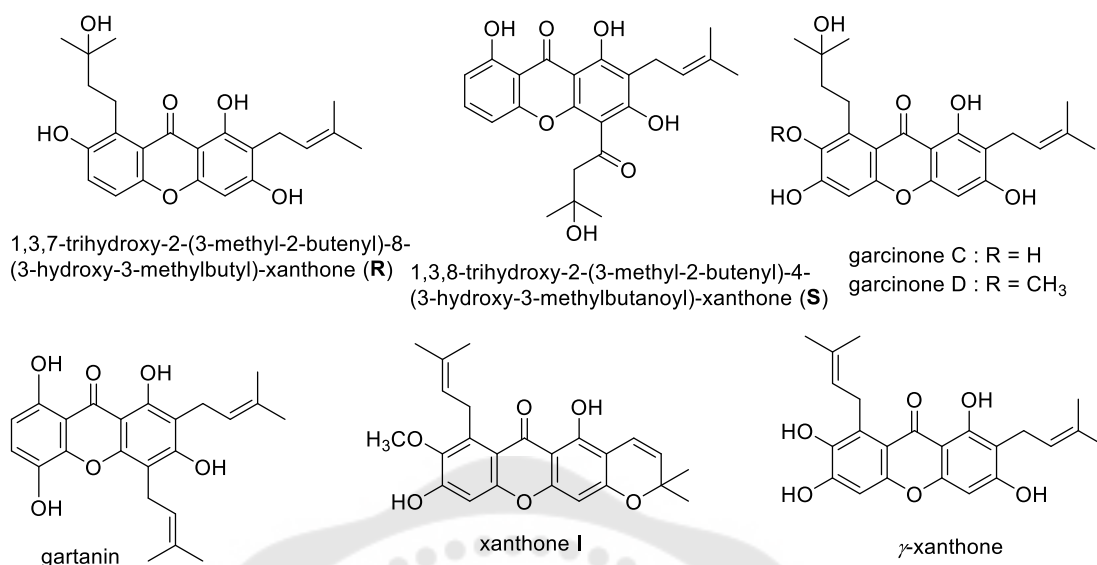
acid, gambogellic acid, gambogenic acid and desoxygambogenin. Epi-gambogic acid C and gambogic acid C are the first examples of caged polyprenylated xanthenes. These isolate compounds showed α -glucosidase inhibitory activities in vitro. Except for 10 α -butoxy gambogic acid, 10 α -ethoxy-9,10-dihydrogambogenic acid, epi-gambogic acid C and gambogic acid C, the remaining compounds were evaluated for α -glucosidase inhibition. Epigambogic acid A and B display moderate α -glucosidase inhibition with IC₅₀ and values 108.75 and 111.80 μ M, respectively (Chen et al., 2016).



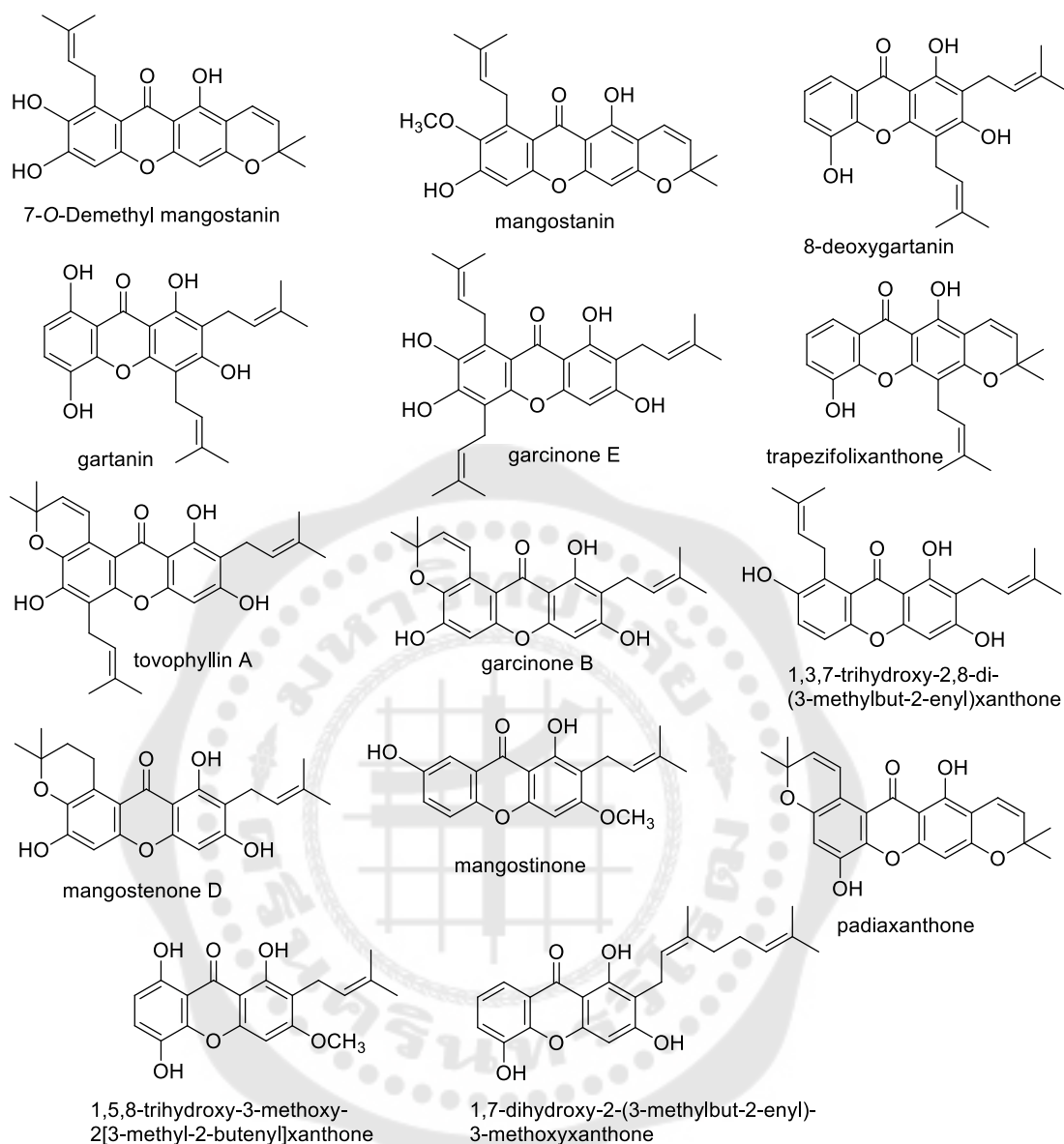
In 2016, Xu; et al. described the isolation of secondary metabolites from an ethanolic extract of *G. mangostana* pericarps to obtain two new xanthenes, compounds R and S, a long with 5 known xanthenes garcinones C-D, gartanin, xanthone I, and γ -mangostin. All isolated compounds displayed significant cytotoxic activities against various human cancer cell lines (Xu, W. J. et al., 2016).



In 2016, Xu; et al. reported one new prenylated xanthone, mangostanate was subjected from the pericarp of *G. mangostana*, together with five known compounds, α -mangostin, γ -mangostin, gartanin, garcinone D and 6-methoxy-bis pyrano xanthone. All compounds were evaluated for their antioxidant activity with DPPH assay. α -mangostin, γ -mangostin, gartanin, garcinone D and 6-methoxy-bis pyrano xanthone showed antioxidant activity with IC₅₀ values of 35.03, 21.52, 25.61, 73.79 and 48.67 μ g/mL, while mangostanate was inactive (Xu, T. et al., 2016).

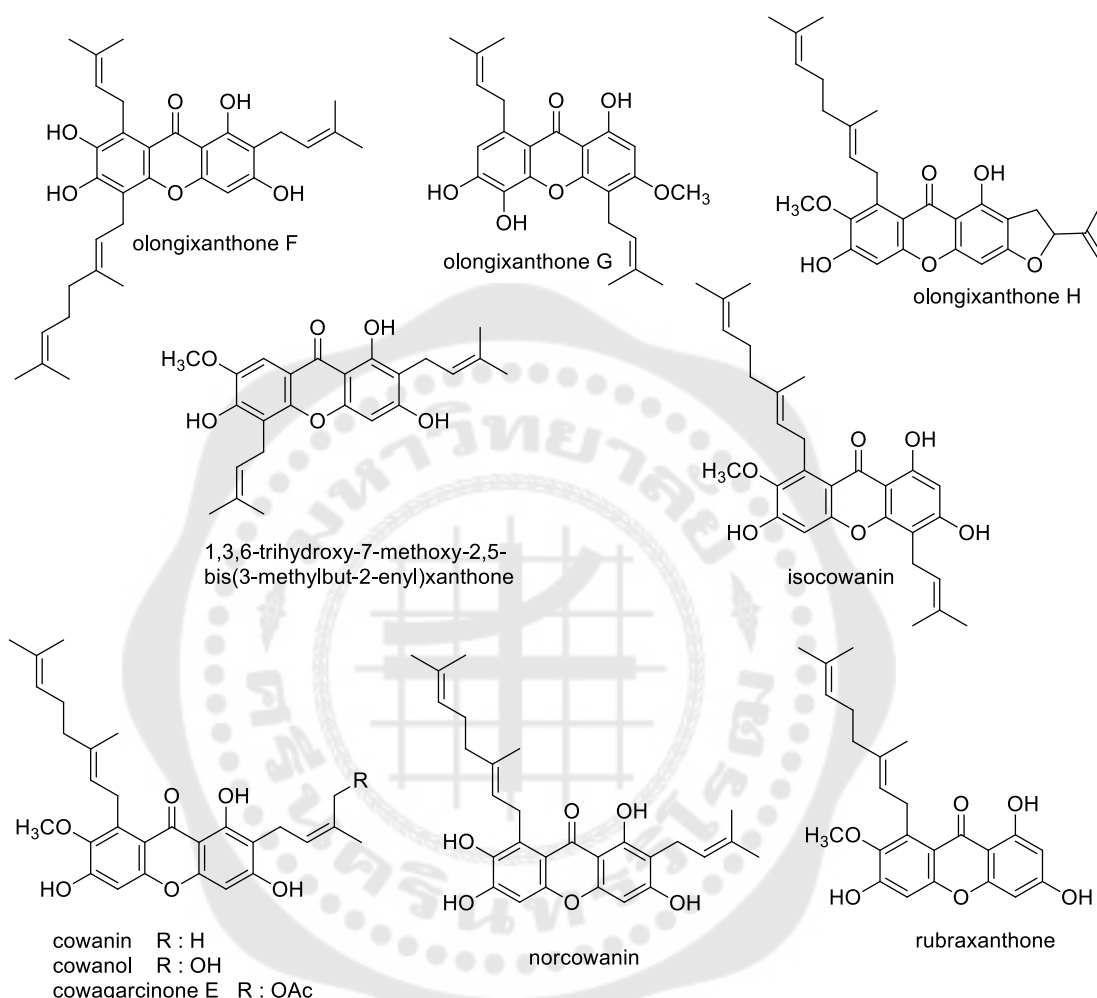


In 2017, Yang; et al. isolated one new prenylated xanthone, 7-O-demethyl mangostanin and thirteen known xanthones, mangostanin, 8-deoxygartanin, gartanin, gartanone E, trapezifolixanthone, padiaxanthone, tovophyllin A, 1,5,8-trihydroxy-3-methoxy-2[3-methyl-2-butenyl]xanthone, gartanone B, 1,3,7-trihydroxy-2,8-di-(3-methylbut2-enyl)xanthone, mangostenone D, 2-geranyl-1,3,5-trihydroxyxanthone (mangostinone), and 1,7-dihydroxy-2-(3-methylbut-2-enyl)-3-methoxyxanthone, from the pericarps of *G. mangostana*. The new compound was tested against seven cancer cell lines and side population growth of CNE-2. The result showed that the compound has potential anti-cancer properties with the half maximal inhibitory concentration (IC₅₀) values 3.35, 4.01, 4.84, 7.84, 6.21, 8.09, 6.39 and 1.26 μ M, respectively. These compounds was also tested from mangosteen flesh extract, which indicated that the popular fruit could have potential cytotoxic activity for cancer cell lines (Yang, R. et al., 2017).



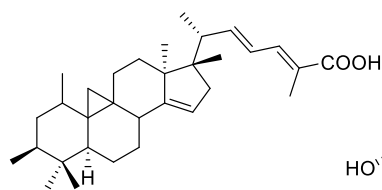
In 2017, Trinh; et al. reported 11 xanthones, of which three new xanthones, oblongixanthone F–H, along with eight known xanthones, 1,3,6-trihydroxy-7-methoxy-2,5-bis(3-methylbut-2-enyl)xanthone, isocowanin, oblongixanthone C, cowanin, cowanol, rubraxanthone, cowagarcinone E, and norcowanin were isolated from an EtOAc extract of the twigs of *G. oblongifolia*. The results indicate that the crude extract of this plant is a potential source of α -glucosidase and PTP1B inhibitors. All isolated compounds were evaluated antidiabetic effects by in vitro α -glucosidase and PTP1B inhibition assays.

Norcowanin was the most active compound, and PTP1B with inhibited α -glucosidase IC_{50} values of 1.7 ± 0.5 and $14.1 \pm 3.5 \mu M$, respectively (Trinh et al., 2017).

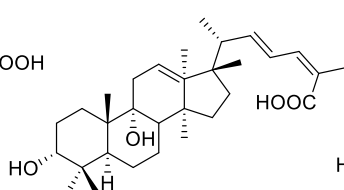


In 2016, Jamila; et al. isolated of CH_2Cl_2 barks extract from *G. hombroniana* to obtain, one new cycloartane triterpene and five known triterpenoids. The extract of this plant obtained a new compound T, a long with 5 known triterpenes U-Y.

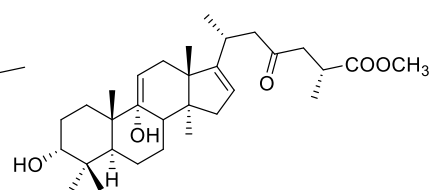
Previously, *G. hombroniana* have been investigated for its benzophenone and biflavonoids, and anticholinesterase activity of isolated compounds. In these activities, triterpenoids and benzophenone displayed more potent the ChE inhibitory effects while biflavonoids did not reasonably contribute to both the enzymes inhibitions (Jamila et al., 2016).



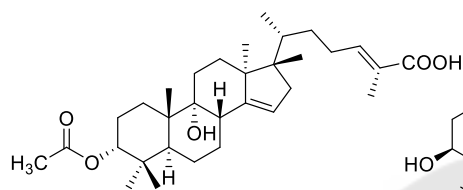
22Z,24E)-3 β -hydroxycycloart-14,22,24-trien-26-oic acid (**T**)



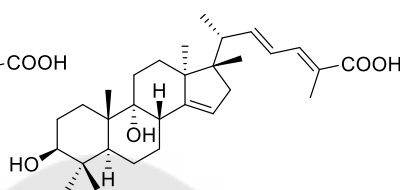
garchihombronane **G (U)**



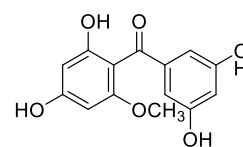
garchihombronane **J (V)**



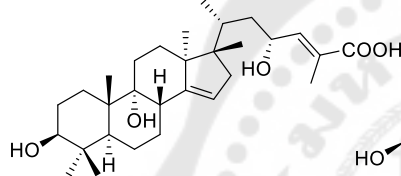
3 β -acetoxy-9 α -hydroxy-17,14-friedlanostan-14,24-dien-26-oic acid (**W**)



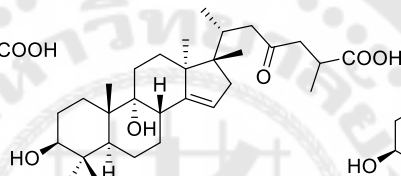
(22Z, 24E)3 β , 9 α -dihydroxy-17,14-friedlanostan-14,22,24-trien-26-oic acid (**X**)



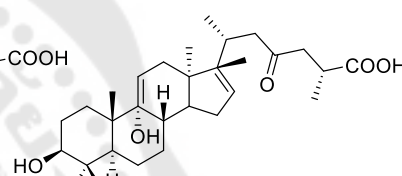
2,3',4,5'-tetrahydroxy-6-methoxybenzophenone



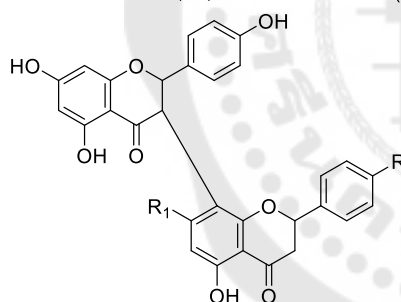
3 β , 23 α -dihydroxy-17,14-friedlanostan-8,14,24-trien-26-oic acid (**Y**)



garchihombronane **B (Z)**

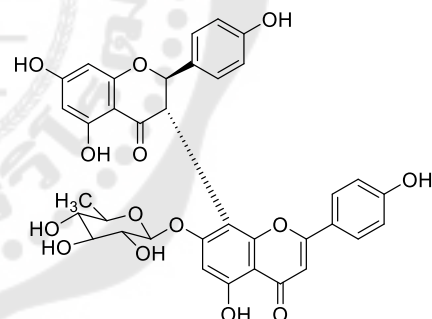


garchihombronane **D**

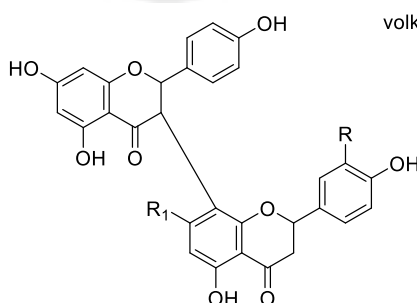


volkensiflavone : R = R₁ = OH

4''-O-methyl-volkensiflavone : R = OCH₃, R₂ = OH



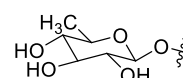
volkensiflavone-7-O-glucopyranoside



morelloflavone : R = R₁ = OH

3''-O-methyl-morelloflavone : R = OCH₃, R₁ = OH

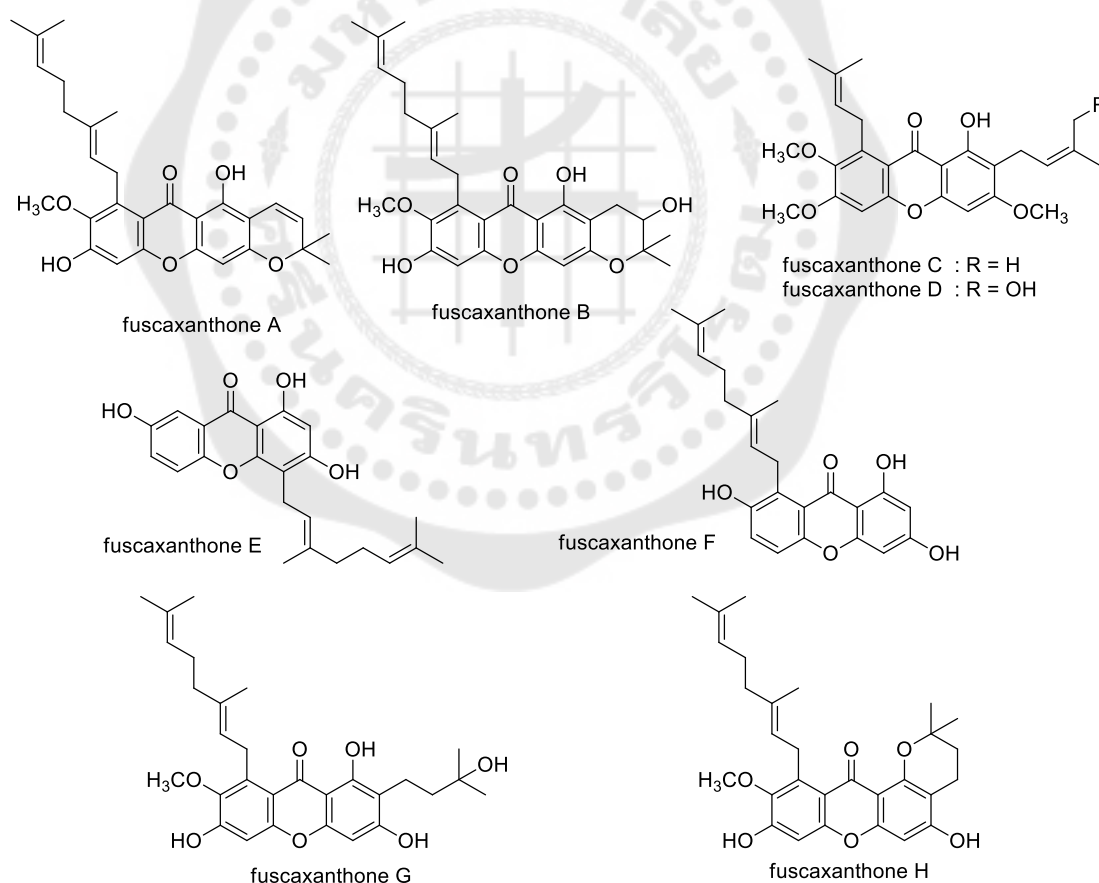
morelloflavone-7-O-glucopyranoside : R = OH, R₁ =

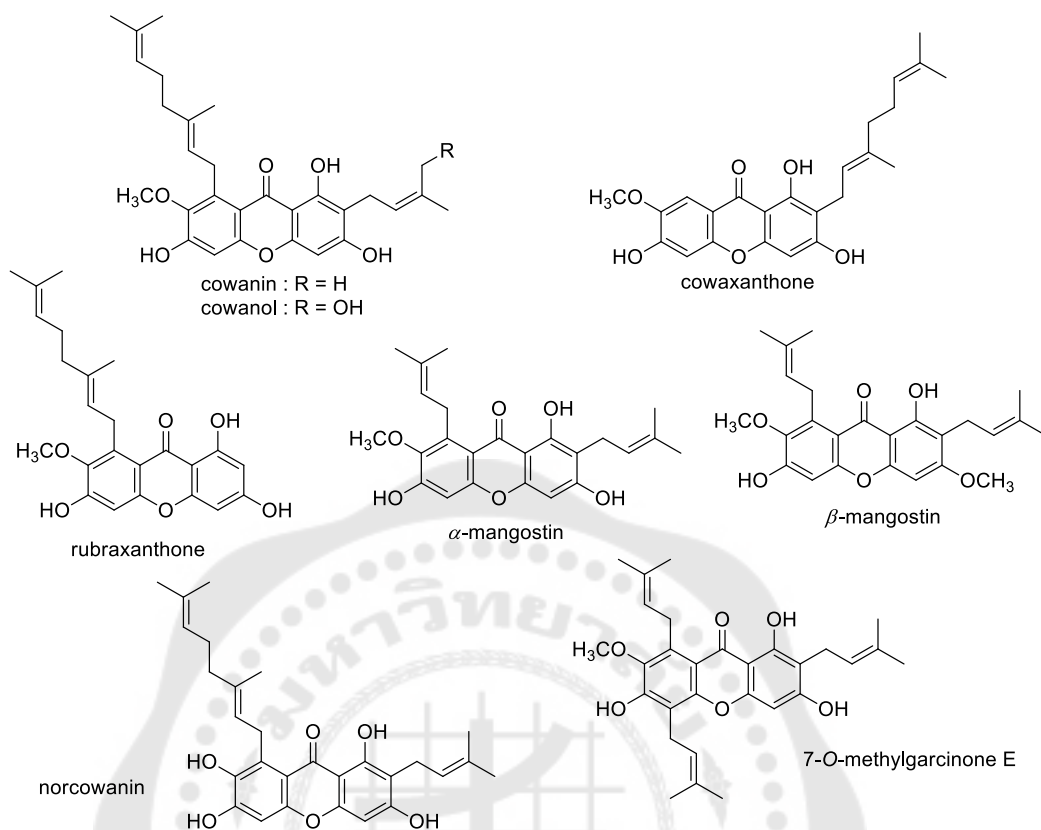


Chemical constituents and their biological activities

In 2003, Ito; et al. reported that eight new xanthenes, fuscaxanthenes A-H, together with eight known xanthenes, namely cowanin, cowanol, cowaxanthone, rubraxanthone, α -mangostin, β -mangostin, norcowanin and 7-O-methylgarcinone E were isolated from the acetone extract of *G. fusca* stem barks collected in Thailand.

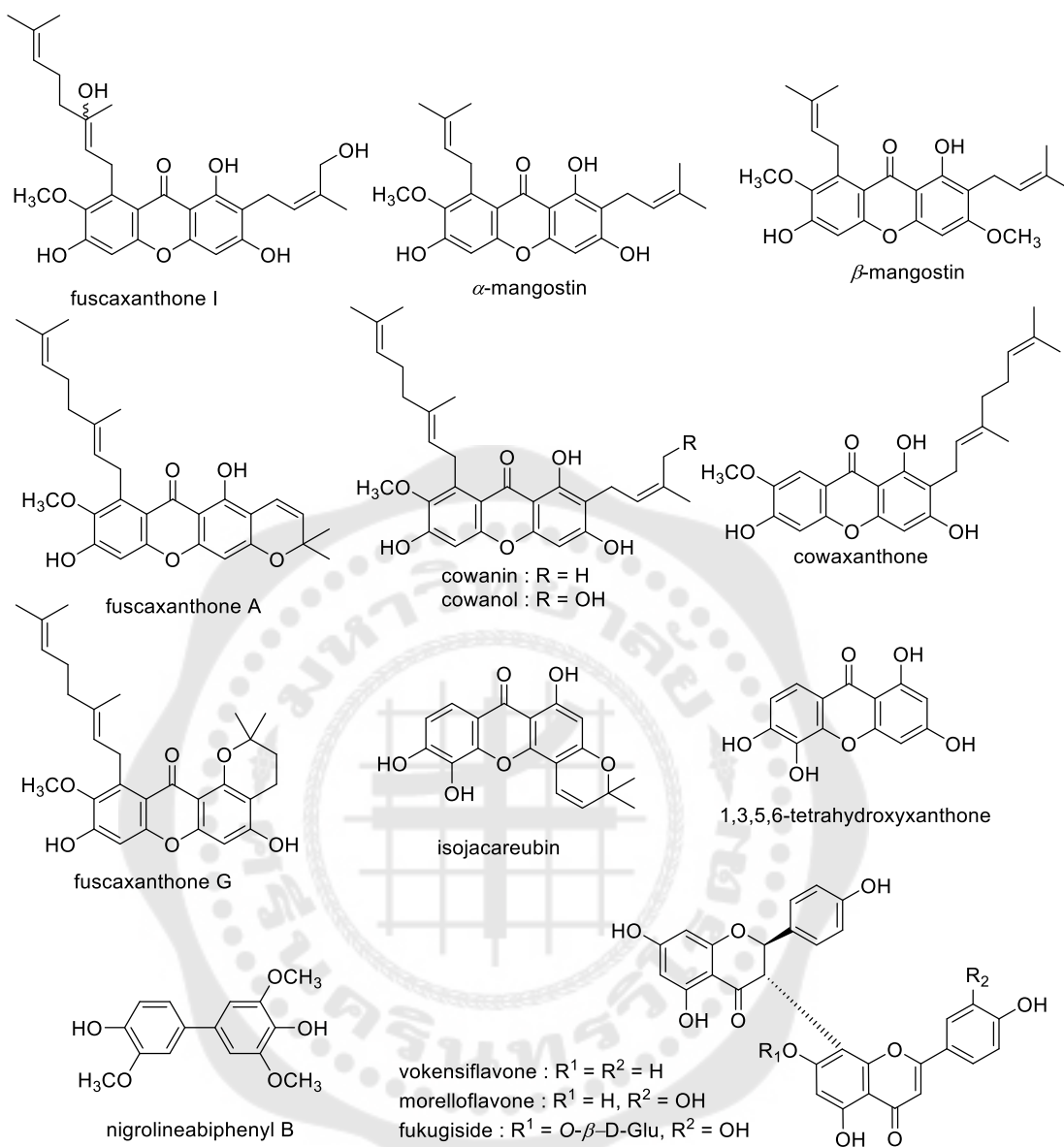
In addition, eight known xanthenes (cowanin, cowanol, cowaxanthone, rubraxanthone, α -mangostin, β -mangostin, norcowanin and 7-O-methylgarcinone E) showed an important role in producing inhibitory effects on Epstein-Barr virus early antigen activation in Raji cells. 7-O-Methylgarcinone displayed the most potent inhibitory activity (Ito, C. et al., 2003).





In 2014, a new geranylated xanthone derivative, fuscaxanthone I, along with nine oxygenated xanthones, β -mangostin, fuscaxanthone A, cowanin, cowaxanthone, α -mangostin, cowanol, isojacareubin, fuscaxanthone G and 1,3,5,6-tetrahydroxyxanthone, a biphenyl, nigrolineabiphenyl B and three bioflavonoids, vokensiflavone, (+)-morelloflavone or fukugetin and (+)-morelloflavone glucoside or (+)-fukugiside were isolated from the roots of *Garcinia fusca* Pierre. Isojacareubin, nigrolineabiphenyl B, 1,3,5,6-tetrahydroxyxanthone, vokensiflavone, morelloflavone and fukugiside were reported from this plant species for the first time.

Two *Helicobacter pylori* strains were used to test the antibacterial activity of the isolated compounds. Cowaxanthone and fukugiside showed stronger antibacterial activities against *H. pylori* DMST strain at MICs 4.6 and 10.8 μM , than that of the standard drug. Isojacareubin showed the most potent activity against *H. pylori* HP40 clinical separate with MIC 23.9 μM , which was approximately 2 times higher than that of the control amoxicillin (Nontakham et al., 2014).



CHAPTER 3

EXPERIMENTAL

Plant materials

The air-dried stem barks of *G. fusca* were collected from Yangtalad District, Kalasin Province, Thailand, in January, 2016. A voucher specimen (Audchara Saenkham001) has been deposited at the Laboratory of Natural Product Research Unit, Chemistry Department of Srinakharinwirot University.

General experimental procedures

Melting points were measured on Griffin melting point apparatus in degree Celsius of temperature.

Optical rotation was recorded on the JASCO-1020 digital polarimeter by using MeOH as a solvent.

UV spectra were obtained on a Jasco V-750 UV-Vis Spectrophotometer in MeOH.

IR spectra were determined by using the Perkin Elmer UATR TWO spectrometer.

^1H - and ^{13}C -NMR spectra were determined on a Bruker AVANCE 300 FT-NMR spectrometer operating at 300 MHz (^1H) and 75 MHz (^{13}C). TMS was calibrated as a reference at 0.00 ppm for both ^1H -NMR and ^{13}C NMR spectra.

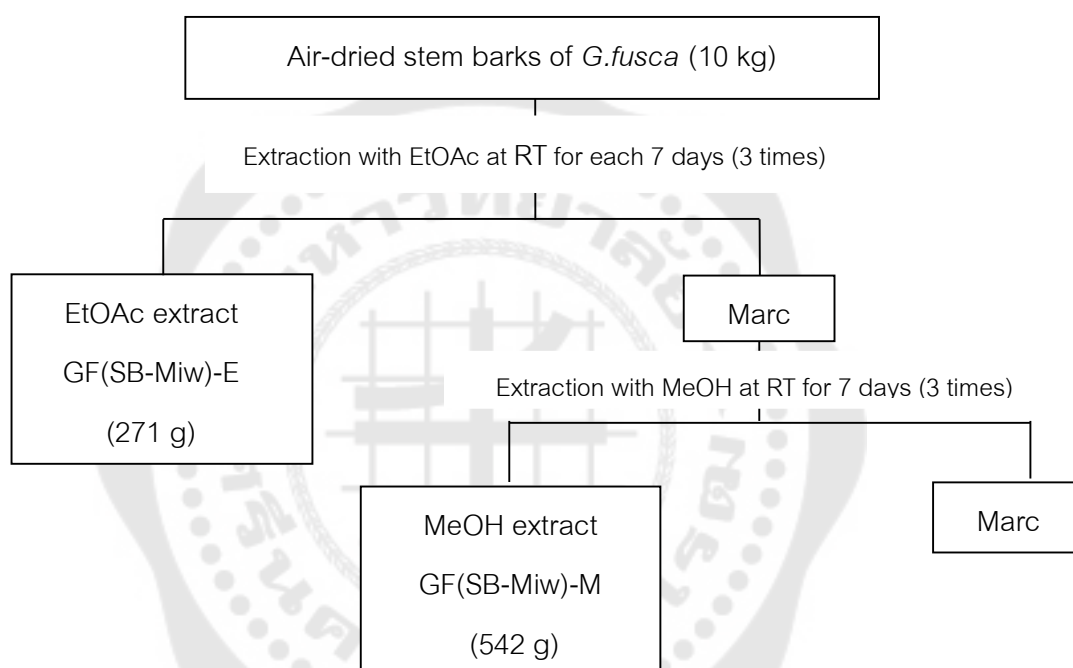
Mass spectra were obtained using a Bruker microTOF mass spectrometer.

Quick column chromatography (QCC) was carried out on silica gel 60 F₂₅₄ (Merck) and column chromatography (CC) was performed on silica gel 60 having either a particle size less than 0.063 mm (Merck 1.07729) or a particle size is 70-230 mesh (SiliCycle, SILIAFLASH G60). Sephadex LH-20 (GE Health care) was also used as an absorbent in size exclusion chromatography.

TLC were monitored using Merck precoated silica gel 60 F254 and were visualized by using UV light (at wavelengths of 254 and 365 nm) and by spraying with anisaldehyde-H₂SO₄ reagent followed by heating.

Extraction of the dried stem barks of *G. fusca*

The air-dried stem barks of *G. fusca* (10 kg) were extracted successively with EtOAc (3 × 20 L) and then with MeOH (3 × 20 L) at room temperature for each one week and the solvents were evaporated to yield the EtOAc (brownish residue, 271 g) and MeOH (reddish brown sticky, 542 g) extracts, respectively. The extraction procedure is shown in Scheme 1.



Scheme 1 Extraction procedure of the stem barks of *G. fusca*

Isolation of compounds from the EtOAc extract of the stem bark of *G. fusca*

A portion of the EtOAc extract (255 g) was fractionated by QCC (ϕ 10 x 15 cm) eluting with a gradient of *n*-hexane–acetone (96:4 to 0:100), acetone–MeOH (95:5–0:100) to afford 13 main fractions (E1–E13). The extraction procedure is shown in Scheme 2.

Isolation of compounds **1** (gartanin), **2** (8 deoxygartanin), **3** (β -mangostin), **4** (Lakoochin A), **5** (cowagarcinone B), **6** (7-*O*-methylgarcinone E), **7** (fuscaxanthone A), and **8** (garbogioliol)

Fraction E3 (15 g) was further chromatographed over silica gel (ϕ 7x 50 cm), eluting with a gradient of *n*-hexane–acetone (96:4 to 0:100), to provide 14 sub-fractions (E3.1–E3.14). Repeated silica gel column (ϕ 2.5x40 cm) of subfraction E3.2 (293 mg) eluting with hexane–acetone (96:2 to 0:100) furnished compound **1** (gartanin, 35 mg), compound **2** (8-deoxygartanin, 13 mg) and compound **3** (β -mangostin, 10 mg) as yellow solids. Compounds **4** (Lakoochin A, 4 mg) and **5** (cowagarcinone B, 42 mg) were successfully yielded from sub-fraction E3.3 (117 mg) using a CC with the same eluent. Repeated CC of sub-fraction E3.5 (629 mg) eluting with hexane–acetone (96:2 to 0:100) gave compound **6** (7-*O*-methylgarcinone E, 110 mg) and compound **7** (fuscaxanthone A, 10 mg) as yellow solids. Sub-fraction E3.5.4 (374.4 mg) was separated to silica gel CC (ϕ 3 x 40 cm) with the same eluent solvent system to obtain compound **8** (garbogioliol, 23 mg) as a pale yellow needle.

Isolation of compound **9** (An oleanane triterpene lactone)

Fraction E4 (388 mg) was purified by a silica gel column (ϕ 3 x 40 cm) eluting with hexane–acetone (95:5) to give compound **9** (An oleanane triterpene lactone or (3 β , 12 α)-3acetyl-12 hydroxy-18 β -olean-28,13 lactone, 4 mg) as a colorless solid.

Isolation of compounds 10 (fuscaxanthone M or 3-O-methylcowanin) and 11 (3-O-methylcowaxanthone)

Fraction E5 (19 g) was purified by silica gel CC (ϕ 5 x 50 cm) eluting with hexane–acetone (96:4 to 0:100) to give 9 sub-fractions (E5.1– E5.9). Two successive re-CC (ϕ 4 x 40 cm) of sub-fraction E5.6 (1.86 g) eluted with hexane–acetone (98:2) to afford compound **10** (fuscaxanthone M or 3-O-methylcowanin, 6 mg) as yellow gum and compound **11** (3-O-methylcowaxanthone, 8 mg) as yellow solids.

Isolation of compound 12 (Rheediaxanthone-A) and compound 13 (fuscaxanthone L or 5-prenyl cowaxanthone)

Fraction E6 (5.2 g) was separated by a silica gel column eluting with hexane–acetone (98:2 to 0:100) to give 14 sub-fractions (E6.1–E6.14). Compound **12** (Rheediaxanthone-A, 6 mg) and compound **13** (fuscaxanthone L or 5-prenyl cowaxanthone, 2 mg) were successfully obtained from sub-fraction E6.2 (55 mg).

Isolation of compound 14 (cowanin) and compound 15 (cowaxanthone)

Fraction E10 (25.6 g) was subjected to silica gel CC (ϕ 5x 50 cm), eluting with a gradient of *n*-hexane–acetone (96:4 to 0:100) to provide 7 sub-fractions (E10.1–E10.7). Sub-fractions E10.1 (15 g) was subjected to silica gel CC (ϕ 5x 50 cm), eluting with *n*-hexane–acetone (96:4 to 0:100) to give 13 subfractions (E10.1.1– E10.1.13). Sub-fractions E10.1.5 was subjected to CC to give the major compound, compound **14** (cowanin, 3.1 g) as yellow solid. Two successive CC over silica gel of sub-fraction E10.1.8 (5.7 g) eluting with *n*-hexane–acetone (ϕ 5x 50 cm) afforded compound **15** (cowaxanthone, 723 mg) as yellow solids.

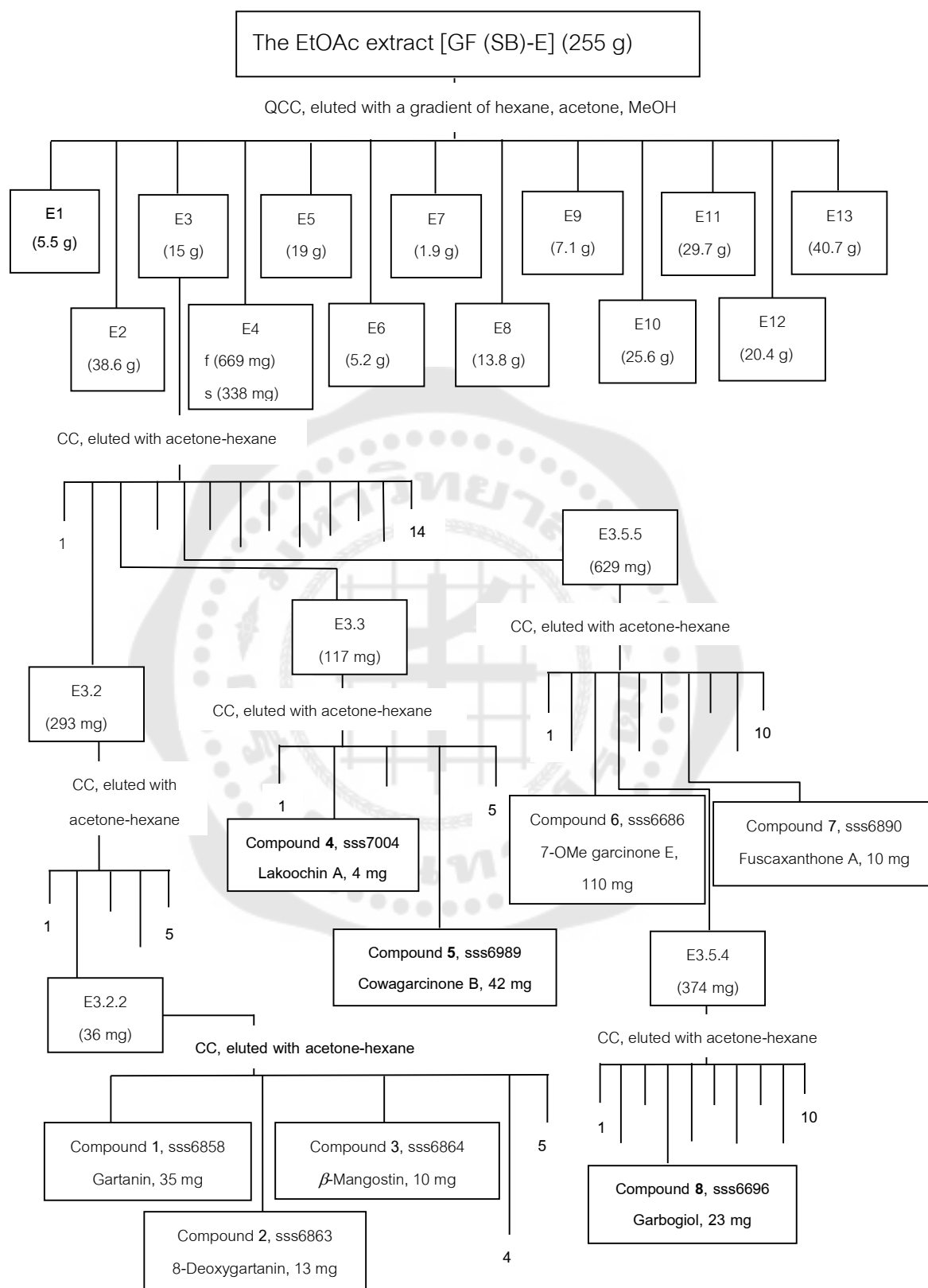
Isolation of compound 16 (cowagarcinone E) and compound 17 (norcowanin), compound 18 (cowanol) and compound 19 (fuscaxanthone N)

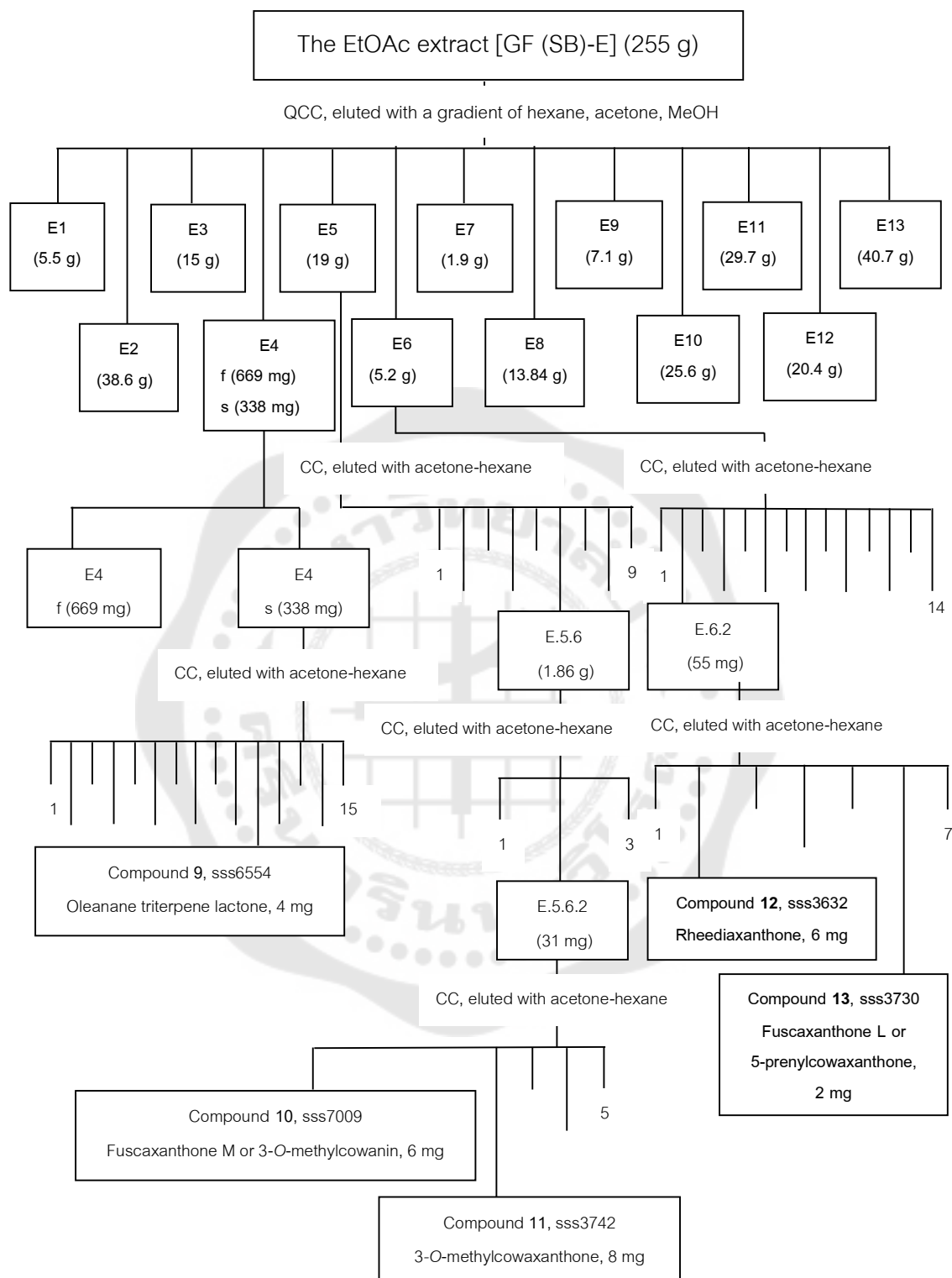
Fraction E11 (29 g) was subjected to silica gel CC (ϕ 5x 50 cm), eluting with a gradient of *n*-hexane–acetone (96:5 to 0:100) to obtain 12 sub-fractions (E11.1–E11.12). Two successive CC over silica gel of sub-fractions E11.6.2 (1.1 g) was separated over

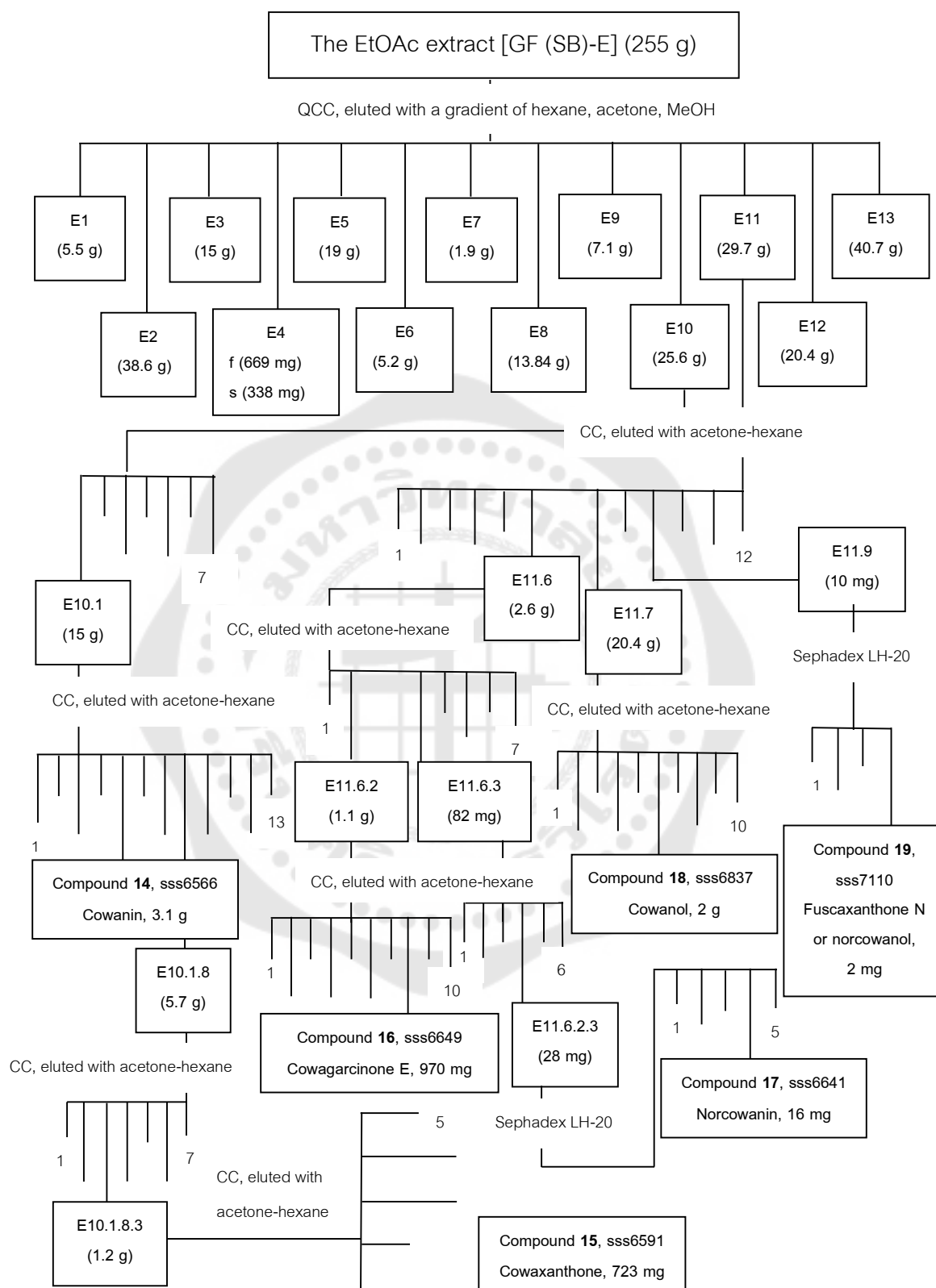
silica gel column (ϕ 5x 50 cm) using of *n*-hexane–acetone (96:5 to 0:100) to afford compound **16** (cowagarcinone E, 970 mg) as yellow solids. The reCC (ϕ 2.5 x 40 cm) of sub-fraction E11.6.3 (82 mg), followed by a Sephadex LH–20 column (MeOH : DCM), a compound **17** (norcowanin) was obtained (16 mg) as a yellow solid. Sub-fractions E11.7 (28 g) was subjected to silica gel CC (ϕ 5x 50 cm), eluting with *n*-hexane–acetone (94:6) to yielded compound **18** (cowanol, 2 g) as yellow solid. Sub-fraction E11.9 (10 mg) was separated by a Sephadex LH-20 column using MeOH to afford compound **19** (fuscaxanthone N, 2.0 mg) as yellow solid.

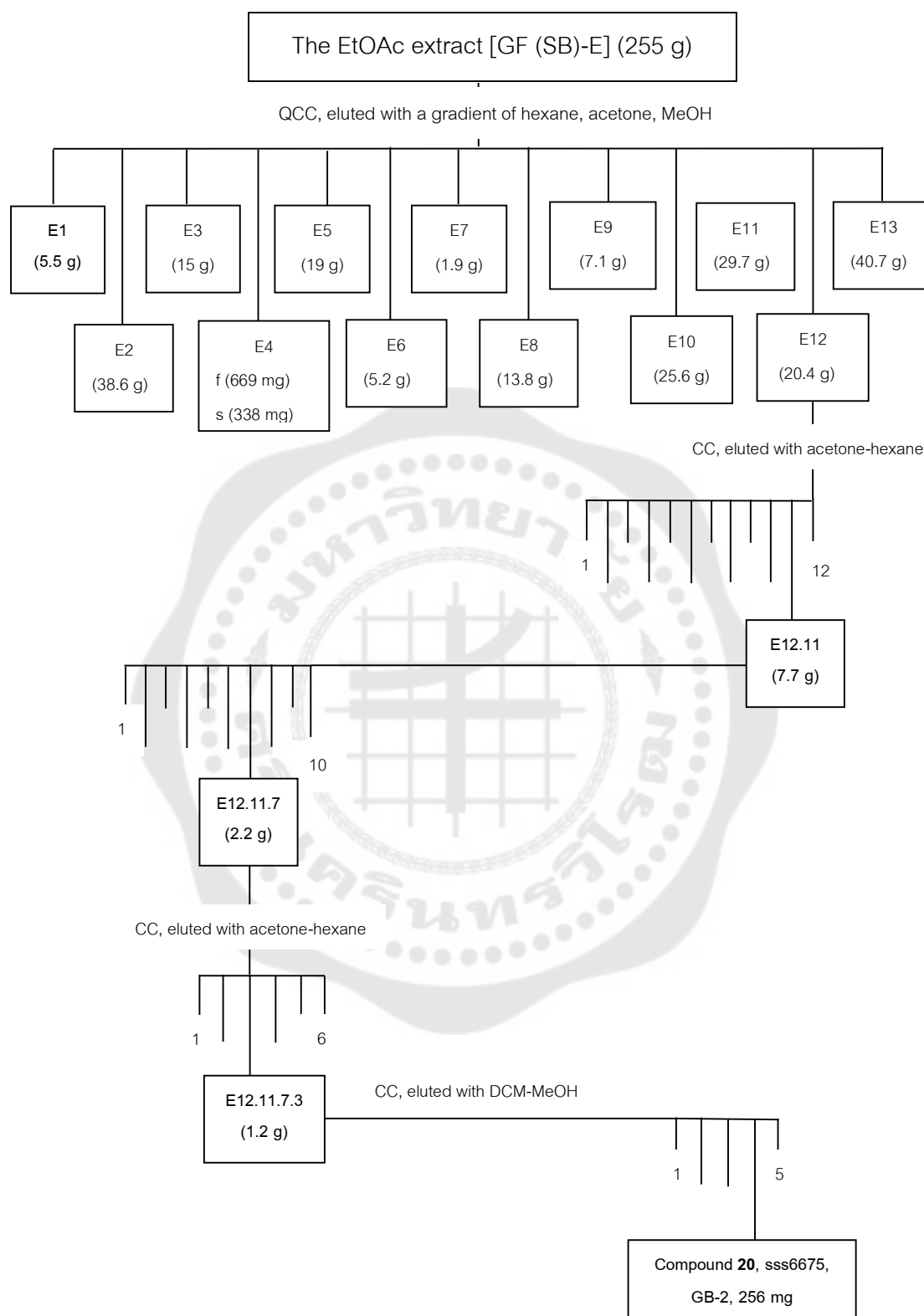
Isolation of compound 20 (GB-2)

Three successive CC over silica gel of fraction E12 (20.4 g) eluting with *n*-hexane–acetone (65:35 to 0:100) to yield 6 sub-fractions (E12.11.7.1–E12.11.7.6) in which compound **2** (GB-2, 256 mg) was furnished as yellow solid from a repeated silica gel column of sub-fraction E12.11.7.6.3, eluting with CH₂Cl₂–MeOH (93:7 to 0:100).

Scheme 2 Extraction procedure of the stem barks of *G. fusca*

Scheme 2 (Continued) Extraction procedure of the stem barks of *G. fusca*

Scheme 2 (Continued) Extraction procedure of the stem barks of *G. fusca*

Scheme 2 (Continued) Extraction procedure of the stem barks of *G. fusca*

Physical and spectral data of compounds 1-20

1. Compound 1 (Gartanin, sss6858)

Yellow solid 35.0 mg, soluble in DCM, acetone, EtOAc and of MeOH

mp : 164-165 °C [lit. 163-165 °C (Parveen & Khan, 1988), 167 °C (Govindachari et al., 1971)]

R_f : 0.42 (30% acetone-hexane)

$^1\text{H-NMR}$: δ ppm, 300 MHz, in CDCl_3 ; Table 10

2. Compound 2 (8-deoxygartanin, sss6863)

Yellow solid 13.1 mg

mp : 163-164 °C [lit. 165.5 °C (Govindachari et al., 1971)]

R_f : 0.42 (30% acetone-hexane)

$^1\text{H-NMR}$: δ ppm, 300 MHz, in CDCl_3 ; Table 10

3. Compound 3 (β -Mangostin, sss6864)

Yellow solid 10 mg

mp : 181-182 °C [lit. 178-179 °C (Gopalakrishnan et al., 1997)]

R_f : 0.42 (30% acetone-hexane)

$^1\text{H-NMR}$: δ ppm, 300 MHz, in CDCl_3 ; Table 8

4. Compound 4 (Lakoochin A, sss7004)

Yellow sticky 4 mg

R_f : 0.68 (30% acetone-hexane)

ESIMS (+ve) m/z (% rel. intensity) (RU-SS693) : 407.4 $[\text{M}+\text{H}]^+$ (100)

$^1\text{H-NMR}$: δ ppm, 300 MHz, in CDCl_3 ; Table 13

$^{13}\text{C-NMR}$: δ ppm, 75 MHz, in CDCl_3 ; Table 13

5. Compound 5 (Cowagarcinone B, sss6989)

Yellow solid 42 mg

mp : 253 °C [lit. 252-253 °C (Mahabusarakam et al., 2005)]

R_f : 0.54 (30% acetone-hexane)

IR ν_{\max} cm^{-1} : 3250, 2914, 2854, 1658, 1607, 1480, 1432, 1288, 1157, 1109, 824, 770

HR-TOFMS (ESI⁺) m/z (RU-SS912) : 379.1156 [M+Na]⁺, calcd 379.1152

¹H-NMR : δ ppm, 300 MHz, in CDCl₃; Table 8

¹³C-NMR : δ ppm, 75 MHz, in CDCl₃; Table 9

6. Compound 6 (7-O-methylgarcinone E, sss6686)

Yellow solid 110 mg

mp : 222-223 °C [lit 220-223 °C (Nguyen et al., 2018)]

R_f : 0.54 (30% acetone-hexane)

IR ν_{\max} cm^{-1} : 3386, 2911, 1641, 1618, 1576, 1486, 1452, 1415, 1279, 1155, 1042, 832, 815, 778

¹H-NMR : δ ppm, 300 MHz, in CDCl₃; Table 8

¹³C-NMR : δ ppm, 75 MHz, in CDCl₃; Table 9

7. Compound 7 (Fuscaxanthone A, sss6669)

Yellow solid 10 mg

mp : 128-130 °C

R_f : 0.54 (30% acetone-hexane)

¹H-NMR : δ ppm, 300 MHz, in CDCl₃; Table 2

8. Compound 8 (Garbogirol, sss6669)

Pale yellow needles 23 mg

mp : 235-237 °C

R_f : 0.46 (30% acetone-hexane)

IR ν_{\max} cm^{-1} : 3587, 3414, 2962, 1667, 1613, 1576, 1491, 1404, 1285, 1223, 1155, 1101, 1056, 998, 810, 745

HR-TOFMS (ESI⁺) m/z (RU-SS926) : 351.0855 [M+Na]⁺, calcd 351.0839

$[\alpha]_{\text{D}}^{26} +79.6$ ($c = 0.11$, MeOH)

¹H-NMR : δ ppm, 300 MHz, in CDCl₃; Table 10

¹³C-NMR : δ ppm, 75 MHz, in CDCl₃; Table 11

9. Compound 9 (An oleanane triterpene lactone, sss6554)

Colorless solid 4 mg

mp : 299-300 °C [lit 295-298 °C (Siewert et al., 2014), 301-303 °C (Katai et al., 1982)]

R_f : 0.54 (30% acetone-hexane)

IR ν_{\max} cm^{-1} : 3526, 3263, 2945, 1735, 1624, 1579, 1514, 1395, 1312, 1244, 1139, 1060, 1029, 983, 904, 870, 830, 774, 680, 623, 558, 487

HR-TOFMS (ESI⁺) m/z (RU-SS915) : 537.3550 [M+Na]⁺, calcd 537.3550

$[\alpha]_{\text{D}}^{26} +25.4$ ($c = 0.30$, CHCl₃) [lit $[\alpha]_{\text{D}} +44.4$ ($c = 0.34$, CHCl₃) (Siewert et al., 2014),

$[\alpha]_{\text{D}}^{25} +37$ ($c = 1$, CHCl₃) (García-Granados et al., 2004)]

¹H-NMR : δ ppm, 300 MHz, in CDCl₃; Table 14

¹³C-NMR : δ ppm, 75 MHz, in CDCl₃; Table 14

10. Compound 10 (Fuscaxanthone M or 3-O-methylcowanin, sss7009)

Yellow gum 6 mg

R_f : 0.50 (30% acetone-hexane)

IR ν_{\max} cm^{-1} : 3403, 2919, 1641 1599, 1460, 1432, 1273, 1155, 1087, 838

UV (MeOH) λ_{\max} (log ϵ) nm: 318 (3.1), 257 (3.2), 244 (3.3)

HR-TOFMS (ESI⁻) m/z (RU-SS917) : 491.2436 [M - H]⁻, calcd 491.2439

¹H-NMR : δ ppm, 300 MHz, in CDCl₃; Table 2

¹³C-NMR : δ ppm, 75 MHz, in CDCl₃; Table 3

11. Compound 11 (3-O-methylcowaxanthone, sss3742)

Yellow solid 8 mg

mp : 223-225 °C

 R_f : 0.48 (30% acetone-hexane)IR ν_{\max} cm^{-1} : 3236, 2916, 1661, 1607, 1480, 1435, 1285, 1155, 1115, 1013, 824, 798, 773HR-TOFMS (ESI⁺) m/z (RU-SS928) : 447.1799 [M+Na]⁺, calcd 447.1778¹H-NMR : δ ppm, 300 MHz, in CDCl₃; Table 6¹³C-NMR : δ ppm, 75 MHz, in CDCl₃; Table 7**12. Compound 12** (Rheediaxanthone-A, sss3632)

Yellow solid 6 mg

mp : 187 °C [lit 187-189 °C (Waterman & Crichton, 1980)]

 R_f : 0.54 (30% acetone-hexane)IR ν_{\max} cm^{-1} : 3346, 2971, 1653, 1636, 1566, 1495, 1478, 1335, 1239, 1197, 1155, 1135, 1107, 892, 819HR-TOFMS (ESI⁺) m/z (RU-SS929) : 415.1153 [M + Na]⁺, calcd 415.1152¹H-NMR : δ ppm, 300 MHz, in CDCl₃; Table 12¹³C-NMR : δ ppm, 75 MHz, in CDCl₃; Table 12**13. Compound 13** (5-Prenyl cowaxanthone or fuscaxanthone L, sss3730)

Yellow solid 2 mg

mp : 187 °C

 R_f : 0.54 (30% acetone-hexane)IR ν_{\max} cm^{-1} : 3522, 2909, 1634, 1610, 1485, 1443, 1287, 1224, 1190, 1159, 773HR-TOFMS (ESI⁺) m/z (RU-SS930) : 501.2262 [M + Na]⁺, calcd 501.2247¹H-NMR : δ ppm, 300 MHz, in CDCl₃; Table 6¹³C-NMR : δ ppm, 75 MHz, in CDCl₃; Table 7

14. Compound 14 (Cowanin, sss6566)

Yellow solid 3.1 g

mp : 138-139 °C [lit 135-137 °C (Nguyen et al., 2018)]

R_f : 0.50 (30% acetone-hexane)

$^1\text{H-NMR}$: δ ppm, 300 MHz, in CDCl_3 ; Table 2

15. Compound 15 (Cowaxanthone, sss6591)

Yellow solid 723 mg

mp : 197 °C [lit 196-197 °C (Nguyen et al., 2018)]

R_f : 0.48 (30% acetone-hexane)

$^1\text{H-NMR}$: δ ppm, 300 MHz, in CDCl_3 ; Table 6

$^{13}\text{C-NMR}$: δ ppm, 75 MHz, in CDCl_3 ; Table 7

16. Compound 16 (Cowagarcinone E, sss6649)

Yellow solid 970 mg

mp : 177 °C

R_f : 0.46 (30% acetone-hexane)

ESIMS (+ve) m/z (% rel. intensity) (RU-SS884) : 559.6 $[\text{M}+\text{Na}]^+$ (100)

$^1\text{H-NMR}$: δ ppm, 300 MHz, in CDCl_3 ; Table 4

$^{13}\text{C-NMR}$: δ ppm, 75 MHz, in CDCl_3 ; Table 5

17. Compound 17 (Norcowanin, sss6641)

Yellow solid 16 mg

mp : 160-161 °C [lit 162-163 °C (na Pattalung et al., 1994)]

R_f : 0.44 (30% acetone-hexane)

IR ν_{max} cm^{-1} : 3411, 2919, 1644, 1613, 1587, 1460, 1282, 1223, 1197, 1172, 1075, 773

ESIMS (+ve) m/z (% rel. intensity) (RU-SS888) : 465.7 $[\text{M}+\text{Na}]^+$ (100)

$^1\text{H-NMR}$: δ ppm, 300 MHz, in CDCl_3 ; Table 2

$^{13}\text{C-NMR}$: δ ppm, 75 MHz, in CDCl_3 ; Table 3

18. Compound 18 (Cowanol, sss6837)

Yellow solid 2 g

R_f : 0.38 (30% acetone-hexane)

mp : 123-124 °C [lit 123-124 °C (Nguyen et al., 2018)]

$^1\text{H-NMR}$: δ ppm, 300 MHz, in CDCl_3 ; Table 4

$^{13}\text{C-NMR}$: δ ppm, 75 MHz, in CDCl_3 ; Table 5

19. Compound 19 (Norcowanol or fuscaxanthone N, sss7110)

Yellow solid 2 mg

R_f : 0.34 (30% acetone-hexane)

IR ν_{max} cm^{-1} : 3360, 2919, 1634, 1613, 1582, 1454, 1279, 1194, 1157, 982, 821, 773

UV (MeOH) λ_{max} (log ϵ) nm: 319 (3.5), 259 (3.8), 244 (3.8)

HR-TOFMS (ESI $^+$) m/z (RU-SS933) : 503.2057 $[\text{M} + \text{Na}]^+$, calcd 503.2040

$^1\text{H-NMR}$: δ ppm, 300 MHz, in CDCl_3 ; Table 4

$^{13}\text{C-NMR}$: δ ppm, 75 MHz, in CDCl_3 ; Table 5

20. Compound 20 (GB-2, sss6675)

Yellow solid 256 mg

mp : 219-220 °C (d) [lit. 220 °C (d) (Jackson et al., 1967)]

R_f : 0.54 (6% MeOH- CH_2Cl_2), an orange coloration with anisaldehyde- H_2SO_4 reagent

IR ν_{max} cm^{-1} : 3192, 2991, 1630, 1593, 1516, 1446, 1358, 1278, 1222, 1156, 1080, 998, 771

$[\alpha]_{\text{D}}^{25.6}$: +9.8 (c = 0.57, MeOH); lit $[\alpha]_{\text{D}}^{25}$ +3 (c = 0.1, MeOH), $[\alpha]_{\text{D}}^{20}$ +3.17 (c = 0.21, MeOH) (Kumar et al., 2004)]

ESIMS ($-ve$) m/z (% rel. intensity) (RU-SS892) : 573.6 $[\text{M}-\text{H}]^-$ (100)

$^1\text{H-NMR}$: δ ppm, 300 MHz, in CDCl_3 ; Table 15

$^{13}\text{C-NMR}$: δ ppm, 75 MHz, in CDCl_3 ; Table 15

Anti-ChE assay

In vitro assay was conducted using the Ellman's method as previously described (Namdaung et al., 2018) employing *Electrophorus electricus* AChE and equine serum BChE (Sigma Aldrich). Briefly, 140 μL of 10 mM sodium phosphate buffer (pH 8.0), 20 μL of AChE (0.2 unit/mL in 10 mM sodium phosphate buffer, pH 8.0) and 20 μL of test compound in % 80 MeOH were mixed and incubated at RT for 10 min. The reaction was started by adding 20 μL of mixture solution of 5 mM DTNB (5,5'-Dithiobis(2-nitrobenzoic acid or Ellman's reagent) in 10 mM sodium phosphate buffer (pH 8.0, containing % 0.1 bovine serum albumin (BSA) and 5 mM acetylthiocholine iodide (ASCh) in 10 mM sodium phosphate buffer, pH 8.0 (5:1). The hydrolysis of ASCh was monitored by the yellow -5 thio--2 nitrobenzoate anion formation as result of the reaction with DTNB and thiocholines (SCh), catalyzed by enzymes at a wavelength of 405 nm and the absorbance was measured after 5 min of incubation at RT. Percentage of inhibition was calculated by comparing the rate of enzymatic hydrolysis of ASCh for the sample to that of the blank (% 80 MeOH in buffer). In the similar manner, BChE inhibition was performed as described for AChE. All the samples were run in triplicate in 96-well microplates and galanthamine was used as a positive control.

CHAPTER 4

RESULTS AND DISCUSSION

The air-dried stem bark of *Garcinia fusca* Pierre was extracted with EtOAc and then with MeOH to obtain the EtOAc and MeOH extracts, respectively. The chemical screening of the extracts was carefully monitored by TLC technique. The EtOAc extract showed the intense green on TLC after treating with an anisaldehyde- H_2SO_4 reagent, indicating the presence of the xanthone content (Pratiwi et al., 2017), whereas the MeOH soluble fraction gave no spot with this reagent. Further chromatographic separations of the former fraction gave three new xanthones, 3-O-methylcowanin (10), 5-prenyl cowaxanthone (13), norcowanol (19), together with fourteen oxygenated xanthones (1-3, 5-8 and 11-12, and 14-18), and the other known metabolites, lakoochin A (4), an oleanane triterpene lactone (9), and GB-2 (20) were isolated from the EtOAc extract. Their chemical structures were characterized using the spectroscopic data analysis (mainly NMR and MS) and comparison of their NMR data with the previous reported data.

TABLES 1 List of isolated compounds from *G. fusca*

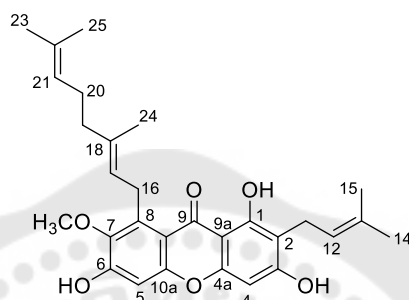
Compounds	NMR code	Weight
1 (Gartanin)	sss6858	35 mg
2 (8-Deoxygartanin)	sss6863	13 mg
3 (β -Mangostin)	sss6864	10 mg
4 (Lakoochin A)	sss7004	4 mg
5 (Cowagarcinone B)	sss6989	42 mg
6 (7-O-methylgarcinone E)	sss6686	110 mg
7 (Fuscaxanthone A)	sss6669	10 mg
8 (Garbogiol)	sss6696	23 mg
9 (An oleanane triterpene lactone)	sss6554	4 mg
10 (New compound or fuscaxanthone M or 3-O-methylcowanin)	sss7009	6 mg
11 (3-O-methylcowaxanthone)	sss3742	8 mg
12 (Rheediaxanthone-A)	sss3632	6 mg
13 (New compound or fuscaxanthone L or 5-prenyl cowaxanthone)	sss3730	2 mg
14 (Cowanin)	sss6566	3.1 g
15 (Cowaxanthone)	sss6591	723 mg
16 (Cowagarcinone E)	sss6649	970 mg
17 (Norcowanin)	sss6641	16 mg
18 (Cowanol)	sss6837	2 g
19 (New compound, fuscaxanthone N or norcowanol)	sss7110	6 mg
20 (GB-2)	sss6675	256 mg

1. Structure determination of the three new xanthenes 10, 13, 19; known xanthenes 1-3, 5-8, 11-12, and 14-18, and other metabolites (4), (9) and (20)

1.1. 1,3,6,7-tetraoxygenated xanthone skeleton

1.1.1. Geranylated xanthenes

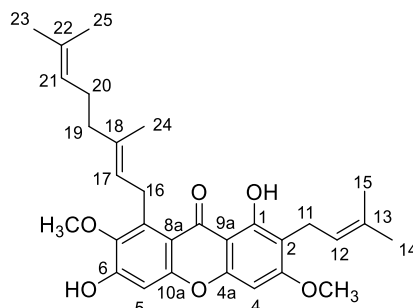
1.1.1.1. Compound 14 (Cowanin)



FIGURES 5 Structure of compound 14

Compound **14** is the major xanthone obtained as a yellow solid. The ^1H - NMR spectra in CDCl_3 (Table 2) exhibited signals of a hydrogen bonded hydroxyl proton at δ_{H} 13.80 (s, 1-OH), a methoxy group at δ_{H} 3.80 (s, 7-OCH₃), and two aromatic protons at δ_{H} 6.30 (s, H-4) and δ_{H} 6.83 (s, H-5). The ^1H - NMR spectra also showed the presence of a prenyl group, which was observed as the following resonances: one olefinic proton at δ_{H} 5.29 (br t, $J = 7.0$ Hz, H-12), methylene protons at δ_{H} 3.46 (d, $J = 7.0$ Hz, H-11), and two allylic methyl groups at δ_{H} 1.83 (s, H-14) and 1.85 (s, H-15). In addition, the presence of a geranyl moiety was also indicated by the remaining signals consisting of: a doublet of methylene protons H-16 (δ_{H} 4.10, $J = 6.1$ Hz); two broad triplets of the olefinic protons H-17 (δ_{H} 5.25) and H-21 (δ_{H} 5.02); two multiplets of the methylene protons H-19 and H-20 at δ_{H} 2.03 (4H); and three singlets of methyl groups H-23, H-24 and H-25 at δ_{H} 1.59, 1.85 and 1.53, respectively. Based on comparison of the patterns of NMR spectrum (Nguyen et al., 2018) and chromatography with those of the authentic cowanin in several solvent systems, the structure of compound **14** was surely identified as cowanin.

1.1.1.2. Compound 10 (Fuscaxanthone M or 3-O-methylcowanin)



FIGURES 6 Structure of compound 10

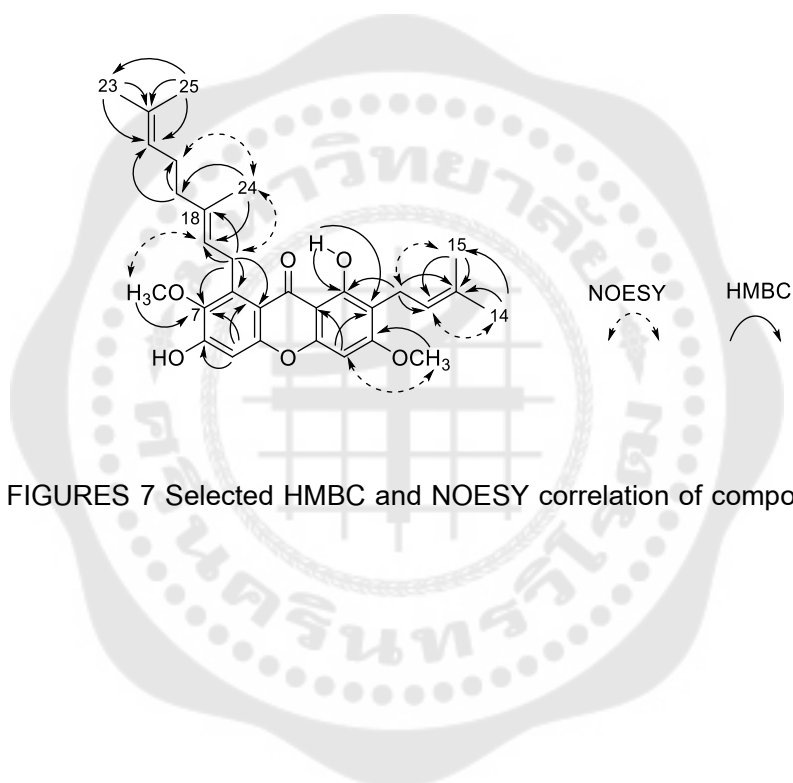
Compound **10** was isolated as a yellow gum and its IR spectrum showed the presence of OH stretching frequency at 3403 cm^{-1} and a conjugated carbonyl moiety at 1641 cm^{-1} . The UV absorption spectra exhibited a xanthone chromophore at λ_{max} 318, 257, and 244 nm (Nontakham et al., 2014). The molecular formula was found to be $\text{C}_{30}\text{H}_{36}\text{O}_6$, which was retrieved from the HR-ESI-TOFMS ion at m/z 491.2436 $[\text{M} - \text{H}]^-$ (calcd. For $\text{C}_{30}\text{H}_{35}\text{O}_6$, 491.2439).

The ^1H -NMR spectrum showed the signals for a chelated hydroxyl group [δ_{H} 13.44 (1H, s, 1-OH)], two isolated aromatic protons at δ_{H} 6.84 and 6.34 (each 1H, each s, H-5 and H-4), a 3-methylbut-2-enyl group, a geranyl group, and two methoxyl singlets (δ_{H} 3.91 and 3.81, each 3H). The NMR spectra (Table 2 and 3) of **10** are quite similar to those of cowanin (**14**) except there is of an extra methoxyl group in **10**. Carefully comparative interpretation of the ^{13}C -NMR spectra of compound **10** to those of the 6-O-methylcowanin (Ha, Ly Dieu et al., 2009), particularly the shifts of C-2, C-3, and C-4, indicated that the extra methoxyl substituent should be located at C-3.

The HMBC and NOESY spectra (Figure 7) revealed that the methoxyl protons at δ_{H} 3.91 (3-OCH₃) showed connectivities to an oxyquaternary carbon at δ_{C} 163.5 (C-3) and to a lone aromatic protons at δ_{H} 6.34 (H-4), which could be supporting the above conclusion. Additionally, the correlations between another methoxyl singlet at δ_{H} 3.81 and C-7 (δ_{C} 142.6) was observed. The proton H-4 correlates to C-2 (δ_{C} 111.5), C-4a (δ_{C}

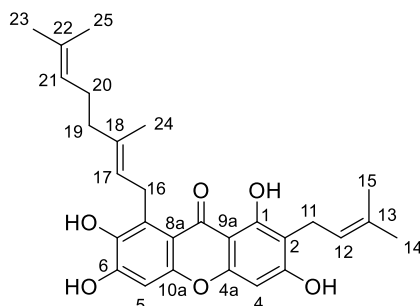
154.3), and C-9a (δ_C 103.8). H-5 (δ_H 6.84) correlates to C-8a (δ_C 112.4), C-7 (δ_C 142.6), and C-6 (δ_C 155.7). The structure of **10** was therefore determined to be (*E*)-1-(3,7-dimethylocta-2,6-dien-1-yl)-3,8-dihydroxy-2,6-dimethoxy-7-(3-methylbut-2-en-1-yl)-9*H*-xanthen-9-one, called 3-*O*-methylcowanin or fuscaxanthone M.

To our knowledge, compound **10** is a new compound having the methyl ether group at position C-3 and belonging to the 1,3,6,7-tetraoxygenated xanthone. It had never been reported before in the previous literatures.



FIGURES 7 Selected HMBC and NOESY correlation of compound **10**

1.1.1.3. Compound 17 (Norcowanin)



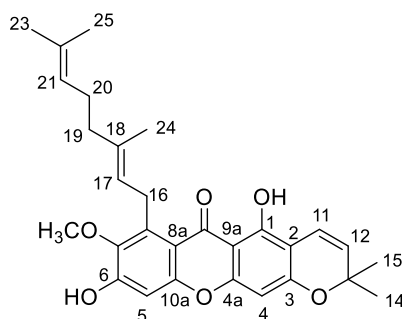
FIGURES 8 Structure of compound 17

Compound **17** was obtained as a yellow solid. The ^1H - and ^{13}C -NMR spectra (Table 2 and 3) showed the characteristics of two aromatic protons [δ_{H} 6.30 (s, H-4), and 6.83 (H-5)], one phenolic hydroxyl proton [δ_{H} 13.78], together with the isoprenyl and isogeranyl moieties. The ^{13}C -NMR and DEPT data revealed there are 28 carbons, which are composed of five methyls, four methylenes, five methines, 14 quaternary carbons including a conjugated carbonyl carbon.

The NMR data showed a similar characteristic to that of cowanin (**14**) except for the absence of a methoxy signal. After comparing the pattern of NMR spectrum of compound **17** with those of 1,3,6,7-tetraoxynated xanthones (na Pattalung et al., 1994), it was found that this compound is norcowanin.

Norcowanin had been found in *G. oblongifolia* (Trinh et al., 2017), *G. pedunculata* (Vo et al., 2015), *G. cowa* (Kaennakam et al., 2015; Laphookhieo et al., 2011; na Pattalung et al., 1994; Siridechakorn et al., 2012) and *G. fusca* (Ito, T. et al., 2013).

1.1.1.4. Compound 7 (Fuscaxanthone A)



FIGURES 9 Structure of compound 7

Compound **7** was chromatographically purified and gave as a yellow solid. The $^1\text{H-NMR}$ spectrum (Table 2) looked almost identical to those of cowanin (**14**) except that the 2,2-dimethylpyran ring was substituted for a prenyl pendant at C-2 and a phenolic hydroxy group at C-3 of compound **14**. This ring is confirmed by two doublet signals of vinylic protons at δ_{H} 6.73 (1H, d, $J = 10.0$, H-11) and 5.56 (1H, d, $J = 10.0$, H-12). Its J -coupling values indicated it is a *cis*-conformation. In addition, two methyl protons of the 2,2-dimethylpyran ring were showed at δ_{H} 1.46 (2x3H, s, H-14 and H-15). The $^1\text{H-NMR}$ spectrum also pointed out that this compound consists of chelated phenolic proton at δ_{H} 13.71 (1-OH), singlet methoxy protons at δ_{H} 3.80 (7-OCH₃), and two singlet signals of two isolated aromatic protons at δ_{H} 6.25 (H-4) and 6.84 (H-5), respectively. The two olefinic protons at δ_{H} 5.03 (1H, t, ca. $J = 6.2$ Hz, H-21) and 5.26 (1H, t, $J = 6.0$ Hz, H-17), three sets of methylene groups at δ_{H} 4.09 (2H, d, $J = 6.0$ Hz, H-16), 2.01 (2H, m, H-19), and 2.03 (2H, m, H-20), and three singlets of vinylic methyl groups at δ_{H} 1.54 (3H, s, H-23), 1.60 (3H, s, H-25), 1.82 (3H, s, H-24) were found and indicated the presence of geranyl pendant.

From the aforementioned NMR spectrum and chromatographic comparison of compound **7** with the authentic of fuscaxanthone A in several solvent systems, it was led to conclude that compound **7** is fuscaxanthone A (Nguyen et al., 2018). This compound is generally isolated from many plants including *Garcinia* such as *G. cowa* (Mahabusarakam et al., 2005), *G. fusca* (Ito, C. et al., 2003).

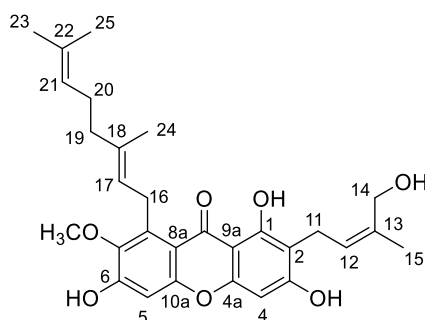
TABLES 2 ^1H -NMR data of cowanin (14), 3-O-methylcowanin (10), norcowanin (17) and fuscaxanthone A (7) in CDCl_3

Position	δ_{H} (mult., J in Hz) CDCl_3			
	Cowanin (14)	3-O-methylcowanin (10)	Norcowanin (17)	Fuscaxanthone A (7)
1-OH	13.80 (1H, s)	13.44 (1H, s)	13.78 (1H, s)	13.71 (1H, s)
2	-	-	-	-
3-OH	6.16 (1H, s)	-	-	-
4	6.30 (1H, s)	6.34 (1H, s)	6.30 (1H, s)	6.25 (1H, s)
4a	-	-	-	-
5	6.83 (1H, s)	6.84 (1H, s)	6.83 (1H, s)	6.84 (1H, s)
6-OH	6.33 (1H, s)	-	-	-
7	-	-	-	-
7-OH	-	-	-	-
8	-	-	-	-
8a	-	-	-	-
9	-	-	-	-
9a	-	-	-	-
10a	-	-	-	-
11	3.46 (2H, d, $J = 7.0$)	3.35 (2H, d, $J = 6.9$)	3.45 (2H, d, $J = 7.1$)	6.73 (1H, d, $J = 10.0$)
12	5.29 (1H, brt, $J = 7.0$)	5.26 (1H, brt, $J = 6.9$)	5.30 (1H, brt, $J = 7.1$)	5.56 (1H, d, $J = 10.0$)
13	-	-	-	-
14	1.83 (3H, s)	1.68 (3H, s)	1.77 (3H, s)	1.46 (3H, s)
15	1.85 (3H, s)	1.80 (3H, s)	1.84 (3H, s)	1.46 (3H, s)
16	4.10 (2H, d, $J = 6.1$)	4.10 (2H, d, $J = 6.2$)	4.37 (2H, d, $J = 6.6$)	4.09 (2H, d, $J = 6.0$)
17	5.25 (1H, brt, $J = 6.1$)	5.22 (2H, brt, $J = 6.2$)	5.30 (1H, brt, $J = 6.6$)	5.26 (1H, t, $J = 6.0$)
18	-	-	-	-
19	2.03 (2H, m)	2.02 (2H, m)	2.11 (2H, m)	2.01 (2H, m)
20	2.03 (2H, m)	2.02 (2H, m)	2.11 (2H, m)	2.03 (2H, m)
21	5.02 (1H, m)	5.02 (1H, brt, $J = 6.0$)	5.03 (1H, brt, $J = 6.6$)	5.03 (1H, t, ca. $J = 6.2$)
22	-	-	-	-
23	1.78 (3H, s)	1.60 (3H, s)	1.67 (3H, s)	1.54 (3H, s)
24	1.85 (3H, s)	1.83 (3H, s)	1.87 (3H, s)	1.82 (3H, s)
25	1.55 (3H, s)	1.55 (3H, s)	1.60 (3H, s)	1.60 (3H, s)
3-OCH ₃	-	3.91 (3H, s)	-	-
7-OCH ₃	3.80 (3H, s)	3.81 (3H, s)	-	3.80 (1H, s)

TABLES 3 ^{13}C -NMR data of cowanin (14), 3-O-methylcowanin (10), norcowanin (17) and fuscaxanthone A (7) in CDCl_3

Position	$\delta_{\text{C}} \text{CDCl}_3$			
	Cowanin (14)	3-O-methylcowanin (10)	Norcowanin (17)	Fuscaxanthone A (7)
1	Not recoded	159.8	160.5	Not recoded
2		111.5	108.3	
3		163.5	161.6	
4		88.8	93.2	
4a		154.3	150.9	
5		101.4	101.2	
6		155.7	155.1	
7		142.6	139.7	
8		137.1	139.5	
8a		112.4	111.4	
9		181.9	182.7	
9a		103.8	103.7	
10a		155.2	153.6	
11		21.3	21.4	
12		122.3	121.3	
13		131.6	132.2	
14		25.8	25.8	
15		17.6	17.7	
16		26.4	25.9	
17		123.2	121.4	
18		135.5	135.7	
19		39.7	39.6	
20		26.5	26.2	
21		124.3	123.7	
22		131.2	127.5	
23		25.5	25.6	
24		16.4	16.3	
25		17.7	17.9	
3-OCH ₃		55.8	-	
7-OCH ₃		62.0	-	

1.1.1.5. Compound 18 (Cowanol)

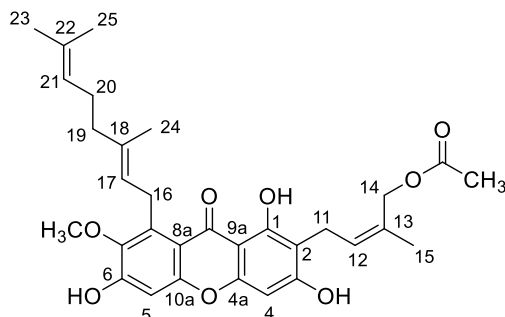


FIGURES 10 Structure of compound 18

Compound **18** was the major xanthone obtained as a yellow solid. The NMR spectra (Table 4 and 5) showed the characteristics of two aromatic protons [δ_{H} 6.24 (s, H-4), and 6.73 (H-5)], one phenolic hydroxyl proton (δ_{H} 13.87), together with the isoprenyl and isogeranyl moieties. The ^{13}C -NMR data revealed there are 29 carbons. These spectra suggested that this compound may belong to xanthone compounds.

From NMR spectra also showed a similar characteristic to those of cowanin (**14**) (Nguyen et al., 2018) except for an extra singlet of vinylic methyl proton at δ_{H} 4.35 (H-14) and δ_{C} 62.59 ppm. Thus, the compound **18** was clearly a derivative of cowanin (**14**) with one of the methyl groups of the prenyl substituent oxidized to a hydroxymethyl group. After comparing the pattern of NMR spectrum of compound **18** with those of 1,3,6,7-tetraoxynated xanthone. It was found that compound **18** and cowanol (Nguyen et al., 2018) have the same spectroscopic features. Thus compound **18** was elucidated as cowanol.

1.1.1.6. Compound 16 (Cowagarcinone E)



FIGURES 11 Structure of compound 16

Compound **16** is a yellow yellow solid. Its ESIMS showed the molecular ion at m/z 559.6 $[M+Na]^+$ (100), which was deduced to the molecular formula $C_{31}H_{36}O_8$.

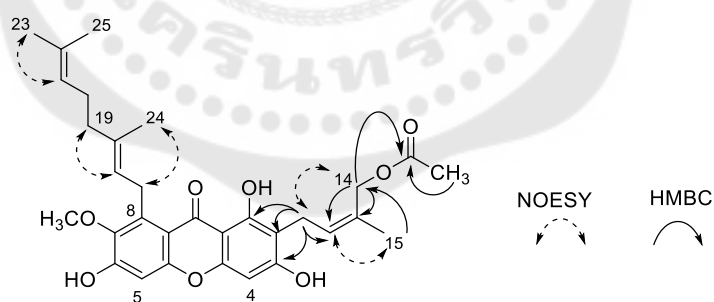
The 1H -NMR spectrum (Table 4) showed the presence of these following signals: a singlet signal of a chelated hydroxy moiety at δ_H 13.79 (s, 1-OH); a singlet resonance of methoxy protons at δ_H 3.80 (s, 7-OCH₃); and two singlet signals of two isolated aromatic protons H-4 and H-5 at δ_H 6.32 and 6.81, respectively. Both alkenyl side chains, a geranyl chain and a prenyl moiety with an acetoxyl group, were also observed. The signals of the geranyl unit appeared as follows: two olefinic protons at δ_H 5.26 (br t, J = 6.0 Hz, H-17) and 5.02 (br t, ca. J = 6.0 Hz, H-21), three sets of methylene groups at δ_H 4.08 (d, J = 6.0 Hz, H-16), 2.02 (m, H-19 and H-20), and three vinylic methyl groups at δ_H 1.82 (H-24), 1.59 (H-23), and 1.54 (H-25). The signals of the isoprenyl pendant appeared in this fashion: an olefinic proton at δ_H 5.42 (br t, J = 6.9 Hz, H-12), methylene protons at δ_H 3.55 (d, J = 6.9 Hz, H-11), and oxymethylene protons δ_H 4.79 (s, H-14). Other signals were assigned to the methyl acetate moiety, which gave the singlet signal at δ_H 2.14 (s, OAc), and a methyl group (C-15) was found at δ_H 1.75 (s, H-15). In fact, the NMR data of **16** was similarly characteristic feature to that of cowanol (**18**) except for the presence of an additional acetoxyl group at C-14 (δ_C 22.7) of **16** in Table 5.

The HMBC spectrum (Figure 12) shows the correlations of benzylic methylene protons H-11/C-1 (δ_C 160.8) with C-2 (δ_C 107.9) and C-3 (δ_C 161.5). This confirmed that

the placement of prenyl group side chain must be at C-2. In addition, the HMBC correlations of methyl acetate protons to the acetyl carbonyl group, oxymethylene proton (H-14) to the acetyl carbonyl group (δ_c 172.2), C-12 (δ_c 128.5), and C-13 (δ_c 131.2), indicating the position of the acetoxyl group. The correlations of benzylic methylene protons H-16/C-7 (δ_c 142.5) to C-8 (δ_c 137.1) and C-8a (δ_c 112.2) also suggested that the geranyl side chain was positioned at C-8 of a parent skeleton.

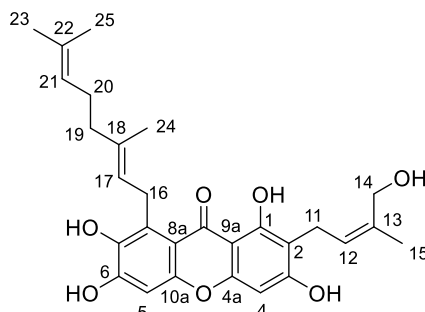
The NOE enhancement of benzylic methylene protons H-11 by irradiation at the oxymethylene protons H-14 and the enhancement of the vinylic methyl protons H-15 by irradiation at the olefinic proton H-12 confirmed the Z configuration of the prenyl moiety (Figure 12).

The structure of compound **16** was also investigated by comparing its spectroscopic data with the literature values of cowagarcinone E, which were reported in a previous publication (Mahabusarakam et al., 2005). It was found that compound **16** and cowagarcinone E have the same spectroscopic features. Thus compound **16** was elucidated as 1,3,6-trihydroxy-7-methoxy-2-(4-acetoxy-3-methyl-2-butenyl)-8-(3,7-dimethyl-2,6-octadienyl)xanthone or cowagarcinone E.



FIGURES 12 Selected HMBC and NOESY correlation of compound **16**

1.1.1.7. Compound 19 (Norcowanol or fuscaxanthone N)



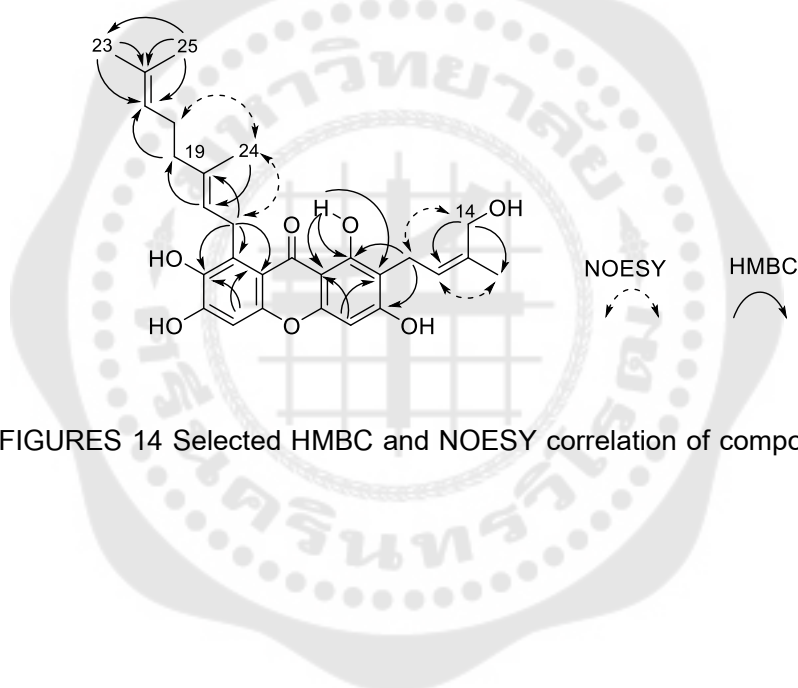
FIGURES 13 Structure of compound 19

Compound **19** was obtained as a yellow amorphous matter and its HRESI-TOFMS exhibited a pseudomolecular ion at m/z 503.2057 $[M+Na]^+$ (calcd. 503.2040) suggesting the molecular formula $C_{26}H_{32}O_7$. Its UV absorption bands at λ_{max} 319, 259, and 244 nm also indicated for a xanthone chromophore.

The 1H - and ^{13}C -NMR data (Table 4 and 5) together with a HSQC experiment disclosed the presence of these characters: a carbonyl moiety, 13 quaternary carbons (six of which are oxygen bearing), five methine protons, five methylene protons, and four methyl groups. These NMR spectroscopic data indicated that the molecule shows the characteristics of xanthone compounds having a tetraoxygenated xanthone skeleton, which bears a geranyl and a modified prenyl moieties. The 1H -NMR spectrum of **19** displayed the signals of a chelated phenolic hydroxyl proton at δ_H 13.94 (1-OH), two isolated aromatic singlets at δ_H 6.77 (H-5) and 6.28 (H-4), and two sets of a geranyl moieties and one prenyl alcohol side chain. The NMR characteristic features of 4-hydroxy-3-methyl-2-butenyl residue was appeared at δ_H 3.51 (2H, d, $J = 7.1$ Hz, H-11), 5.46 (1H, br t, $J = 7.1$ Hz, H-12), 4.33 (2H, s, H-14), and 1.79 (3H, s, H-15). This unit is connected to C-2 (δ_C 108.0) by cross-peaks determined from the H-11 to C-1, C-2, C-3 and C-13 in its HMBC spectrum (Figure 14).

Compound **19** showed the 1H - and ^{13}C -NMR spectra similar to those of cowanol (**18**) except the methoxyl group in **19** is replaced by a hydroxy group in cowanol. From

NOESY spectrum (Figure 14), the geometric isomer of the double bond at C-12/C-13 is *Z*, which was assigned by more significant NOE enhancements marked between those pairs of the CH₂OH (δ_{H} 4.33) / H-11 (δ_{H} 3.51) and of H-12 (δ_{H} 5.46) / H-15 (δ_{H} 1.79). On the other hand, the geometric arrangement of the C-17/C-18 double bond is *E* as evidenced by correlations displayed between the methyl protons (δ_{H} 1.86) of C-24 and the methylene protons (δ_{H} 4.29) of C-16. Thus, **19** was established as 1-((*E*)-3,7-dimethylocta-2,6-dien-1-yl)-2,3,6,8-tetrahydroxy-7-((*Z*)-4-hydroxy-3-methylbut-2-en-1-yl)-9*H*-xanthen-9-one and was named fuscaxanthone N.



FIGURES 14 Selected HMBC and NOESY correlation of compound 19

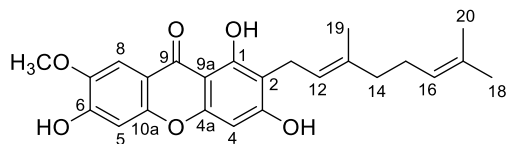
TABLES 4 ^1H -NMR data of cowanin (14), cowanol (19), cowagarcinone E (16) and norcowanol (19) in CDCl_3

Position	δ_{H} (mult., J in Hz) CDCl_3			
	Cowanin (14)	Cowanol (19)	Cowagarcinone E (16)	Norcowanol (19)
1-OH	13.80 (1H, s)	13.87 (1H, s)	13.79 (1H, s)	13.94 (1H, s)
2	-	-	-	-
3-OH	6.16 (1H, s)	-	-	-
4	6.30 (1H, s)	6.24 (1H, s)	6.32 (1H, s)	6.28 (1H, s)
4a	-	-	-	-
5	6.83 (1H, s)	6.73 (1H, s)	6.81 (1H, s)	6.77 (1H, s)
6-OH	6.33 (1H, s)	-	-	-
7	-	-	-	-
7-OH	-	-	-	-
8	-	-	-	-
8a	-	-	-	-
9	-	-	-	-
9a	-	-	-	-
10a	-	-	-	-
11	3.46 (2H, d, $J = 7.0$)	3.47 (2H, d, $J = 7.7$)	3.55 (2H, d, $J = 6.9$)	3.51 (2H, d, $J = 7.1$)
12	5.29 (1H, brt, $J = 7.0$)	5.47 (1H, brt, $J = 7.7$)	5.42 (1H, brt, $J = 6.9$)	5.46 (1H, brt, $J = 7.1$)
13	-	-	-	-
14	1.83 (3H, s)	4.35 (2H, s)	4.79 (3H, s)	4.33 (3H, s)
15	1.85 (3H, s)	1.80 (3H, s)	1.75 (3H, s)	1.79 (3H, s)
16	4.10 (2H, d, $J = 6.1$)	4.05 (2H, d, $J = 5.6$)	4.08 (2H, d, $J = 6.0$)	4.29 (2H, d, $J = 6.6$)
17	5.25 (1H, brt, $J = 6.1$)	5.23 (1H, brt, $J = 5.6$)	5.26 (1H, brt, $J = 6.0$)	5.30 (1H, brt, ca. $J = 6.6$)
18	-	-	-	-
19	2.03 (2H, m)	2.01 (2H, m)	2.02 (2H, m)	2.08 (2H, m)
20	2.03 (2H, m)	2.01 (2H, m)	2.02 (2H, m)	2.08 (2H, m)
21	5.02 (1H, m)	5.01 (1H, brt, ca. $J = 6.7$)	5.02 (1H, brt, ca. $J = 6.1$)	5.04 (1H, brt, ca. $J = 6.7$)
22	-	-	-	-
23	1.78 (3H, s)	1.59 (3H, s)	1.59 (3H, s)	1.65 (3H, s)
24	1.85 (3H, s)	1.81 (3H, s)	1.82 (3H, s)	1.86 (3H, s)
25	1.55 (3H, s)	1.53 (3H, s)	1.54 (3H, s)	1.58 (3H, s)
7-OCH ₃	3.80 (3H, s)	3.87 (1H, s)	3.80 (3H, s)	-
OAce	-	-	2.14 (3H, s)	-

TABLES 5 ^{13}C -NMR data of cowanin (14), cowanol (19), cowagarcinone E (16) and norcowanol (19) in CDCl_3

Position	$\delta_{\text{C}} \text{CDCl}_3$			
	Cowanin (14)	Cowanol (19)	Cowagarcinone E (16)	Norcowanol (19)
1	Not recoded	160.3	160.8	160.3
2		108.0	107.9	108.0
3		161.3	161.5	161.3
4		93.4	93.5	93.4
4a		154.8	154.5	154.8
5		100.9	101.5	100.9
6		150.7	155.8	150.7
7		139.7	142.5	139.7
8		127.5	137.1	127.5
8a		111.1	112.2	111.1
9		182.3	181.9	182.3
9a		103.2	103.4	103.2
10a		153.2	155.2	153.2
11		21.4	20.8	21.4
12		127.0	128.5	127.0
13		133.2	131.2	133.2
14		62.5	21.1	62.5
15		22.7	63.9	22.7
16		25.8	26.4	25.8
17		121.7	123.2	121.7
18		138.2	135.5	138.2
19		39.7	39.6	39.7
20		26.4	26.5	26.4
21		123.9	124.2	123.9
22		131.8	130.4	131.8
23		25.6	25.5	25.6
24		16.3	16.4	16.3
25		17.6	17.6	17.6
7-OCH ₃		-	62.0	-
OAc		-	172.2	-
			20.9	

1.1.1.8. Compound 15 (Cowaxanthone)



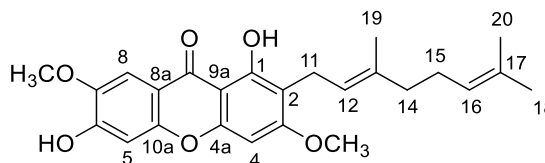
FIGURES 15 Structure of compound 15

Compound **15** was obtained as a yellow solid. The ^1H - and ^{13}C -NMR spectra showed the characteristics of three aromatic protons [δ_{H} 6.39 (s, H-4), 6.94 (H-5), and 7.60 (H-8)], methoxy protons [δ_{H} 4.02 (s, OCH_3 -7)], three phenolic hydroxyl protons [δ_{H} 6.26, 6.36 and 13.41], together with one set of isogeranyl unit. The ^{13}C -NMR and DEPT data contains 24 carbons, which are composed of one methoxy, three methyls, three methylenes, five methines, 12 quaternary carbons including a conjugated carbonyl carbon (Table 6).

Analysis of the ^1H - and ^{13}C -NMR spectroscopic data of **15** indicated that this compound has the 1,3,6,7-tetraoxygenated xanthone as the skeleton, in which the six oxygenated aromatic carbons were observed at δ_{C} 162.2, 160.1, 156.0, 152.6, and 152.5 ppm, respectively.

The comparison of the patterns of NMR spectrum (Nguyen et al., 2018) and TLC with those of the authentic cowaxanthone in several solvent systems, it could conclude that the structure of compound **15** was identified as cowaxanthone.

1.1.1.9. Compound 11 (3-O-methylcowaxanthone)



FIGURES 16 Structure of compound 11

Compound 11 was thoroughly purified and given as yellow amorphous powder. The HRESI-TOFMS exhibited a molecular ion at m/z 447.1799 $[M+Na]^+$ (calcd. 447.1778), suggesting that the molecular formula of this compound is $C_{25}H_{28}O_6$. The IR spectrum clearly showed that the broad hydroxyl stretching peak falls at 3236 cm^{-1} and the stretching vibration of a conjugated carbonyl absorbs at 1661 cm^{-1} .

The $^1\text{H-NMR}$ spectrum of 11 (Table 6) exhibited the signals of a 1,3,6,7-tetraoxygenated xanthone, including of a chelated phenolic hydroxy proton at δ_H 13.04 (s, 1-OH); a geranyl group [δ_H 1.98 and 2.19 (2H each, m, H-14 and H-15), 3.37 (2H, d, $J = 7.0\text{ Hz}$, H-11), 5.07 (1H, t, $J = 6.3\text{ Hz}$, H-16), 5.23 (1H, t, $J = 7.0\text{ Hz}$, H-12), 1.57, 1.64, and 1.80 (3H each, s, H-20, H-18, and H-19)]; and two methoxy groups at δ_H 3.91 (s, 3-OCH₃), and 4.01 (s, 7-OCH₃).

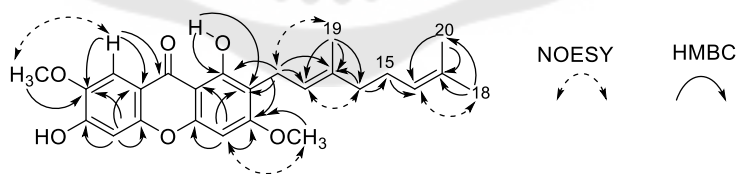
Analysis of its $^{13}\text{C-NMR}$, DEPT, and HMQC spectra (Table 7) revealed this compound contains 25 carbons, consisting of one conjugated carbonyl carbon (δ_C 179.8, C-9), eleven quaternary carbons [δ_C 103.3 (C-9a), 111.7 (C-2), 113.5 (C-8a), 131.1 (C-17), 135.3 (C-13), 144.2 (C-7), 152.3 (C-6), 152.4 (C-10a), 156.1 (C-4a), 159.3 (C-1), and 163.8 (C-3)], five methine carbons [δ_C 89.5 (C-4), 102.4 (C-5), 104.5 (C-8), 122.0 (C-12), and 124.4 (C-16)], two methylene carbons, and two methoxy groups [δ_C 56.4 (7-OCH₃) and 55.8 (3-OCH₃)].

The aromatic proton (δ_H 7.59) was assigned to be H-8 as it was deshielded by a C-9 carbonyl group. By comparing the $^1\text{H-}$ and $^{13}\text{C-NMR}$ spectra of compound 11 with those of the known xanthone, cowaxanthone (15) which was isolated from this plant, it was found that spectra look very similar to each other except there is one extra methoxy

group at a C-3 position of compound **11**. This causes the position of C-4 peak to be shifted. The location of the extra methoxy substituent at C-3 was also confirmed by conducting the HMBC experiment. HMBC spectrum of **11** showed the correlations of the methoxy proton (δ_{H} 3.91) with an oxyquaternary carbon (δ_{C} 163.8) (Figure 17).

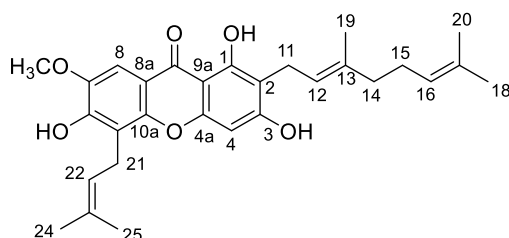
In addition, the NMR spectra of compound **11** looks the same characteristic peaks to those of 3-O-methylcowaxanthone (Na, Z. et al., 2013), which was previously published. By comparison of their ^{13}C -NMR spectra, it was revealed that the methoxy groups should be positioned at C-3 and C-7. The 3-OCH₃ was also confirmed to be adjacent to H-4 by performing the NOESY experiment. On one hand, another methoxy group was assigned to be at C-7 (δ_{C} 144.2) since HMBC spectrum displayed the correlation of methoxy protons at δ_{H} 4.01 with C-7 and the NOE spectrum exhibited the correlations of methoxy protons with H-8 as well. Furthermore, the geranyl pendent was assigned to be bonding with C-2, which was confirmed by the HMBC correlations of benzylic methylene protons H-11 (δ_{H} 3.37) to C-2 (δ_{C} 111.7), C-1 (δ_{C} 159.3), and C-3 (δ_{C} 163.8), respectively. The positions of other protons were also verified as shown in Figure 17.

Therefore, **11** was characterized as 1,6-dihydroxy-6,7-dimethoxy-2-(3,7-dimethyloct-2,6-dienyl) xanthone or 3-O-methylcowaxanthone. To the best of our knowledge, this is the first report, which found 3-O-methylcowaxanthone in *G. fusca*.



FIGURES 17 Selected HMBC and NOESY correlation of compound **11**

1.1.1.10 Compound 13 (5-Prenyl cowaxanthone or fuscaxanthone L)



FIGURES 18 Structure of compound 13

Compound **13** was obtained as a yellow amorphous solid and the molecular formula was deduced to be $C_{29}H_{34}O_6$ on the basis of HR-ESITOFMS data (m/z 501.2262 $[M+Na]^+$, calcd 501.2247). The IR absorptions indicated the presence of hydroxyl (3522 cm^{-1}) and conjugated carbonyl (1634 cm^{-1}) functionalities.

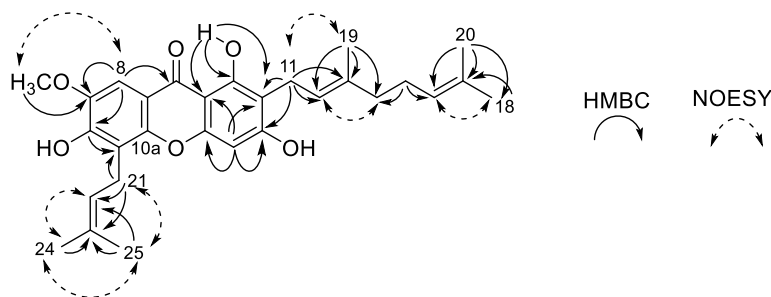
The $^1\text{H-NMR}$ spectrum (Table 6) of compound **13** in CDCl_3 showed the three hydroxyl group at δ_{H} 13.48 (1-OH), δ_{H} 6.43 and 6.28, two aromatic singlets at δ_{H} 7.49 (H-8) and 6.42 (H-4), methoxy protons (δ_{H} 4.00) together with two sets of isoprenyl units. The $^{13}\text{C-NMR}$, DEPT, and HSQC data contains 29 carbons which are composed of one methoxy, five methyls, four methylenes, five methines, and 13 quaternary carbons including a conjugated carbonyl carbon (Table 7).

The HBMBC experiment (Figure 19) showed the correlations of the chelated hydroxyl proton with three aromatic carbons C-1 (δ_{C} 160.0), C-2 (δ_{C} 108.3), and C-9a (δ_{C} 103.0). The aromatic singlet H-4 exhibited correlation with C-3 (δ_{C} 162.1) and the deshielded aromatic signal at δ_{H} 7.49 (H-8) also displayed correlations with the C-7 (δ_{C} 143.9), C-6 (δ_{C} 150.7), and the C-9 carbonyl group (δ_{C} 180.3). In addition, the NOE experiment confirmed the correlation of methoxy protons with H-8 (Figure 19). The presence of two isoprenyl units was also observed. For the geranyl or 3,7-dimethyloct-2,6-dienyl pendant, the following observations were noticed: the two olefinic protons at δ_{H} 5.31 (1H, br t, $J = 7.3\text{ Hz}$, H-12) and 5.06 (1H, br t, $J = 7.3\text{ Hz}$, H-16); three methylenes at δ_{H} 3.49 (2H, d, $J = 7.3\text{ Hz}$, H-11) and 2.10 (4H, m, H-14 and H-15); and three methyl singlets at δ_{H} 1.84 (H-19), 1.68 (H-18) and 1.59 (H-20) including a set of carbon chemical

shifts at δ_{H} 139.8 (C-13), 132.1 (C-17), 123.6 (C-16), 121.2 (C-12), 39.7 (C-14), 26.3 (C-15), 25.6 (C-18), 21.3 (C-11), 17.7 (C-20), and 16.2 (C-19). A prenyl moiety was interpreted from the two methylenes at δ_{H} 3.61 (2H, d, $J = 7.2$ Hz, H-21) and two methyls at δ_{H} 1.68 (3H, s, H-24), and 1.88 (3H, s, H-25), as well as their carbon signals at δ_{C} 132.7 (C-23), 120.8 (C-22), 17.9 (C-24), 22.3 (C-21), 25.6 (C-25).

The HMBC spectrum showed these following interactions: the methylene protons at δ_{H} 3.49 (H-11) versus the C-2, oxygenated C-3, and C-13; the methyl signal at δ_{H} 1.84 (H-19) versus the C-12, C-13, and C-14; another methyl singlet at δ_{H} 1.59 (H-20) versus the C-16, C-17, and C-18. These data suggested that the geranyl residue was resided at C-2 carbon. Moreover, the stereogenic configuration of double bond at C-12/C-13 was assigned as *E*, which was confirmed by strong NOE enhancements showing among those pairs of H-11 / H-19 and of H-12 / H-14 in the NOESY data. Placement of the prenyl unit at C-5 was deduced by the HMBC correlations from the methylene protons (δ_{H} 3.61, H-21) to C-5 and C-22 and from H-22 to C-24 and C-25. The NOESY also pointed out the correlations of H-21 to H-25, H-22 to H-24, H-24 to H-25, respectively (Figure 19).

In fact, the ^1H -NMR spectrum of **13** was similarly characteristic feature to that of cowaxanthone (**15**) except for the presence of an additional 3-methylbut-2-enyl positioning at C-5 of **13**. Thus, the structure of compound **13** was identified as (*E*)-2-(3,7-dimethylocta-2,6-dien-1-yl)-1,3,6-trihydroxy-7-methoxy-5-(3-methylbut-2-en-1-yl)-9*H*-xanthen-9-one or 5-prenylcowaxanthone named fuscaxanthone L. Importantly, **15** is a new compound, which had never been reported before in previous publications.



FIGURES 19 Key HMBC and NOESY correlations for compound **13**

TABLES 6 ^1H -NMR data of cowaxanthone (15), 3-O-cowaxanthone (11) and 5-prenyl cowaxanthone (13) in CDCl_3

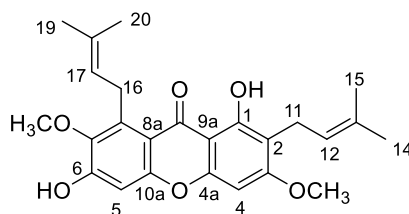
Position	δ_{H} (mult., J in Hz) CDCl_3		
	Cowaxanthone (15)	3-O-cowaxanthone (11)	5-Prenyl cowaxanthone (13)
1-OH	13.41 (1H, s)	13.04 (1H, s)	13.48 (1H, s)
2	-	-	-
3-OH	-	-	6.28 (1H, s)
4	6.39 (1H, s)	6.42 (1H, s)	6.42 (1H, s)
4a	-	-	-
5	6.94 (1H, s)	6.93 (1H, s)	-
6-OH	-	-	6.43 (1H, s)
7	-	-	-
8	7.60 (1H, s)	7.59 (1H, s)	7.49 (1H, s)
8a	-	-	-
9	-	-	-
9a	-	-	-
10a	-	-	-
11	3.49 (2H, d, $J = 7.1$)	3.37 (2H, d, $J = 7.0$)	3.49 (2H, d, $J = 7.3$)
12	5.30 (1H, brt, $J = 7.1$)	5.23 (1H, brt, $J = 7.0$)	5.31 (1H, brt, $J = 7.3$)
13	-	-	-
14	2.10 (2H, m)	1.98 (2H, m)	2.10 (2H, m)
15	2.10 (2H, m)	2.19 (2H, m)	2.10 (2H, m)
16	5.05 (1H, brt, $J = 7.1$)	5.07 (1H, brt, $J = 6.3$)	5.06 (1H, brt, $J = 7.3$)
17	-	-	-
18	1.68 (3H, s)	1.64 (3H, s)	1.68 (3H, s)
19	1.84 (3H, s)	1.80 (3H, s)	1.84 (3H, s)
20	1.60 (3H, s)	1.57 (3H, s)	1.59 (3H, s)
21	-	-	3.61 (2H, d, $J = 7.2$)
22	-	-	5.27 (1H, brt, $J = 7.2$)
23	-	-	-
24	-	-	1.68 (3H, s)
25	-	-	1.88 (3H, s)
3-OCH ₃	-	3.91 (3H, s)	-
7-OCH ₃	4.02 (3H, s)	4.01 (3H, s)	4.00 (3H, s)

TABLES 7 ^{13}C -NMR data of cowaxanthone (15), 3-O-cowaxanthone (11) and 5-prenyl cowaxanthone (13) in CDCl_3

Position	$\delta_{\text{C}} \text{CDCl}_3$		
	Cowaxanthone (15)	3-O-cowaxanthone (11)	5-Prenyl cowaxanthone (13)
1	160.1	159.3	160.0
2	108.6	111.7	108.3
3	162.2	163.8	162.1
4	94.2	89.5	94.1
4a	156.0	156.1	156.0
5	102.5	102.4	115.4
6	152.5	152.3	150.7
7	144.2	144.2	143.9
8	104.5	104.5	101.9
8a	113.3	113.5	112.9
9	179.9	179.8	180.3
9a	103.0	103.3	103.0
10a	152.6	152.4	149.9
11	21.3	21.2	21.3
12	121.1	122.0	121.2
13	139.7	135.3	139.8
14	39.7	39.7	39.7
15	26.3	26.7	26.3
16	123.6	124.4	123.6
17	132.1	131.1	132.1
18	25.6	25.6	25.6
19	16.2	16.1	16.2
20	17.6	17.6	17.7
21	-	-	22.3
22	-	-	120.8
23	-	-	132.7
24	-	-	17.9
25	-	-	25.6
3-OCH ₃	-	55.8	-
7-OCH ₃	56.4	56.4	56.3

1.2. Prenylated xanthenes

1.2.1. Compound 3 (β -mangostin)

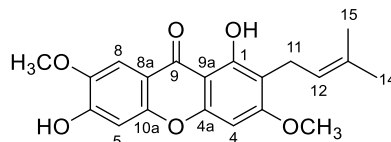


FIGURES 20 Structure of compound 3

Compound **3** was obtained as a yellow solid. The $^1\text{H-NMR}$ spectra (Table 8) indicates the presence of a xanthone skeleton. The chelated phenolic hydroxyl group is at δ_{H} 13.42 and two methoxy groups locate at δ_{H} 3.81 (7- OCH_3) and δ_{H} 3.91 (3- OCH_3), respectively. There are two singlet aromatic protons; H-4 at δ_{H} 6.34 and H-5 at δ_{H} 6.83 ppm. Clearly, there are two prenyl groups [δ_{H} 5.24 (2H, br t); δ_{H} 4.10 (2H, d, $J = 6.0$ Hz); δ_{H} 3.35 (2H, d, $J = 6.8$ Hz); δ_{H} 1.68 (2 x CH_3); δ_{H} 1.80 (CH_3), 1.83 (CH_3)].

The $^1\text{H-NMR}$ spectra of compound **3** is similar to those of α -mangostin except compound **3** has an additional methoxy group at δ_{H} 3.91, which is attached at C-3. By comparing the $^1\text{H-NMR}$ spectrum pattern and chromatographic value to those of the authentic β -mangostin, it was confirmed that compound **3** is β -mangostin, which is commonly found in *Garcinia* plants such as *G. mangostana* (Suksamram et al., 2006), *G. cowa* (Auranwiwat et al., 2014), and *G. fusca* (Ito, C. et al., 2003) and *G. oliver* (Ha, Ly Dieu et al., 2009).

1.2.2. Compound 5 (Cowagarcinone B)



FIGURES 21 Structure of compound 5

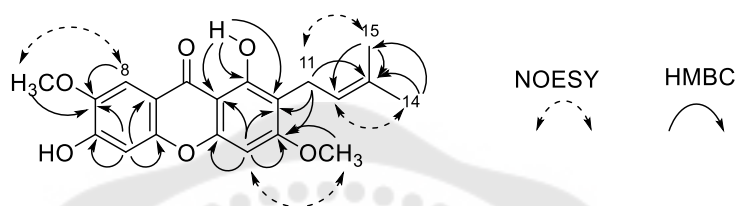
Compound **5** was obtained as a yellow solid. Deducing the basis of HR-ESITOFMS data (m/z 379.1156 $[M+Na]^+$, calcd 379.1152), the molecular formula is $C_{20}H_{20}O_6$. The IR absorptions indicated the presence of hydroxyl (3250 cm^{-1}) and conjugated carbonyl (1658 cm^{-1}) functionalities.

The NMR data of **5** is presented in Table 8. The ^1H -NMR spectra exhibited the signals of a chelated phenolic hydroxyl proton at δ_{H} 13.04 (1-OH, s), two methoxy protons at δ_{H} 3.92 (3-OCH₃, s) and 4.02 (7-OCH₃, s), a phenolic hydroxyl proton at δ_{H} 6.36 (6-OH, s), and three aromatic protons at δ_{H} 6.42 (H-4, s), 6.94 (H-5, s), and 7.61 (H-8, s), respectively. The aromatic proton at δ_{H} 7.61 was assigned to be the H-8, which is deshielded by the C-9 (δ_{C} 179.8) carbonyl group. Lastly, there is a one of isoprenyl unit in this molecule. The NMR data showed a similar characteristic to that of β -mangostin (**3**) except for the absence of the isoprenal signal at C-8.

Irradiation of the methoxy protons at δ_{H} 3.92 gave a NOESY enhancement of the H-4 signal and likewise irradiation of the signal at δ_{H} 4.02 enhanced the H-8 signal, thus the methoxy groups should be at C-3 (δ_{C} 163.8) and C-7 (δ_{C} 144.3), respectively. A prenyl moiety was also present: two methyl group singlets at δ_{H} 1.69 and 1.81, a doublet from methylene protons at δ_{H} 3.37 (2H, d, $J = 6.8\text{ Hz}$, H-11), and an olefinic proton signal at δ_{H} 5.23 (1H, t, $J = 6.8\text{ Hz}$, H-12). The position of the prenyl group was deduced to be at C-2 (δ_{C} 111.7) by the HMBC correlations of H-11 to C-1 (δ_{C} 159.3), C-2, and C-3 (Figure 22).

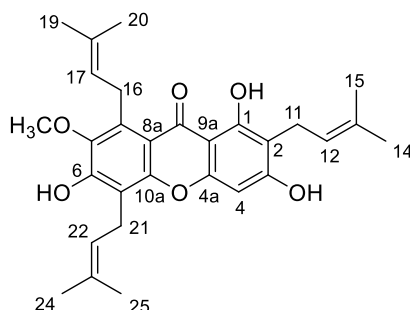
Compound **5** was also confirmed by comparing its spectroscopic data with the literature values (Mahabusarakam et al., 2005). Based on the aforementioned data, it was

concluded that the structure of compound 5 is 1,6-dihydroxy-3,7-dimethoxy-2-(3-methyl-2-butenyl)xanthone or cowagarcinone B. This compound is commonly found in *Garcinia* plants such as *G. mangostana* (Ee, G. C. et al., 2014), *G. cowa* (Mahabusarakam et al., 1986; Siridechakorn et al., 2012), and *G. oliveri* (Ha, L. D. et al., 2012). To the best of our knowledge, compound 5, found in this research, is first reported from *G. fusca*.



FIGURES 22 Selected HMBC and NOESY correlation of compound 5

1.2.3. Compound 6 (7-O-methylgarcinone E)



FIGURES 23 Structure of compound 6

Compound **6** was obtained as a yellow solid. The $^1\text{H-NMR}$ spectra (Table 8) indicated the aromatic proton at δ_{H} 6.33 (s, H-4), three OH signals at δ_{H} 6.13 (br s, 3-OH), 6.42 (s, 6-OH), and 13.85 (s, 1-OH), respectively. In addition, there are three olefinic protons at δ_{H} 5.28 (m, H-12, H-17, and H-22), three of methylene protons at δ_{H} 3.46 (d, $J = 7.5$ Hz, H-11), 3.57 (d, $J = 7.3$ Hz, H-21), and 4.07 (d, $J = 6.5$ Hz, H-16), and six methyl protons at δ_{H} 1.69 (s, H-24), 1.77 (s, H-19), 1.78 (s, H-14), 1.83 (s, H-20), 1.85 (s, H-15), and 1.87 (s, H-25), which confirms the presence of three prenyl pendants in this compound.

Comparatively, the $^1\text{H-NMR}$ spectral feature of compound **6** is similar to that of β -mangostin (**3**), except at C-3 of compound **6** is a hydroxyl group at δ_{H} (6.13s, 3-OH) instead of a methoxy group as shown in compound **3**. Also, there is the extra prenyl side chain at C-5 (δ_{C} 113.9), whereas compound **3** has an aromatic proton (H-5) at this position (Table 9).

On the basis of $^1\text{H-}$ and $^{13}\text{C-NMR}$ data and comparison with those reported in the literature (Nguyen et al., 2018), it would conclude that compound **6** was 1,3,6-trihydroxy-7-methoxy-2,5,8-triprenylxanthone or 7-O-methylgarcinone E. This molecule is commonly found in *Garcinia* plants such as *G. fusca* (Ito, C. et al., 2003), *G. mangostana* (Zhao et al., 2010) and *G. cowa* (Sriyatep et al., 2015).

TABLES 8 ^1H -NMR data of β -mangostin (3), cowagarcinone B (5) and 7-O-methylgarcinone E (6) in CDCl_3

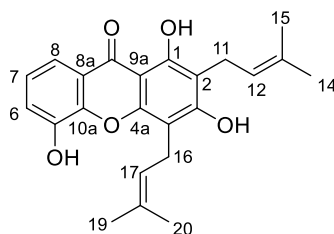
Position	δ_{H} (mult., J in Hz) CDCl_3		
	β -mangostin (3)	cowagarcinone B (5)	7-O-methylgarcinone E (6)
1-OH	13.42 (1H, s)	13.04 (1H, s)	13.85 (1H, s)
2	-	-	-
3-OH	-	-	6.13 (1H, s)
4	6.34 (1H, s)	6.42 (1H, s)	6.33 (1H, s)
4a	-	-	-
5	6.83 (1H, s)	6.94 (1H, s)	-
6-OH	-	6.36 (1H, s)	6.42 (1H, s)
7	-	-	-
8	-	7.61 (1H, s)	-
8a	-	-	-
9	-	-	-
9a	-	-	-
10a	-	-	-
11	3.35 (2H, d, $J = 6.8$)	3.37 (2H, d, $J = 6.8$)	3.46 (2H, d, $J = 7.5$)
12	5.24 (1H, brt, $J = 6.8$)	5.23 (1H, brt, $J = 6.8$)	5.28 (1H, m)
13	-	-	-
14	1.68 (3H, s)	1.69 (3H, s)	1.78 (3H, s)
15	1.83 (3H, s)	1.81 (3H, s)	1.85 (3H, s)
16	4.10 (2H, d, $J = 6.0$)	-	4.07 (2H, d, $J = 6.5$)
17	5.24 (1H, brt, $J = 6.0$)	-	5.28 (1H, m)
18	-	-	-
19	1.68 (3H, s)	-	1.77 (3H, s)
20	1.80 (3H, s)	-	1.83 (3H, s)
21	-	-	3.57 (2H, d, $J = 7.3$)
22	-	-	5.28 (1H, m)
23	-	-	-
24	-	-	1.69 (3H, s)
25	-	-	1.87 (3H, s)
3-OCH ₃	3.91 (3H, s)	3.92 (3H, s)	-
7-OCH ₃	3.81 (3H, s)	4.02 (3H, s)	3.80 (1H, s)

TABLES 9 ^{13}C -NMR data of β -mangostin (3), cowagarcinone B (5) and 7-O-methylgarcinone E (6) in CDCl_3

Position	$\delta_{\text{C}} \text{CDCl}_3$		
	β -mangostin (3)	Cowagarcinone B (5)	7-O-Methylgarcinone E (6)
1	Not recoded	159.3	160.5
2		111.7	108.2
3		163.8	161.5
4		89.5	93.2
4a		156.2	155.0
5		102.4	113.9
6		152.3	152.3
7		144.3	142.2
8		104.60	135.8
8a		113.6	111.9
9		179.8	182.4
9a		103.3	103.5
10a		152.5	153.5
11		21.3	21.4
12		122.2	121.4
13		131.8	133.8
14		25.7	25.7
15		17.7	17.9
16		-	26.3
17		-	123.4
18		-	132.6
19		-	25.8
20		-	18.2
21		-	22.6
22		-	121.1
23		-	131.8
24		-	25.8
25		-	17.9
3-OCH ₃		55.9	-
7-OCH ₃		56.5	62.0

1.3. Other oxynatedxanthone frame work (1,3,5,-trioxynated, 1,3,5,8-tetraoxynated and 1,3,5,6-tetraoxynated xanthenes)

1.3.1. Compound 2 (8-Deoxygartanin)

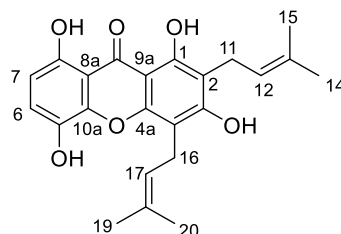


FIGURES 24 Structure of compound 2

The minor compound 2 was obtained as yellow solid. The $^1\text{H-NMR}$ spectrum (Table 10) of compound 2 shows the only one chelated OH at δ_{H} 13.20, indicating the presence of two prenyl (3,3-dimethylallyl) side chains at the same circumstance. The aromatic region confirms the clear ABX pattern of H-6, H-7, and H-8 protons. The H-8 proton appears as a doublet of doublet at δ_{H} 7.78 (1H, dd, $J = 7.9, 1.8$ Hz), while the H-6 displays the doublet of doublet at δ_{H} 7.31 (1H, dd, $J = 7.9, 1.8$ Hz). A proton H-7 emerges as the triplet at δ_{H} 7.24 (1H, t, $J = 7.9, 7.8$ Hz).

From the above results, compound 2 was first reported from this plant species, and the structure of 2 was therefore determined to be 1,3,5-trihydroxy-2,4-bis(3-methylbut-2-en-1-yl)-9*H*-xanthen-9-one and was named 8-deoxygartanin (2) (Govindachari et al., 1971; Ragasa et al., 2010; Suksamrarn et al., 2006).

1.3.2. Compound 1 (Gartanin)



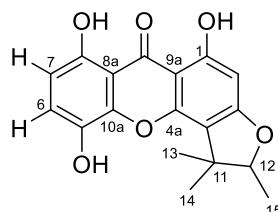
FIGURES 25 Structure of compound 1

Compound 1 was chromatographically purified to yield yellow solid. The $^1\text{H-NMR}$ spectrum (Table 10) shows a similar pattern to that of compound 2 except there is addition of the hydroxyl signal at H-8, indicating that there is addition of the hydroxyl group at C-8.

$^1\text{H-NMR}$ spectrum display discloses the one chelated phenolic hydroxyl moiety [δ_{H} 12.36 (1-OH, s)], two sets of benzylic allylic methylene protons at δ_{H} 3.47 (2H, d, $J = 7.0$ Hz) and 3.53 (2H, d, $J = 6.8$ Hz); olefinic protons at δ_{H} 5.23 (1H, br t, $J = 7.0$ Hz) and 5.28 (1H, br t, $J = 6.8$ Hz). The presence of two aromatic protons doublets at δ_{H} 6.67 (H-7) and 7.23 (H-6) with a large coupling constant ($J = 8.8$ Hz) indicates that the substituents are in the *ortho*. The four allylic methyl singlets are at δ_{H} 1.86, 1.86, 1.79, and 1.76 ppm. Also, there are three aromatic hydroxy proton singlets at δ_{H} 5.15, 6.61, and 11.27 ppm. The hydroxyl group at δ_{H} 12.36 is deshielded because it forms the H-bonding with a carbonyl oxygen. Lastly, there is no methoxyl signal.

Based on the characteristic feature of $^1\text{H-NMR}$ spectrum, it should be noted that compound 1 is surely not 1,3,6,7-tetraoxygenated xanthone since two singlet signals of H-4 and H-5 protons do not show up on the spectrum. In addition, it is found that the $^1\text{H-NMR}$ data of compound 1 looks the same as that of gartanin isolated by our group (Ragasa et al., 2010; Suksamrarn et al., 2006). To the best of our knowledge, it is the first time that compound 1 is found in this plant species and its chemical structure is carefully identified as 1,3,5,8-tetrahydroxy-2,4-bis(3-methylbut-2-en-1-yl)-9*H*-xanthen-9-one or gartanin (1).

1.3.3 Compound 8 (Garbogiol)



FIGURES 26 Structure of compound 8

Compound **8** was obtained as pale yellow needle-shaped solid and its HR-TOFMS exhibited a pseudomolecular ion at m/z 351.0855 $[M+Na]^+$ (calcd. 351.0839) suggesting that the molecular formula is $C_{18}H_{16}O_6$. The IR spectrum showed the presence of hydroxyl groups at 3587 and 3414 cm^{-1} and a conjugated carbonyl at 1667 cm^{-1} . Its positive specific rotation $[\alpha]_D^{26}$ is +79.6 ($c = 0.11$, MeOH). By comparing the specific rotation value with that of garbogiol reported in a previous publication (Linuma et al., 1998; Nguyen et al., 2018), it should be noted that compound **8** is akin to garbogiol.

The 1H -NMR spectrum (Table 10) showed the signals of an isolated aromatic proton [δ_H 6.27 (1H, s, H-2)] and two *ortho*-coupled protons [δ_H 6.68 and 7.24 (1H each, d, $J = 8.8$ Hz, H-7 and H-6, respectively)]. The signals of a 1,1,2-trimethyldihydrofuran ring [δ_H 1.32 (3H, s, H-13), 1.57 (3H, s, H-14), and 1.43 (3H, d, $J = 6.6$ Hz, H-15), and 4.56 (1H, qt, $J = 6.6$ Hz)] were also observed. In addition, the 1H -NMR spectrum indicated that presence of two resonance signals of chelated hydroxyl groups at δ_H 11.34 (1H, s, 8-OH), and 12.31 (1H, s, 1-OH). A non-chelated hydroxyl signal at δ_H 4.81 (1H, br s, 5-OH), were also existed.

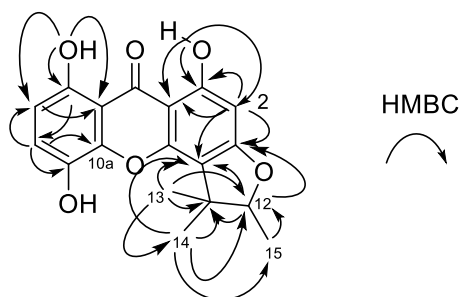
The ^{13}C -NMR, DEPT and HMQC experiments (Table 11) displayed the 18 carbon signals, consisting of three methyl groups at δ_C 14.2 (C-15), 21.6 (C-13), and 26.1 (C-14); four methines at δ_C 90.9 (C-12), 94.6 (C-2), 110.1 (C-7), and 123.3 (C-6); ten quaternary carbons at δ_C 43.6 (C-11), 102.6 (C-9a), 107.3 (C-8a), 113.1 (C-4), 135.4 (C-5), 142.6 (C-10a), 152.2 (C-4a), 154.2 (C-8), 164.1 (C-1), and 167.1 (C-3); and one carbonyl carbon at δ_C 184.1 (C-9).

In the HMBC spectrum (Figure 27), the less shielding of chelated hydroxyl signal at δ_{H} 12.31 (s, 1-OH) correlated with carbon C-1, C-2, C-9, and C-9a. Cross-peaks of the isolated aromatic signal H-2 at δ_{H} 6.27 showed the correlations to C-1, C-3, C-4, C-9, and C-9a. This data confirms that there is this pendant in this compound, in which it is fused at C-3 and C-4 and it forms a five-numbering ring via an ether linkage at C-3. In addition, the two tertiary methyl protons (3H, H-13 and H-14) correlated to C-4 (δ_{C} 113.1), supporting that the 1,1,2-trimethyldihydrofuran ring was condensed with the xanthone A ring at C-3 and C-4 with the latter being oxygenated. The tertiary methyl proton H-13 also correlates with C-4, C-11, C-12, and C-14. Similarly, the correlations between the tertiary methyl group of H-14 with C-4, C-11, C-12, and C-13 were observed. While the methyl proton H-15 showed correlations with C-11, and C-12. Furthermore, the second chelated hydroxyl proton at δ_{H} 11.34 (1H, s, 8-OH) correlated to C-6, C-7, C-8, C-8a, and C-9. This reveals that C-8 was hydroxylated. The two *ortho* coupled protons were therefore attached to C-6 and C-7. Other HMBC correlations supported the structure of the subunit.

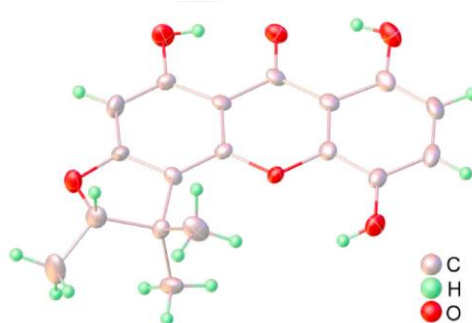
In addition, it should be noted that compound **8** is surely not 1,3,6,7-tetraoxygenated xanthone since two singlet signals of H-4 and H-5 protons do not show up on the spectrum. The xanthone B ring therefore carried the remaining two hydroxyl groups. Compound **8** was also confirmed by comparing its spectroscopic data with the literature values reported in a previous report (Linuma et al., 1998).

The X-ray crystallography had been used to characterize the crystal structure of compound **8**, Its result confirmed a 1,3,5,8-oxygenated xanthone featuring with a furano group attached at C-3/C-4 position. The absolute configuration was defined as 14S (Figure 28). The structure of **8** was therefore deduced as (+) (S)-5,7,10-trihydroxy-1,1,2-trimethyl-1H-furo[2,3-c]xanthen-6(2H)-one or (+) (S)-garbogioli.

In general, (+) (S)-garbogioli is commonly isolated from many plants including *Garcinia* such as *G. fusca* (Nguyen et al., 2018), *G. cambogia* (Tharachand & Mythili, 2013), *G. pedunculata* (Vo et al., 2012), and *G. cantleyana* (Shadid et al., 2007).



FIGURES 27 Selected HMBC correlation of compound 8



FIGURES 28 ORTEP plot of the X-ray crystal structure for compound 8

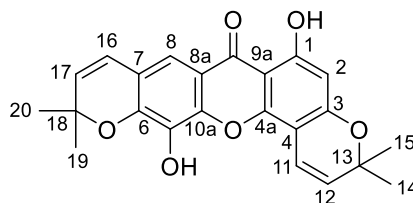
TABLES 10 ^1H -NMR data of 8-deoxygartanin (2), gartanin (1) and garbogiol (8) in CDCl_3

Position	δ_{H} (mult., J in Hz) CDCl_3		
	8-Deoxygartanin (2)	Gartanin (1)	Garbogiol (8)
1-OH	13.20 (1H, s)	12.36 (1H, s)	12.31 (1H, s)
2	-	-	6.27 (1H, s)
3-OH	6.53 (1H, s)	6.61 (1H, s)	-
4	-	-	-
4a	-	-	-
5-OH	5.67 (1H, s)	5.15 (1H, s)	4.81 (1H, brs)
6	7.31 (1H, dd, $J = 7.9, 1.8$)	7.23 (1H, d, $J = 8.8$)	7.24 (1H, d, $J = 8.8$)
7	7.24 (1H, t, $J = 7.9, 7.7$)	6.67 (1H, d, $J = 8.8$)	6.68 (1H, d, $J = 8.8$)
8	7.78 (1H, dd, $J = 7.7, 1.8$)	-	-
8-OH	-	11.27 (1H, s)	11.34 (1H, s)
8a	-	-	-
9	-	-	-
9a	-	-	-
10a	-	-	-
11	3.50 (2H, d, $J = 7.1$)	3.47 (2H, d, $J = 7.0$)	-
12	5.27 (1H, brt, $J = 7.1, 6.4$)	5.23 (1H, brt, $J = 7.0$)	4.56 (1H, qt, $J = 6.6$)
13	-	-	1.32 (3H, s)
14	1.80 (3H, s)	1.86 (3H, s)	1.57 (3H, s)
15	1.87 (3H, s)	1.79 (3H, s)	1.43 (3H, d, $J = 6.6$)
16	3.56 (2H, d, $J = 6.4$)	3.53 (2H, d, $J = 6.8$)	-
17	5.27 (1H, brt, $J = 7.1, 6.4$)	5.28 (1H, brt, $J = 6.8$)	-
18	-	-	-
19	1.88 (3H, s)	1.86 (3H, s)	-
20	1.77 (3H, s)	1.76 (3H, s)	-

TABLES 11 ^{13}C -NMR data of 8-deoxygartanin (2), gartanin (1) and garbogiol (8) in CDCl_3

Position	$\delta_{\text{c}} \text{CDCl}_3$		
	8-Deoxygartanin (2)	Gartanin (1)	Garbogiol (8)
1	Not recoded	Not recoded	164.1
2			94.6
3			167.1
4			113.1
4a			152.2
5			135.4
6			123.3
7			110.1
8			154.2
8a			107.3
9			184.1
9a			102.6
10a			142.6
11			43.6
12			90.9
13			21.6
14			26.1
15			14.2
16			-
17			-
18			-
19			-
20			-

1.3.4. Compound 12 (Rheediaxanthone-A)



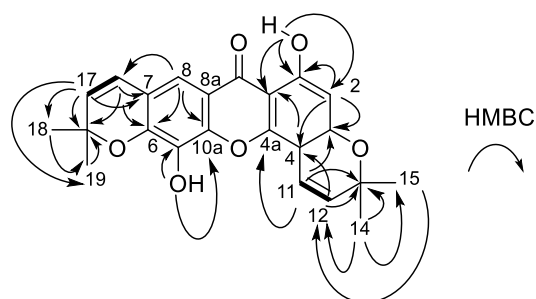
FIGURES 29 Structure of compound 12

Compound 12 is a yellow solid. The molecular formula was found to be $C_{23}H_{20}O_6$ based on HR-TOFMS ion at $(m/z\ 415.1153\ [M + Na]^+)$, calcd. $C_{23}H_{20}O_6Na$, 415.1152). The IR spectrum showed the presence of hydroxyl group at $3346\ cm^{-1}$ and a conjugated carbonyl at $1636\ cm^{-1}$.

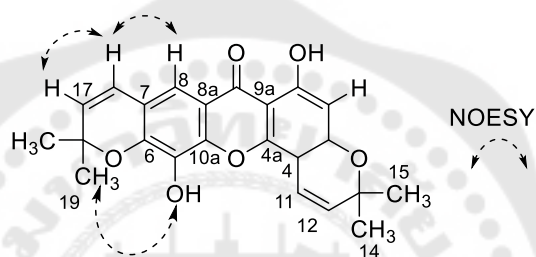
The 1H -NMR spectrum revealed the presence of two hydroxy substituents at δ_H 13.08 (1H, s); two aromatic protons [(H-2, δ_H 6.25, 1H, s), (H-8, δ_H 7.47, 1H, s)]; two 2,2-dimethylpyrano-substituents [(H-11, δ_H 6.88, 1H, d, $J = 6.8\ Hz$), (H-12, δ_H 5.60, 1H, d, $J = 10.0\ Hz$), (H-16, δ_H 6.44, 1H, d, $J = 10.0\ Hz$), (H-17, δ_H 5.73, 1H, d, $J = 10.0\ Hz$)]. The ^{13}C -NMR and HMQC experiments displayed 23 carbon signals, including four methyl groups at δ_C 28.4 (C-14 and C-15) and δ_C 28.2 (C-19 and C-20), six methines at δ_C 99.3 (C-2), 113.4 (C-8), 115.1 (C-11), 121.4 (C-16), 127.1 (C-12) and 130.9 (C-17), twelve quaternary carbons at δ_C 163.0 (C-1), 160.4 (C-3), 151.5 (C-4a), 145.0 (C-10a), 144.7 (C-6), 132.3 (C-5), 114.6 (C-8a), 117.7 (C-7), 103.2 (C-9a), 101.3 (C-4), 78.9 (C-18) and 78.1 (C-13) and one carbonyl carbon at δ_C 180.2 (C-9) (Table 12).

The 1D NMR spectra of this compound could confirm there are two pyrano rings flanking the main xanthone skeleton and its chemical structure is similar to pyranojacareubin, which was isolated from *Calophyllum inophyllum* (Ee, G. C. L. et al., 2009). Also, the chemical constituent of this compound is akin to mesuaferriin B, which was isolated from *Mesua ferrea* (Teh et al., 2011). Both pyranojacareubin and mesuaferriin B have two pyrano rings on their structures.

In addition, the COSY spectrum indicated that the proton signal at δ_{H} 6.88 (H-11, 1H, d, $J = 6.8$ Hz) was coupled to the H-12 at δ_{H} 5.60 (1H, d, $J = 10.0$ Hz). Meanwhile, the proton signal at δ_{H} 6.44 (H-16, 1H, d, $J = 10.0$ Hz) was coupled to the H-17 at δ_{H} 5.73 (1H, d, $J = 10.0$ Hz). HMBC experiment gives correlations between H-11 and C-3 (δ_{C} 160.4), C-4a (δ_{C} 151.5), and C-13 (δ_{C} 78.1), while methine proton H-12 shows the correlations with C-4 (δ_{C} 101.3) and C-13 (δ_{C} 78.1). In addition, the methyl protons of H-14 and H-15 (δ_{H} 1.48, each H-14 and H-15) correlates with C-12 (δ_{C} 127.1) and C-13 (δ_{C} 78.1), respectively. These data supports that the olefinic protons H-11/H-12 show a *cis* conformer since. Moreover, HMBC pulse sequence for long-range heteronuclear correlation also confirm the presence of pyrano rings; one ring is fused at C-3 and C-4 via an ether linkage at C-3 and second pyrano ring is deduced to be bonded to C-6 and C-7, which is supported by evidence of the correlations of H-16 (δ_{H} 6.44) with C-6 (δ_{C} 144.7), C-7 (δ_{C} 117.7), C-8 (δ_{C} 113.4), and C-18 (δ_{C} 78.9). The methine proton H-17 (δ_{H} 5.73) also correlates with C-7 and C-18. Similarly, the correlations between the methyl groups of H-19 and H-20 at δ_{H} 1.53 (each H-19 and H-20) with C-17 (δ_{C} 130.9) and C-18 (δ_{C} 78.9) confirms the presence of this unit, which was fused at C-6 and C-7 with an ether linkage at C-6. Two pyrano rings were therefore assigned to be attached to C-3, C-4 and C-6, C-7 by HMBC correlations between these carbons and a couple of *cis* olefinic hydrogens. In addition, the long-range correlations between the two pair of *cis* olefinic protons H-11, H-12 and H-16, H-17 were confirmed to be adjacent to the quaternary carbon C-13 and C-18, respectively. The hydroxyl proton at δ_{H} 13.08 shows correlations with C-1 (δ_{C} 163.0), C-9a (δ_{C} 103.2), and C-2 (δ_{C} 99.3). The other hydroxyl proton at δ_{H} 5.56 (H-5, s) correlates with C-10a and C-5. The signal of aromatic proton at δ_{H} 6.25 (H-2) gives correlations with C-1 (163.0), C-3 (160.4), and C-4 (101.3). Also, the isolated methine proton at δ_{H} 7.47 (H-8) displays the long-range heteronuclear correlations with C-9 (103.2), C-10a (145.0), and C-6 (144.7) in HMBC spectrum (Figure 30).



FIGURES 30 Key COSY and HMBC correlations for compound 12



FIGURES 31 Key NOESY correlations for compound 12

All spectral and physical data obtained were in close agreement with that recently reported for rheedioxanthone-A, which was isolated from *G. staudtii* (Waterman & Ussain, 1982). Furthermore, this compound was first reported in *Rheedia benthamiana* (Monache et al., 1981) but there are no reports isolating this compound in *G. fusca*. Therefore, to the best of our knowledge, this is the first report finding rheedioxanthone-A in *G. fusca*.

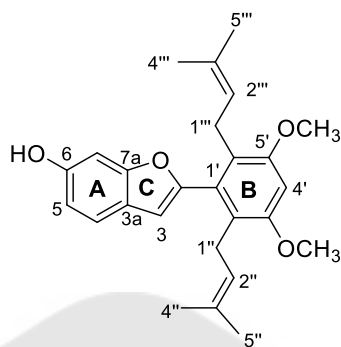
TABLES 12 Comparison ^1H - and ^{13}C -NMR data of compound 12 with rheediaxanthone-A in CDCl_3

Position	δ_{H} (mult., J in Hz) CDCl_3		δ_{C}	
	Rheediaxanthone-A ^a	Compound 12	Rheediaxanthone-A ^a	Compound 12
1-OH	13.20 (1H, s)	13.08 (1H, s)		163.0
2	6.16 (1H, s)	6.25 (1H, s)		99.3
3				160.4
4	6.30 (1H, s)			101.3
4a				151.5
5-OH		5.56 (1H, s)		132.3
6				144.7
7				117.7
8	7.45 (1H, s)	7.47 (1H, s)		113.4
8a				114.6
9				108.2
9a				103.2
10a				145.0
11	6.94 (1H, d, $J = 8.0$)	6.88 (1H, d, $J = 10.0$)		115.1
12	5.73 (1H, d, $J = 8.0$)	5.60 (1H, d, $J = 10.0$)		127.1
13				78.1
14	1.46 (3H, s)	1.48 (3H, s)		28.2
15	1.46 (3H, s)	1.48 (3H, s)		28.2
16	6.54 (1H, d, $J = 8.0$)	6.44 (1H, d, $J = 10.0$)		121.4
17	5.90 (1H, d, $J = 8.0$)	5.73 (1H, d, $J = 10.0$)		130.9
18				78.9
19	1.49 (3H, s)	1.53 (3H, s)		28.4
20	1.49 (3H, s)	1.53 (3H, s)		28.4

^a (Waterman & Ussain, 1982)

1.3. Non-xanthones

1.3.1. Compound 4 (Lakoochin A)



FIGURES 32 Structure of compound 4

Compound **4** was isolated as yellow viscous liquid. Its ESIMS showed the molecular ion at m/z 407.4 $[M+H]^+$ (100), corresponding to the molecular formula $C_{26}H_{30}O_4$.

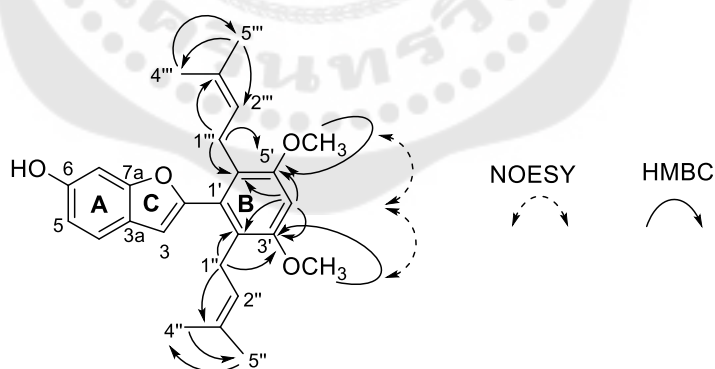
The 1H -NMR spectrum (Table 13) of **4** revealed the ABX aromatic spin system in which aromatic protons appear at δ_H 6.78 (dd, $J = 8.3, 2.2$ Hz), δ_H 6.96 (d, $J = 2.2$ Hz), and δ_H 7.39 (d, $J = 8.3$ Hz), including two downfield singlets at δ_H 6.53 and 6.60, two methyl ether singlets (both resonances at δ_H 3.86), respectively. From the observation, there are two sets of signals for a prenyl group at δ_H 5.07 (2x2H, br t, $J = 6.8$ Hz, H-2'' and H-2'''), 3.13 (2x2H, d, $J = 6.8$ Hz, H-1'' and H-1'''), 1.64 (2x3H, s, H-4'' and H-5'''), 1.38 (2x3H, s, H-5'' and H-4''').

Analysis of the 1D and 2D NMR spectral data of **4** also disclosed the symmetrical methoxy and prenyl groups. There are 26 carbons, which are composed of four methyls, two methylenes, seven methines, and 13 quaternary carbons.

Interpretation of the HMBC spectrum (Figure 33) of **4** indicates that two prenyl and methoxy groups are located on an aromatic ring, which is the formation of a symmetrical ring B. The HMBC correlations are seen from an aromatic proton H-4' to C-2', C-3', C-5', and C-6'; the methoxy protons 5'-OCH₃ to C-5' and 3'-OCH₃ to C-3'; the methylene protons H-1''' to C-5', C-6', C-3''; H-1'' to C-2', C-3', C-3''.

In NOESY spectrum, the location of two methoxy groups is also confirmed by intense cross-peak of a OCH_3 group to aromatic proton H-4'. Furthermore, the correlations of aromatic protons (H-4') to two oxygenated quaternary carbons (C-3' and C-5') at δ_{C} 156.3 and to two quaternary carbon (C-2' and C-6') at δ_{C} 122.5 were displayed on the HMBC spectrum. A gross structure for **4** was established by analysis of the HMBC spectral data. The HMBC correlations pointed out that H-3 is correlated with C-1' and C-2' (Figure 33). Therefore, it may conclude that the symmetrical unit **B** is linked with an ring **C** through a C2—C1' bond.

Compound **4** was also confirmed by comparing its spectroscopic data with the literature values reported in a previous publications (Namdaung et al., 2018; Puntumchai et al., 2004). The structure of the compound is thus concluded as 2-(3,5-dimethoxy-2,6-bis(3-methylbut-2-enyl)phenyl)benzofuran-6-ol or lakoochin A, which is an isoprenylated derivative of 2-arylbenzofuran. Generally, the arylbenzofuran compounds, such as garcinol (Niwa et al., 1993) and garcifurans A-B (Niwa et al., 1994) have been found in *G. Kola* but there are no reports found these compounds in *G. fusca* before. This is therefore the first report to isolate the lakoochin A (**4**) from *G. fusca*.



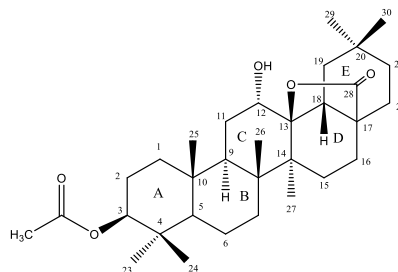
FIGURES 33 Selected HMBC and NOESY correlation of compound **4**

TABLES 13 Comparison ^1H - and ^{13}C -NMR data of compound 4 with lakoochin A in CDCl_3

Position	δ_{H} (mult., J in Hz) CDCl_3		δ_{C}	
	Lakoochin A ^a	Compound 4	Lakoochin A ^a	Compound 4
2			153.0	153.0
3	6.54 (1H, s)	6.53 (1H, s)	106.2	106.2
3a			123.2	122.5
4	7.40 (1H, d, $J = 8.1$)	7.39 (1H, d, $J = 8.3$)	120.8	120.8
5	6.78 (1H, dd, $J = 8.1, 2.1$)	6.78 (1H, dd, $J = 8.3, 2.2$)	111.5	111.5
6			153.3	153.2
7	6.97 (1H, d, $J = 2.1$)	6.96 (1H, d, $J = 2.2$)	98.2	98.2
7a			155.6	155.6
1'			131.8	131.8
2'			122.5	122.5
3'			156.3	156.3
4'	6.61 (1H, s)	6.60 (1H, s)	97.3	97.3
5'			156.3	156.3
6'			122.5	122.5
1''	3.15 (2H, d, $J = 6.8$)	3.13 (2H, d, $J = 6.8$)	26.5	26.5
2''	5.05 (1H, br t, $J = 7.1$)	5.07 (1H, br t, $J = 6.8$)	123.6	123.5
3''			130.3	130.3
4''	1.58 (3H, s)	1.58 (3H, s)	25.7	25.7
5''	1.39 (3H, s)	1.38 (3H, s)	17.6	17.6
1'''	3.15 (2H, d, $J = 6.8$)	3.13 (2H, d, $J = 6.8$)	26.5	26.5
2'''	5.05 (1H, d, $J = 7.1$)	5.07 (1H, br t, $J = 6.8$)	123.6	123.5
3'''			130.3	130.3
4'''	1.39 (3H, s)	1.38 (3H, s)	17.6	17.6
5'''	1.58 (3H, s)	1.58 (3H, s)	25.7	25.7
3'-OCH ₃	3.87 (3H, s)	3.86 (3H, s)	55.9	55.9
5'-OCH ₃	3.87 (3H, s)	3.86 (3H, s)	55.9	55.9

^a (Puntumchai et al., 2004)

1.3.2 Compound 9 (An oleanane triterpene lactone)



FIGURES 34 Structure of compound 9

The minor compound **9** was obtained as a colorless solid. It gave a violet spot with anisaldehyde reagent on TLC, indicating it was a triterpene. Its HR-TOFMS showed a pseudomolecular ion at m/z 537.3550 [$M + Na$] $^+$, calcd. $C_{32}H_{50}O_5Na$, 537.3550). The IR absorption bands for free hydroxyl (3526 cm^{-1}) and carbonyl ester (1735 cm^{-1}) functions were observed.

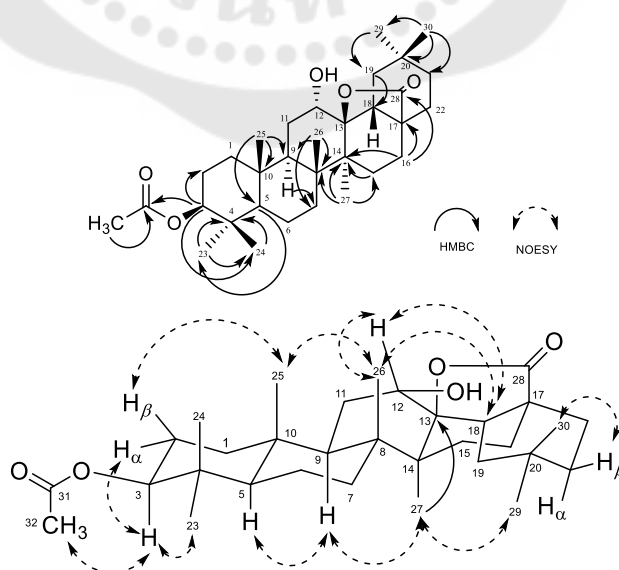
The ^1H -NMR spectrum of **9** revealed the seven methyl signals at δ_{H} 0.85, 0.87, 0.90 (6H), 0.98, 1.14, and 1.30, and an acetate group at δ_{H} 2.05 ppm. The pattern of the methyl protons is similar to that of oleanane-type triterpene with an acetate group. The comparison of the ^1H - and ^{13}C -NMR spectra pattern of this compound with oleanolic acid, they were similarity except there was no alkene protons signals at C-11 and C-12 in **9**.

The ^{13}C -NMR, DEPT and HMQC spectra of **9** exhibited 32 carbons, consisting of seven methyls at δ_{C} 16.3 (C-25), 16.4 (C-24), 18.5 (C-26), 18.5 (C-27), 23.8 (C-30), 27.9 (C-23), and 33.2 (C-29), ten methylenes, five methines [two of which were carbon bearing oxygen at δ_{C} 76.3 (C-12) and 80.7 (C-3)], and nine quaternary carbons [including a C-O (δ_{C} 90.5, C-13) and two carbonyls at δ_{C} 179.9 (C-28) and 171.0 (C-31)].

The doublet of doublet signal at δ_{H} 4.49, dd, $J = 6.6, 9.4\text{ Hz}$ (H-3) in **9** was showed down field shift when compared with the signal of H-3 (δ_{H} 4.14, m) in oleanolic acid structure (Hichri et al., 2003), together with the HMBC correlations shown between H-3 and C-2 (δ_{C} 23.5) and C-31 (δ_{C} 171.0), suggesting the acetate moiety was located at C-3. Furthermore, a broad signal at δ_{H} 3.88 (1H), δ_{C} 76.3 (C-12), a hydroxyl moiety, showed

the COSY interactions between the H-12/H-11 α and H-12/H-11 β . From the DEPT and ^{13}C -NMR spectra, there observed a quaternary carbon at δ_{C} 90.5 (C-13), tertiary carbon of lactone carbonyl at δ_{C} 179.0 (C-28), in addition, HMBC displayed between H-27/C-13, H-16/C-17 and H-16/C-28 supported an oxycarbonyl-lacton-group placed at carbons 13 and 17.

The NOESY experiment was also conducted in order to confirm the stereochemistry of this compound. NOESY spectrum showed the enhancements between H-3 to H-2, H-23, and H-32, which indicated the H α -2 and H β -3 orientation in the oleanane nucleus. Also the ring junctions are *trans* as displayed in NOESY experiment (Froelich et al., 2017; García-Granados et al., 2004; Hichri et al., 2003; Poehland et al., 1987; Siewert et al., 2014) as shown in Figure 35, and in accordance with its biosynthetic pathway (Pollier & Goossens, 2012). Its optical rotation is $[\alpha]_{\text{D}}^{26} +25.4$ ($c = 0.30$, CHCl_3) [lit $[\alpha]_{\text{D}}^{25} +37$ ($c = 1$, CHCl_3) (García-Granados et al., 2004) and $[\alpha]_{\text{D}} +44.4$ ($c = 0.34$, CHCl_3) (Siewert et al., 2014)]. Therefore, it could concluded that the structure of the compound 9 is 3 β -acetoxy-12 α -hydroxyoleanan-28,13 β -olide or (3 β , 12 α) 3-acetyl-12-hydroxy-18 β -olean-28-oic acid 28,13-lactone. This compound was also found in *Rhodomystrotopnentosa* (Siewert et al., 2014) and *Pieris japonica* D. Don (Katai et al., 1982). Thus, this research is the first time to report the oleanane triterpene lactone (9) in this plant.



FIGURES 35 HMBC and NOESY correlations of compound 9

TABLES 14 Comparison ^1H - and ^{13}C -NMR data of compound 9 with 3β -acetoxy- 12α -hydroxyoleanan-28, 13β -olide in CDCl_3

Position	δ_{H} (mult., J in Hz) CDCl_3		δ_{C}	
	A ^a	Compound 9	A ^a	Compound 9
1a	1.76-1.66 (1H, m)	1.74, 1.07 (2H, m)	38.6	38.5
1b	1.13-1.09 (1H, m)			
2	1.69-1.52 (2H, m)	1.74, 1.64 (2H, m)	23.6	23.5
3	4.48 (1H, dd, $J = 5.7, 9.7$)	4.49 (1H, dd, $J = 6.6, 9.4$)	80.9	80.7
4			37.9	37.8
5	0.85-0.86 (1H, m)	0.86 (1H, m)	55.4	55.3
6	1.69-1.52 (2H, m)	1.50, 1.42 (2H, m)	17.7	17.6
7a	2.06-1.84 (1H, m)	1.55, 1.36 (2H, m)	34.0	34.1
7b	1.69-1.52 (1H, m)			
8			42.4	42.0
9	1.69-1.52 (1H, m)	1.62 (1H, m)	44.6	44.5
10			36.4	36.3
11	1.69-1.52 (2H, m)	1.68, 1.36 (2H, m)	27.6	27.4
12	3.87 (1H, dd, $J = 2.5$)	3.88 (1H, brs)	76.3	76.3
12-OH				
13			90.7	90.5
14			42.1	42.3
15a	1.84 (1H, ddd, $J = 6.1, 13.5, 13.5$)	1.60, 1.11 (2H, m)	28.1	28.0
15b	1.29-1.22 (1H, m)			
16a	2.13 (1H, ddd, $J = 5.8, 13.3, 13.3$)	2.14 (1H, ddd, $J = 13.2, 7.5, 5.7$)	21.3	21.3
16b	1.29-1.22 (1H, m)	1.24 (1H, m)		
17			44.8	44.7
18	2.06-1.84 (1H, m)	2.02 (1H, m)	51.2	51.1
19	2.06-1.84 (2H, m)	1.96 (1H, m)	39.4	39.3
		1.50 (1H, m)		
20			31.6	31.5
21	1.29-1.22 (2H, m)	1.28, 1.18 (2H, m)	34.2	33.9
22a	1.69-1.52 (1H, m)	1.91, 1.47 (2H, m)	28.9	28.8
22b	1.69-1.52 (1H, m)			

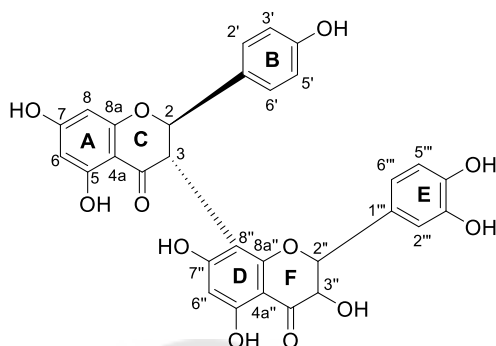
TABLES 14 (Continued)

Position	δ_{H} (mult., J in Hz) CDCl_3		δ_{C}	
	Oleanane triterpene lactone ^a	Compound 9	Oleanane triterpene lactone ^a	Compound 9
23	0.86 (3H, s)	0.87 (3H, s)	28.0	27.9
24	0.84 (3H, s)	0.85 (3H, s)	16.5	16.4
25	0.89 (3H, s)	0.90 (3H, s)	16.5	16.3
26	1.13 (3H, s)	1.14 (3H, s)	18.6	18.5
27	1.29 (3H, s)	1.30 (3H, s)	18.7	18.5
28			180.1	179.9
29	0.89 (3H, s)	0.90 (3H, s)	33.3	33.2
30	0.97 (3H, s)	0.98 (3H, s)	24.0	23.8
31			171.2	171.0
32	2.04 (3H, s)	2.05 (3H, s)	21.4	21.2

A = 3 β -acetoxy-12 α -hydroxyoleanan-28,13 β -olide

^a (García-Granados et al., 2004)

1.3.3 Compound 20 (GB-2)



FIGURES 36 Structure of compound 20

Compound **20** was obtained as a yellow solid. The molecular formula was $C_{30}H_{22}O_{12}$ as deduced from ESIMS ($[M-H]^-$ at m/z 573.6). The IR spectrum showed the presence of hydroxy groups at 3192 cm^{-1} and conjugated carbonyl groups at 1630 cm^{-1} . In general, biflavonoid shows two sets of signals in its ^1H - and ^{13}C -NMR spectra due to its rotameric behavior (atropisomerism). Its ^1H - and ^{13}C -NMR and DEPT spectra (Table 15) showed signals of respective pairs (relative ratio; 1:1.23) indicating the presence of a biflavonoid skeleton. The ^{13}C -NMR and DEPT spectra displayed 30 major signals attributable to 14 methines and 16 quaternary carbons.

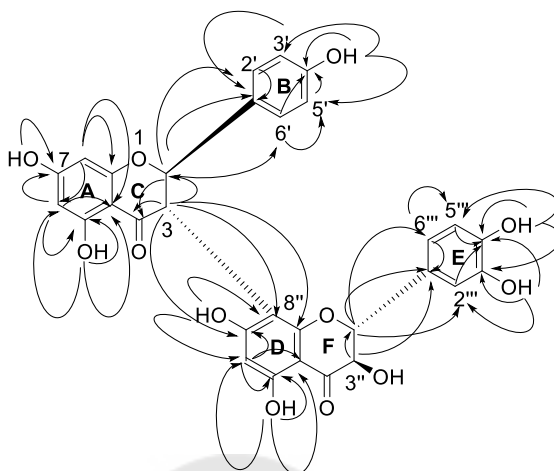
The methine doublets of H-2 exhibited at δ_{H} 5.65 (1H, $J = 12.2\text{ Hz}$) and H-3 at δ_{H} 4.45 (1H, $J = 12.2\text{ Hz}$) on ring C including COSY correlations observed between of protons indicating the presence of flavanone unit. In same manner the doublets signal of H-2'' [δ_{H} 4.86 (d, $J = 11.6\text{ Hz}$)] and H-3'' [δ_{H} 3.95 (dd, $J = 11.6$ and 6.0 Hz)] of ring F, as well as COSY correlations suggesting a dihydroflavanol group (Figure 37). By COSY and HMBC correlations the aromatic protons (ring A) at δ_{H} 5.87 (1H, d, $J = 2.1\text{ Hz}$) and 5.87 (1H, d, $J = 2.1\text{ Hz}$) were assigned to be located at C-6 and C-8 moiety. Broad doublets of aromatic *ortho* coupled protons (ring B) appearing at H-2' (δ_{H} 7.10) and H-6' (δ_{H} 7.08), H-3' (δ_{H} 6.75), and H-5' (δ_{H} 6.58) with J coupling constant of 8.3 Hz were attributed to the position C-2', C-6', C-3', and C-5', respectively, confirming the flavonone part. Two doublets at δ_{H} 4.86 (d, $J = 11.6\text{ Hz}$, H-2'') and 3.95 (dd, $J = 11.6$ and 6.0 Hz , H-3'') indicate

the presence of a dihydroflavonol moiety (ring F). Aromatic protons (ring D) emerging at H-6'' (δ_{H} 5.91) was attributed to the position C-6'. The aromatic protons at δ_{H} 6.83 (br s, H-2''') and two doublets aromatic *ortho* coupled protons (ring E) at δ_{H} 6.79 (d, H-5'''), δ_{H} 6.64 (d, H-6''') with *J* coupling constant of 8.1 Hz were attributed to the position C-2''', C-5''', and C-6''', respectively. Furthermore, the two singlet signals of chelated hydroxy at δ_{H} 12.12 and 11.83 and five signals of phenolic hydroxy showed singlets and broad singlets at δ_{H} 9.60, 8.99, 8.97, 5.81, and 5.73, respectively.

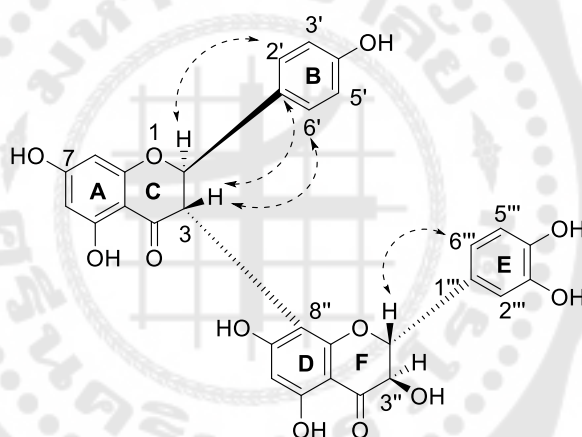
Connections among rings A, B, and C of flavanone subgroup were provided by analysis of its HMBC and NOESY spectra (Figures 37 and 38). The NOESY correlations were observed for methine proton at δ_{H} 5.65 (H-2) to H-2' (δ_{H} 7.10) and δ_{H} 4.45 (H-3) to H-6' (δ_{H} 7.08) of aromatic protons together with HMBC correlations of H-2 to C-2' (δ_{C} 129.0), the correlations of H-3 to C-6' (δ_{C} 129.0) in HMBC spectra, indicating that ring B connects to ring C. The HMBC correlation of chelated hydroxy OH-5 (δ_{H} 12.12) and H-6 (δ_{H} 5.87) to C-4a (δ_{C} 101.3), and H-8 (δ_{H} 5.87) to C-8a (δ_{C} 162.8) confirmed that ring A connected to ring C.

Linkage between rings D, E, and F of dihydroflavonol subgroup were confirmed by analysis of its HMBC and NOESY spectra. The correlations of H-2'' (δ_{H} 4.86) to C-2''' (δ_{C} 115.3) and C-6''' (δ_{C} 119.0), and H-3'' (δ_{H} 3.95) to C-2''' (δ_{C} 115.3) and C-1''' (δ_{C} 127.8) in HMBC spectra together with NOESY correlations of H-6''' (δ_{H} 6.64) to H-2'' (δ_{H} 4.86), indicates that ring E links to ring F. The HMBC correlations deduced from H-6'' (δ_{H} 5.91) and chelated hydroxy 5''-OH (δ_{H} 11.83) to C-4a'' (δ_{C} 99.7) confirms that ring D connects to ring F.

Furthermore, HMBC interactions seen between the methine protons at δ_{H} 4.45 (H-3) to C-8'' (δ_{C} 101.0), C-8a'' (δ_{C} 160.1) and C-7'' (δ_{C} 164.5), Figures 37 and 38, support the linkage of the flavanone and dihydroflavonol units via C-3 and C-8''.



FIGURES 37 Key HMBC correlations for compound 20



FIGURES 38 Key NOESY correlations for compound 20

The relative configurations at the two stereogenic centers of flavanone (C-2 and C-3) and dihydroflavonol (C-2'' and C-3'') moieties are *trans*-diaxial were confirmed by ^1H -NMR coupling constants ($J = 12.2$ Hz) (Messi et al., 2012). The dextrorotatory optical rotation of compound **20** is $[\alpha]_{\text{D}}^{25.6} = +9.8$, [lit $[\alpha]_{\text{D}}^{25} = +3$ ($c = 0.1$, MeOH) (Messi et al., 2012), $[\alpha]_{\text{D}}^{20} = +3.17$ ($c = 0.57$, MeOH) (Kumar et al., 2004)]. The structure of compound **20** is thus assigned to be (+) GB-2.

GB-2 was found in *Garcinia* plants such as *G. kola* (Adaramoye et al., 2005; Farombi et al., 2000; Iwu, M. M. et al., 1990; Iwu, W. M. et al., 1987; Kabangu et al., 1987; Okoko, Tebekeme 2009; Okoko, T., 2009; Okoko & Ere, 2013; Tchimine et al., 2016), *G.*

Buchananii (Jackson et al., 1967), *G. preussii* (Messi et al., 2012), *G. terphophylla* (Ollis, 1975) , this is the first report of the *G. fusga*.



TABLES 15 Comparison ^1H - and ^{13}C -NMR data of compound 20 with GB-2 in $\text{DMSO}-d_6$

Position	δ_{H} (mult., J in Hz) $\text{DMSO}-d_6$				δ_{C}			
	GB-2 ^a		20		GB-2 ^a	GB-2 ^a	20	20
	Major	Minor	Major	Minor	Major	Minor	Major	Minor
2	5.70	5.36	5.65 (1H, d, $J = 12.2$)	5.33 (1H, d, $J = 12.2$)	81.7	81.4	81.3	81.7
3	4.66	4.48	4.45 (1H, d, $J = 12.2$)	4.64 (1H, d, $J = 12.2$)	47.2	-	47.1	47.2
4	-	-	-	-	196.6	196.5	196.6	196.5
4a	-	-	-	-	101.1	-	101.3	-
5	-	-	-	-	-	-	-	-
6	5.90	5.88	5.87 (1H, d, $J = 2.1$)	5.83 (1H, d, $J = 2.1$)	96.2	-	96.1	95.0
7	-	-	-	-	-	-	-	-
8	5.96	5.90	5.87 (1H, d, $J = 2.1$)	5.57 (1H, brs)	95.9	95.4	96.1	94.9
8a	-	-	-	-	162.8	162.6	162.8	162.6
1'	-	-	-	-	128.2	-	128.1	128.2
2'	7.11	-	7.10 (1H, d, $J = 8.3$) ^b	-	129.0	128.3	129.0	-
3'	6.66	-	6.75 (1H, d, $J = 8.3$)	-	114.9	-	114.9	-
4'	-	-	-	-	-	-	-	-
5'	6.78	-	6.58 (1H, d, $J = 8.3$)	-	114.9	-	114.7	-
6'	7.11	-	7.08 (1H, d, $J = 8.3$) ^b	-	129.0	128.3	129.0	-
2''	5.00	4.89	4.86 (1H, d, $J = 11.0$)	4.98 (1H, d, $J = 11.0$)	82.9	-	82.8	-
3''	4.20	3.86	3.95 (1H, dd, $J = 11.0$, 6.0)	4.18 (1H, dd, $J = 11.0$, 6.0)	72.4	72.0	72.0	72.4
4''	-	-	-	-	197.5	-	197.6	197.6
4a''	-	-	-	-	100.3	99.8	99.7	100.3
5''	-	-	-	-	-	-	162.2	161.8
6''	5.84	5.74	5.91 (1H, br s)	5.79 (1H, brs)	95.0	-	95.8	95.3
7''	-	-	-	-	-	-	-	-
8''	-	-	-	-	101.3	-	101.0	-
8a''	-	-	-	-	160.2	159.5	160.1	159.5
1'''	-	-	-	-	127.9	-	127.8	-
2'''	6.85	-	6.83 (1H, brs)	-	115.4	-	115.3	-
3'''	-	-	-	-	-	-	-	-
4'''	-	-	-	-	-	-	-	-
5'''	6.78	-	6.79 (1H, d, $J = 8.1$)	-	115.2	-	115.1	-
6'''	6.68	-	6.64 (1H, d, $J = 8.1$)	6.63 (d, $J = 8.1$)	119.1	117.5	119.0	117.4
5-OH	12.21	12.15	12.12 (1H, s)	12.19 (1H, s)	163.8	163.1	163.6	163.7
7-OH	11.18	10.88	-	-	166.4	166.3	166.4	166.3
4'-OH	9.55	9.47	9.60 (1H, s)	9.53 (1H, s)	157.8	157.6	157.8	157.6
3''-OH	5.70	5.60	5.81 (1H, d, $J = 6.2$)	5.73 (1H, d, $J = 6.2$)	72.4	72.0	72.0	72.4
5''-OH	11.85	11.95	11.83 (1H, s)	11.73 (s, 1H)	162.2	161.9	162.2	161.8
7''-OH	10.72	10.12	5.73 (1H, d, $J = 6.2$)	-	165.0	164.5	164.5	165.0
3'''-OH	8.90	8.81	8.99 (1H, s)	9.16 (1H, s)	145.0	144.6	145.9	145.3
4'''-OH	9.09	8.81	8.97 (1H, s)	8.86 (1H, s)	145.9	145.4	145.0	144.6

^a (Kumar et al., 2004), ^b Signals interchangeable in the same column.

2. Cholinesterase inhibitory activities

TABLES 16 The ChE inhibitory activity (IC_{50}) of compounds (1-8, 10-12 and 14-20).

Compounds	IC_{50} (μ M)	
	AChE	BChE
1 (Gartanin)	9.35 ± 0.0003	1.46 ± 0.00003
2 (8-Deoxygartanin)	20.41 ± 0.14	1.23 ± 0.00003
3 (β -Mangostin)	Inactive	82.00 ± 0.60
4 (Lakoochin A)	27.22 ± 0.40	13.65 ± 0.05
5 (Cowagarcinone B)	Inactive	Inactive
6 (7-O-methylgarcinone E)	10.95 ± 0.13	2.92 ± 0.06
7 (Fuscaxanthone A)	81.26 ± 5.9	25.67 ± 0.23
8 (Garbogiol)	23.90 ± 0.59	14.04 ± 0.66
9 (An oleanane triterpene lactone)	Not tested	Not tested
10 (3-O-methylcowanin)	97.22 ± 0.26	42.95 ± 0.53
11 (3-O-methylcowaxanthone)	73.15 ± 0.32	108.28 ± 0.47
12 (Rheediaxanthone-A)	Inactive	126.42 ± 0.19
13 (5-Prenyl cowaxanthone)	Not tested	Not tested
14 (Cowanin)	1.09 ± 0.09	0.51 ± 0.006
15 (Cowaxanthone)	3.89 ± 0.15	4.25 ± 1.09
16 (Cowagarcinone E)	0.79 ± 0.05	0.048 ± 0.003
17 (Norcowanin)	0.33 ± 0.04	0.35 ± 0.03
18 (Cowanol)	0.72 ± 0.05	1.84 ± 0.29
19 (Norcowanol)	Not tested	Not tested
20 (GB-2)	Inactive	16.75 ± 0.23
Gаланthamine	1.56 ± 0.28	3.67 ± 0.04

In this work, *in vitro* AChE and BChE inhibitory activities of the isolated compounds, except for 5-prenyl cowaxanthone (**13**), norcowanol (**19**) and oleanane triterpene lactone (**9**), were assessed using the standard drug, galanthamine, as a reference. The results (Table 16), cowanin (**14**) (IC_{50} 1.09 μ M), cowagarcinone E (**16**) (IC_{50} 0.79 μ M), norcowanin (**17**) (IC_{50} 0.33 μ M) and cowanol (**18**) (IC_{50} 0.72 μ M) showed, at the submicromolar level, more pronounced anti-AChE effects than the reference drug (IC_{50} 1.56 μ M) and norcowanin (**17**) was the most active compound which was approximately 5-fold more active than the control. The rest xanthenes, biflavonoid (**20**) and arylbenzofuran (**4**) compounds exhibited moderate to inactive activity.

In the anti-BChE mode (Table 16), cowagarcinone E (**16**) exerted the highest inhibition with the IC_{50} value of 0.048 μ M and was 76-fold higher activity than galanthamine (IC_{50} 3.67 μ M), followed by the strong activity of xanthenes norcowanin (**17**), cowanin (**13**), 8-deoxygartanin (**2**), gartanin (**1**), cowanol (**18**) and 7-O-methylgarcinone E (**6**) (IC_{50} 0.35, 0.51, 1.23, 1.46, 1.84 and 2.92 μ M, respectively), while cowaxanthone (**15**) (IC_{50} 4.25 μ M) was moderately active. The biflavonoid (**20**), aryl benzofuran (**4**) and other xanthenes displayed weak to inactive action under the same test.

Based on the observed activity, for the high anti-AChE effect, the xanthone scaffold should obviously bear a 1,3,6,7-tetraoxygenated function carrying two isoprenyl substituents at both positions of C-2 and C-8, as observed in compounds cowanin (**14**), cowagarcinone E (**16**), norcowanin (**17**), cowanol (**18**) (IC_{50} 0.33–1.09 μ M), when compared with the lower activity of cowaxanthone (IC_{50} 3.89 μ M) which have only a geranyl group at C-2 position. The higher inhibitory potency was shown for the preference of free hydroxyl groups in the core structure as shown in the series of norcowanin (IC_{50} 0.33 μ M) / cowanin (IC_{50} 1.09 μ M) / 3-O-methylcowanin (IC_{50} 97.22 μ M), in addition to those pair of cowaxanthone (IC_{50} 3.89 μ M) / 3-O-methylcowaxanthone (IC_{50} 73.15 μ M). A terminal hydroxyl and its acetate derivative of the prenyl side chain in cowanol (**18**) and cowagarcinone E (**16**) seemed to display a slightly better inhibitory activity than cowanin (**14**).

Similar trend was observed in the BChE inhibitory activity, for the most pronounced effect, the 1,3,6,7-tetraoxygenated xanthone possessing two hydrophobic isoprenyl substituents at C-2 and C-8 is also important. Therefore, cowagarcinone E (**16**) was at least 76-fold more active than that of the drug, followed by norcowanin (**17**) (IC_{50} 0.35 μM), cowanin (**14**) (IC_{50} 0.51 μM) and norcowanin (**17**) (IC_{50} 1.84 μM), in which a terminal acetate group in cowagarcinone E (**16**) was obviously associated for a remarkable inhibition enhancement. Whereas an additional prenyl group in 7-O-methylgarcinone E (**6**) (IC_{50} 2.92 μM) or a lesser isoprenyl unit content in cowaxanthone (**15**) (IC_{50} 4.25 μM) lowered the activity. Modified prenyl group in garbogiol (**8**) (IC_{50} 14.04 μM), fuscaxanthone A (**7**) (IC_{50} 25.67 μM), and rheediaxanthone-A (**12**) (IC_{50} 126.42 μM) gradually decline the effect.

From the results, it could be concluded that the oxygenated xanthone core of the lead cowagarcinone E (**16**) was highly potent and selective BChE inhibitor, while those of the geranylated cowanin (**14**), norcowanin (**17**) and cowanol (**18**) inhibition of AChE and BChE enzymes which breakdown acetylcholine, are considered as a promising strategy for the treatment of Alzheimer's disease (AD).

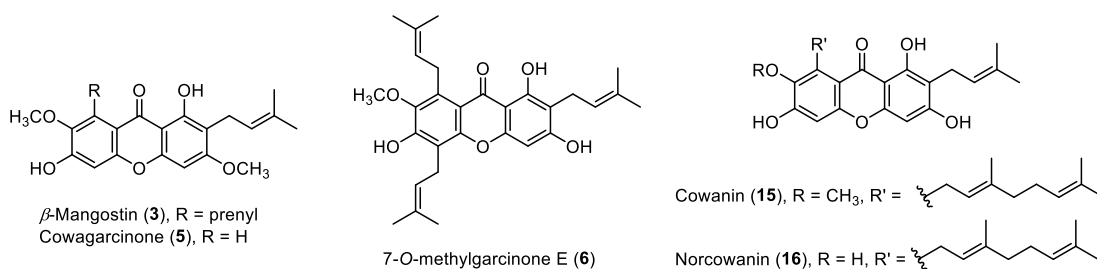
CHAPTER 5

CONCLUSION

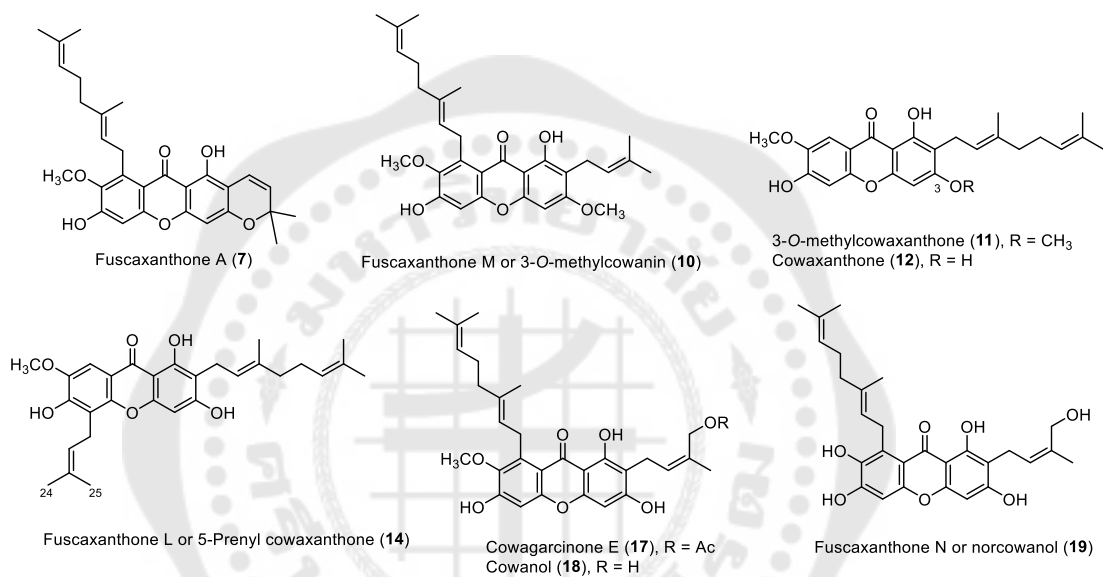
Investigation of the chemical constituents of the EtOAc extract of stem barks of *G. fusca* led to the isolation of three new oxygenated xanthenes fuscaxanthone M or 3-O-methylcowanin (**10**), fuscaxanthone L or 5-Prenyl cowaxanthone (**13**), fuscaxanthone N or norcowanol (**19**), and 14 known xanthenes **1-3**, **5-8**, **10-19** named, gartanin (**1**), 8-deoxygartanin (**2**), β -mangostin (**3**), cowagarcinone B (**5**), 7-O-methylgarcinone E (**6**), fuscaxanthone A (**7**), garbogiol (**8**), 3-O-methylcowaxanthone (**11**), rheedioxanthone-A (**12**), cowanin (**14**), cowaxanthone (**15**), cowagarcinone E (**16**), norcowanin (**17**), cowanol (**18**) (Figure 39), together with the other known metabolites **4**, **9**, **20** named, lakoochin A (**4**), oleanane triterpene lactone (**9**), and GB-2 (**20**) in Figure 40. The structures of known compounds were elucidated by spectroscopic techniques and by comparison of spectroscopic data with those of reported values and including chromatographic comparison with authentic samples in several solvent systems.

In this work, we discovered that geranylated xanthenes of *G. fusca* are good sources of anti-ChE agents in Alzheimer's disorder. Compounds **14** and **17-18** demonstrated a comparable level of dual ChE inhibition and more potent than the reference drug galanthamine. Compound **16** showed a remarkable BChE inhibitory property, which was 76-fold superior to that of the reference drug. The presence of a geranyl unit at C-8 in the xanthone nucleus exhibited superior inhibition to the prenylated xanthenes. The results of this study represent the discovery of geranylated xanthenes from *G. fusca* as an additional potential new class of the multi-target ChE inhibitors.

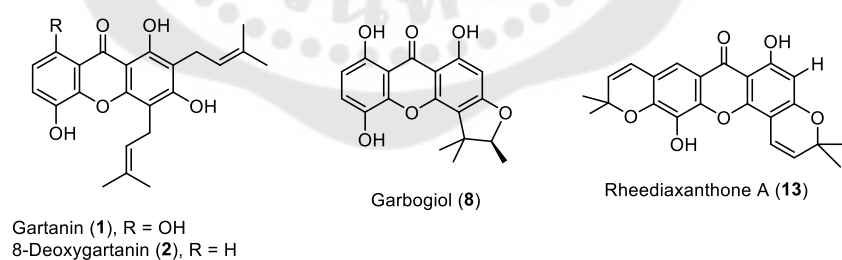
1,3,6,7-tetraoxygenated xanthone skeleton : Prenylated xanthenes

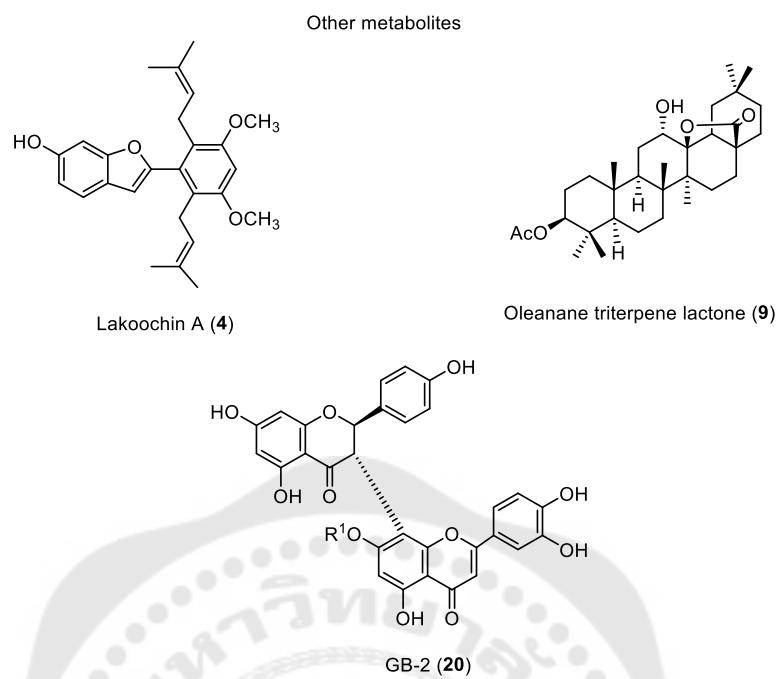


1,3,6,7-tetraoxygenated xanthone skeleton : Geranylated xanthenes



Other oxynated xanthone framework

FIGURES 39 Prenylated and geranylated xanthenes from *G. fusca*



FIGURES 40 Other known metabolites from *G. fusca*

REFERENCES

- Adaramoye, O. A., et al. (2005). Possible anti-atherogenic effect of kolaviron (a *Garcinia kola* seed extract in hypercholesterolaemic rats. *Clin. Exp. Pharmacol. Physiol.*, 32, 40–46.
- Al-Hazimi, H. M. G., & Miana, G. A. (1990). Naturally occurring xanthenes in higher plants and ferns *Journal of the Chemical Society of Pakistan*, 12(2), 174–188.
- Aldred, E. M. (2008). Terpenes. *Pharmacology: A Handbook for Complementary Healthcare Professionals*, Chapter 22, 168–174.
- Auranwiwat, C., et al. (2014). Antibacterial tetraoxygenated xanthenes from the immature fruits of *Garcinia cowa*. *Fitoterapia*, 98, 179–183.
- Balasubramanian, K., & Rajagopalan, K. (1988). Novel xanthenes from *Garcinia mangostana*, structures of BR-xanthone-A and BR-xanthone-B. *Phytochemistry*, 27(5), 1552–1554.
- Bui, D. A., et al. (2014). A protostane and two lanostanes from the bark of *Garcinia ferrea*. *Phytochem. Lett.*, 10, 123–126.
- Chantarasriwong, O., et al. (2010). Chemistry and biology of the caged *Garcinia* xanthenes. *Chem. Eur. J.*, 16(33), 9944–9962.
- Chen, Y., et al. (2016). Caged polyprenylated xanthenes from the resin of *Garcinia hanburyi*. *Fitoterapia*, 109, 106–112.
- Chen, Y., et al. (2013). Chemical constituents of *Gentiana rhodantha*. *Zhongguo Zhong Yao Za Zhi*, 38(8), 362–365.
- Chomnawang, M. T., et al. (2007). Effect of *Garcinia mangostana* on inflammation caused by propionibacterium acnes. *Fitoterapia*, 78(6), 401–408.
- Chung, M. I., et al. (1999). *J. Nat. Prod.*, 62, 1033.
- Demirkiran, O. (2005). PhD thesis. Trakya University, Turkey.
- Demirkiran, O. (2007). Xanthenes in *Hypericum*: Synthesis and biological activities. *Top. Heterocycl. Chem.*, 9, 139–178.

- Denisova-Dyatlova, O. A., & Glyzin, V. I. (1982). Natural xanthenes *Usp. Khim.*, 51(10), 1753–1774.
- Ee, G. C., et al. (2014). A new furanoxanthone from *Garcinia mangostana*. *J. Asian. Nat. Prod. Res.*, 16(7), 790–794.
- Ee, G. C. L., et al. (2009). Xanthenes from *Calophyllum inophyllum*. *Pertanika J. Sci. & Technol.*, 17 (2), 307–312
- El-Seedi, H. R., et al. (2010). Recent insights into the biosynthesis and biological activities of natural xanthenes. *Curr. Med. Chem.*, 17, 854–901.
- Farombi, E. O., et al. (2000). Chemoprevention of 2-acetylaminofluorene-induced hepatotoxicity and lipid peroxidation in rats by kolaviron-A *Garcinia kola* seed extract. *Food Chem. Toxicol.*, 38, 535–541.
- Fouotsa, H., et al. (2015). Antibacterial and antioxidant xanthenes and benzophenone from *Garcinia smeathmannii*. *Planta. Med.*, 81(7), 594–599.
- Froelich, A., et al. (2017). Beckmann rearrangement within the ring C of oleanolic acid lactone: Synthesis, structural study and reaction mechanism analysis. *Journal of Molecular Structure*, 1136, 173–181.
- Garcia-Granados, A., et al. (2004). Partial synthesis of C-ring derivatives from oleanolic and maslinic acids. Formation of several triene systems by chemical and photochemical isomerization processes. *Tetrahedron*, 60(7), 1491–1503.
- Gopalakrishnan, G., et al. (1997). Evaluation of the antifungal activity of natural xanthenes from *Garcinia mangostana* and their synthetic derivatives. *J. Nat. Prod.*, 60, 519–524.
- Govindachari, T. R., et al. (1971). Xanthenes of *Garcinia mangostana* Linn. *Tetrahedron*, 27, 3919–3926.
- Ha, L. D., et al. (2012). Oliveridepsidones A-D, antioxidant depsidones from *Garcinia oliveri*. *Magn. Reson. Chem.*, 50(3), 242–245.
- Ha, L. D., et al. (2009). Cytotoxic geranylated xanthenes and O-alkylated derivatives of α -mangostin. *Chem. Pharm. Bull.*, 57(8), 830–834.

- Hauck, M., et al. (2010). Norstictic acid: Correlations between its physico-chemical characteristics and ecological preferences of lichens producing this depsidone. *Environ. Exp. Bot.*, 68(3), 309–313.
- Hemshekhar, M., et al. (2011). An overview on genus *Garcinia*: phytochemical and therapeutical aspects. *Phytochem. Rev.*, 10(3), 325–351.
- Hichri, F., et al. (2003). Antibacterial activities of a few prepared derivatives of oleanolic acid and of other natural triterpenic compounds. *Comptes Rendus Chimie*, 6(4), 473–483.
- Hostettmann, K., & Hostettmann, M. (1989). Xanthones. *Methods in Plant Biochemistry*, 1, 493–508.
- Hostettmann, K., & Miura, I. (1977). A new xanthone diglucoside from *Swertia perennis* L. *Helv. Chim. Acta*, 60, 262–264.
- Iinuma, M., et al. (1996). Two xanthones from roots of *Cratoxylum formosanum*. *Phytochemistry*, 42(4), 1195–1198.
- Ishiguro, K., et al. (2002). Bisxanthones from *Hypericum japonicum*: Inhibitors of PAF-Induced Hypotension. *Planta. Med.*, 68, 258–261.
- Ito, C., et al. (2003). Chemical constituents of *Garcinia fusca*: structure elucidation of eight new xanthones and their cancer chemopreventive activity. *J. Nat. Prod.*, 66, 200–205.
- Ito, T., et al. (2013). Isolation of six isoprenylated biflavonoids from the leaves of *Garcinia subelliptica*. *Chem. Pharm. Bull.*, 61 (5), 551–558.
- Iwu, M. M., et al. (1990). Prevention of thioacetamide-induced hepatotoxicity by biflavanones of *Garcinia kola*. *Phytother. Res.*, 4(4), 157–159.
- Iwu, W. M., et al. (1987). Evaluation of the antihepatotoxic activity of the biflavonoids of *Garcinia kola* seed. *J. Ethnopharmacol.*, 21, 127–138.
- Jackson, B., et al. (1967). The isolation of a new series of biflavanones from heartwood of *Garcinia buchananii*. *Tetrahedron Lett.*, 9, 787–792.
- Jamila, N., et al. (2014). Cytotoxic benzophenone and triterpene from *Garcinia hombroniana*. *Bioorg. Chem.*, 54, 60–67.

- Jamila, N., et al. (2016). A bioactive cycloartane triterpene from *Garcinia hombroniana*. *Nat. Prod. Res.*, 30(12), 1388–1397.
- Jensen, S. R., & Schripsema, J. (2002). Chemotaxonomy and pharmacology of Gentianaceae. *Gentianaceae -Systematics and Natural History, Chapter 6*, 573–631.
- Kabangu, K., et al. (1987). A new biflavanone from the bark of *Garcinia kola*. *Planta Med.*, 275–277.
- Kaennakam, S., et al. (2015). Kaennacowanols A-C, three new xanthenes and their cytotoxicity from the roots of *Garcinia cowa*. *Fitoterapia*, 102, 171–176.
- Katai, M., et al. (1982). Triterpenoids of the bark of *Pieris japonica* D. Don (Japanese name: Aseni). II. ^{13}C nuclear magnetic resonance of the α -Lactones of ursane- and oleanane-type triterpenes. *Chem. Pharm. Bull.*, 5, 1567–1571.
- Khaw, K. Y., et al. (2014). Prenylated xanthenes from *mangosteen* as promising cholinesterase inhibitors and their molecular docking studies. *Phytomedicine*, 21(11), 1303–1309.
- Kijjoo, A., et al. (2008). Cytotoxicity of prenylated xanthenes and other constituents from the wood of *Garcinia merguensis*. *planta. med. lett.*, 74, 864–866.
- Kleemann, G., et al. (1990). Tetrahymanol from the phototrophic bacterium *Rhodospseudomonas palustris*: first report of a gammacerane triterpene from a prokaryote. *J. Gen. Microbiol.*, 136, 2551–2553.
- Krstić, D., et al. (2003). Secoiridoids and xanthenes in the shoots and roots of *centaurium pulchellum* cultured *In vitro*. *In Vitro Cell. Dev. Biol. Plant*, 39(2), 203–207.
- Kumar, V., et al. (2004). Conformational analysis of the biflavanoid GB-2 and a polyhydroxylated flavanone-chromone of *Cratoxylum neriifolium*. *Planta. Med.*, 70(7), 646–651.
- Lang, G., et al. (2007). Excelsione, a depsidone from an endophytic fungus isolated from the New Zealand endemic tree *Knightia excelsa*. *J. Nat. Prod.*, 70, 310–311.
- Laphookhieo, S., et al. (2011). A new depsidone from the twigs of *Garcinia cowa*. *Heterocycles*, 83(5), 1139–1144.

- Lee, C. W., et al. (2008). Biflavonoids isolated from *Selaginella tamariscina* regulate the expression of matrix metalloproteinase in human skin fibroblasts. *Bioorg. Med. Chem.*, 16(2), 732–738.
- Linuma, M., et al. (1998). A xanthone from *Garcinia cambogia*. *Phytochemistry*, 47(6), 1169–1170.
- Mahabusarakam, W., et al. (2005). Xanthoness from *Garcinia cowa* Roxb. latex. *Phytochemistry*, 66(10), 1148–1153.
- Mahabusarakam, W., et al. (1986). Antimicrobial activities of chemical constituent from *Garcinia mangostana* Linn. *J. Sci. Soc. Thailand*, 12, 239–242.
- Mandal, S., et al. (1992). Naturally occurring xanthoness from *terrestrial flora*. *J. Indian Chem. Soc.*, 69, 611–636.
- Masters, K. S., & Brase, S. (2012). Xanthoness from fungi, lichens, and bacteria: the natural products and their synthesis. *Chem. Rev.*, 112(7), 3717–3776.
- Messi, B. B., et al. (2012). Preussianone, a new flavanone-chromone biflavonoid from *Garcinia preussii* Engl. *Molecules*, 17(5), 6114–6125.
- Monache, F. D., et al. (1981). Three new xanthoness and macluraxanthone from *Rheedia benfarniana* Pl. Triana (Guttiferae). *J.C.S. Perkin I*, 484–488.
- na Pattalung, P., et al. (1994). Xanthoness of *Garcinia cowa*. *Planta Med.*, 60, 365–368.
- Na, Y. (2009). Recent cancer drug development with xanthone structures. *JPP*, 61(6), 707–712.
- Na, Z., et al. (2013). A New prenylated xanthone from latex of *Garcinia cowa* Roxb. *Rec. Nat. Prod.*, 7(3), 220–224.
- Namdaung, U., et al. (2018). 2-Arylbenezofurans from *Artocarpus lakoocha* and methyl ether analogs with potent cholinesterase inhibitory activity. *Eur. J. Med. Chem.*, 143, 1301–1311.
- Negi, J. S., et al. (2013). Naturally occurring xanthoness: Chemistry and biology. *J. Appl. Chem.*, 2013, 1–9.
- Ngernsaengsaruy, C., & Suddee, S. (2016). *Garcinia nuntasaenii* (Clusiaceae), a new species from Thailand. *Thai Forest Bulletin (Botany)*, 44(2), 134–139.

- Nguyen, A. K., et al. (2018). Tetraoxygenated xanthenes from the Latex of *Garcinia Cowa*. *VJST*, 56(5), 560–566.
- Niwa, M., et al. (1993). Garcinol, A novel arylbenzofuran derivative from *Garcinia Kola*. *Heterocycles*, 36(4), 671–673.
- Niwa, M., et al. (1994). Two novel arylbenzofurans, Garcifuran-A and Garcifuran-B from *Garcinia kola*. *Heterocycles*, 38(1994), 1071–1076.
- Nkengfack, A. E., et al. (2002). Globulixanthenes C, D and E: three prenylated xanthenes with antimicrobial properties from the root bark of *Symphonia globulifera*. *Phytochemistry*, 61, 181–187.
- Nontakham, J., et al. (2014). Anti-*Helicobacter pylori* xanthenes of *Garcinia fusca*. *Arch. Pharm. Res.*, 37, 972–977.
- Okoko, T. (2009). Chromatographic characterisation, in vitro antioxidant and free radical scavenging activities of *Garcinia kola* seeds. *Afr. J. Biotechnol.*, 8(24), 7133–7137.
- Okoko, T. (2009). In vitro antioxidant and free radical scavenging activities of *Garcinia kola* seeds. *Food Chem Toxicol.*, 47(10), 2620–2623.
- Okoko, T., & Ere, D. (2013). Some bioactive potentials of two biflavanols isolated from *Garcinia kola* on cadmium-induced alterations of raw U937 cells and U937-derived macrophages. *Asian Pacific Journal of Tropical Medicine*, 6(1), 43–48.
- Ollis, W. D. (1975). biflavonoids and xanthenes of *Garcinia terphophylla* and *G. Echinocarpa*. *Phytochemistry*, 14, 1878–1880.
- Panthong, K., et al. (2009). Cowaxanthone F, a new tetraoxygenated xanthone, and other anti-inflammatory and antioxidant compounds from *Garcinia cowa*. *Can. J. Chem.*, 87, 1636–1640.
- Parveen, M., & Khan, N. U.-D. (1988). Two xanthenes from *Garcinia mangostana*. *Phytochemistry*, 27(11), 3694–3696.
- Peres, V., & Nagem, T. J. (1997). Trioxynated naturally occurring xanthenes. *Phytochemistry*, 44(2), 191–214.
- Peres, V., et al. (2000). Tetraoxygenated naturally occurring xanthenes. *Phytochemistry*, 55, 683–710.

- Pinheiro, L., et al. (2003). Antibacterial xanthenes from *Kielmeyera variabilis* Mart. (Clusiaceae). *Mem. Inst. Oswaldo. Cruz.*, 98(4), 549–552.
- Pinto, M., et al. (2005). Xanthone derivatives: new insights in biological activities. *Curr. Medi. Chem.*, 12(21), 2517–2538.
- Poehland, B. L., et al. (1987). In vitro antiviral activity of dammar resin triterpenoids. *J. Nat. Prod.*, 50(4), 706–713.
- Pollier, J., & Goossens, A. (2012). Oleanolic acid. *Phytochemistry*, 77, 10–15.
- Poomipamorn, S., & Kumkong, A. (1997). Edible multipurpose tree species. *Faung Fa printing, Bangkok.*, 486.
- Pratiwi, L., et al. (2017). Development of TLC and HPTLC method for determination α -mangostin in mangosteen peels (*Garcinia Mangostana* L.). *IJPPR*, 9(3), 297–302.
- Puntumchai, A., et al. (2004). Lakoochins A and B, new antimycobacterial stilbene derivatives from *Artocarpus lakoocha*. *J. Nat. Prod.*, 67(3), 485–486.
- Ragasa, C. Y., et al. (2010). Antimicrobial xanthenes from *Garcinia mangostana* L. *Philipp. Scient.*, 47, 63–75.
- Ritthiwigrom, T., et al. (2013). Chemical constituents and biological activities of *Garcinia cowa* Roxb. . *MIJST*, 7(2), 212–231.
- Roberts, J. C. (1961). Naturally occurring xanthenes. *Chem. Rev.*, 61(6), 591–605.
- Ronco, A. L., & De Stéfani, E. (2013). Squalene: a multi-task link in the crossroads of cancer and aging. *FFHD*, 3(12), 462–476.
- Rukachaisirikul, V., et al. (2003). Antibacterial xanthenes from the leaves of *Garcinia nigrolineata*. *J. Nat. Prod.*, 66, 1531–1535.
- Rukachaisirikul, V., et al. (2003). Anti-HIV-1 protostane triterpenes and digeranylbenzophenone from trunk bark and stems of *Garcinia speciosa*. *Planta. Med.*, 69, 1141–1146.
- Sangsuwon, C., & Jiratchariyakul, W. (2015). Antiproliferative effect of lung cancer cell lines and antioxidant of macluraxanthone from *Garcinia speciosa* wall. *Procedia Soc. Behav. Sci.*, 197, 1422–1427.

- Saputri, F. C., & Jantan, I. (2012). Inhibitory activities of compounds from the twigs of *Garcinia hombroniana* Pierre on human low-density lipoprotein (LDL) oxidation and platelet aggregation. *Phytother. Res.*, 26(12), 1845–1850.
- See, I., et al. (2014). Two new chemical constituents from the stem bark of *Garcinia mangostana*. *Molecules*, 19(6), 7308–7316.
- Shadid, K. A., et al. (2007). Cytotoxic caged-polyprenylated xanthonoids and a xanthone from *Garcinia cantleyana*. *Phytochemistry*, 68(20), 2537–2544.
- Shagufta, & Ahmad, I. (2016). Recent insight into the biological activities of synthetic xanthone derivatives. *Eur. J. Med. Chem.*, 116, 267–280.
- Siewert, B., et al. (2014). The chemical and biological potential of C ring modified triterpenoids. *Eur. J. Med. Chem.*, 72, 84–101.
- Siridechakorn, I., et al. (2012). Antibacterial dihydrobenzopyran and xanthone derivatives from *Garcinia cowa* stem barks. *Fitoterapia*, 83(8), 1430–1434.
- Sosef, M. S., & Dauby, G. (2012). Contribution to the taxonomy of *Garcinia* (Clusiaceae) in Africa, including two new species from gabon and a key to the lower Guinean species. *PhytoKeys*(17), 41–62.
- Sriyatep, T., et al. (2015). Bioactive prenylated xanthones from the young fruits and flowers of *Garcinia cowa*. *J. Nat. Prod.*, 78(2), 265–271.
- Sukandar, E. R., et al. (2016). New depsidones and xanthone from the roots of *Garcinia schomburgkiana*. *Fitoterapia*, 111, 73–77.
- Suksamrarn, S., et al. (2006). Cytotoxic prenylated xanthones from the young fruit of *Garcinia mangostana*. *Chem. Pharm. Bull.*, 54(3), 301–305.
- Suksamrarn, S., et al. (2003). Antimycobacterial activity of prenylated xanthones from the fruits of *Garcinia mangostana*. *Chem. Pharm. Bull.*, 51(7), 857–859.
- Syed, V. B., et al. (1988). A biflavonoid from *Garcinia nervosa*. *Phytochemistry*, 27(10), 3332–3335.
- Tang, Z. Y., et al. (2015). Four new cytotoxic xanthones from *Garcinia nuijiangensis*. *Fitoterapia*, 102, 109–114.

- Tchimene, M. K., et al. (2016). Anti-diabetic profile of extract, kolaviron, biflavonoids and garcinoic acid from *Garcinia kola* seeds. *Int. J. Curr. Microbiol. Appl. Sci.*, 5(2), 317–322.
- Teh, S. S., et al. (2011). Pyranoxanthones from *Mesua ferrea*. *Molecules*, 16(7), 5647–5654.
- Tharachand, S. I., & Mythili, A. (2013). Medicinal properties of *Malabar tamarind* [*Garcinia cambogia* (Gaertn.) Desr.]. *Int. J. Pharm. Sci. Rev. Res.*, 19(2), 101–107.
- Trinh, B. T. D., et al. (2017). Xanthones from the twigs of *Garcinia oblongifolia* and their antidiabetic activity. *Fitoterapia*, 118, 126–131.
- Vieira, L. M. M., & Kijjoa, A. (2005). Naturally-occurring xanthones: recent developments. *Curr. Med. Chem.*, 12, 2413–2446.
- Vo, H. T., et al. (2015). Geranylated tetraoxygenated xanthones from the pericarp of *Garcinia pedunculata*. *Phytochemistry Letters*, 13, 119–122.
- Vo, H. T., et al. (2012). Xanthones from the bark of *Garcinia pedunculata*. *Phytochem. Lett.*, 5(4), 766–769.
- Wagenaar, M. M., & Clardy, J. (2001). Dicerandrols, new antibiotic and cytotoxic dimers produced by the fungus *phomopsis iongicolla* isolated from an *Endangered mint*. *J. Nat. Prod.*, 64, 1006–1009.
- Waterman, P. G., & Crichton, E. G. (1980). Xanthones and biflavonoids from *Garcinia densivenia* stem bark. *Phytochemistry*, 19, 2723–2726.
- Waterman, P. G., & Ussain, R. A. (1982). Major xanthones from *Garcinia quadrifaria* and *Garcinia staudtii* stem barks. *Phytochemistry*, 21(8), 2099–2101.
- Winter, S. E., et al. (2013). Host-derived nitrate boosts growth of *E. coli* in the inflamed gut. *Science*, 339(6120), 708–711.
- Xu, R., et al. (2004). On the origins of triterpenoid skeletal diversity. *Phytochemistry*, 65(3), 261–291.
- Xu, T., et al. (2016). A new xanthone from the pericarp of *Garcinia mangostana*. *J. Chem. Res.*, 40(1), 10–11.

- Xu, W. J., et al. (2016). Polyprenylated tetraoxygenated xanthenes from the roots of *Hypericum monogynum* and their neuroprotective activities. *J. Nat. Prod.*, 79(8), 1971–1981.
- Yang, R., et al. (2017). Xanthenes from the Pericarp of *Garcinia mangostana*. *Molecules*, 22(5), 683–692.
- Yang, Y.-B. (1980). Naturally occurring xanthone compounds. *Yunnan Zhiwu Yanjiu*, 2(3), 345–369.
- Yoon, C. S., et al. (2016). A prenylated xanthone, cudraticusxanthone A, isolated from *Cudrania tricuspidata* inhibits lipopolysaccharide-Induced neuroinflammation through inhibition of NF-kappaB and p38 MAPK pathways in BV2 microglia. *Molecules*, 21(9), 1240–1251.
- Zhang, H., et al. (2014). Cytotoxic and anti-inflammatory prenylated benzoylphloroglucinols and xanthenes from the twigs of *Garcinia esculenta*. *J. Nat. Prod.*, 77(7), 1700–1707.
- Zhao, Y., et al. (2010). Isolation and identification of several xanthenes from the pericarp of *Garcinia mangostana*. *Journal of Jilin Agricultural University*, 32 (5), 513–517.



APPENDIX



Highly potent cholinesterase inhibition of geranylated xanthenes from *Garcinia fusca* and molecular docking studies

Audchara Saenkham^a, Amornmart Jaratrungratwee^b, Yuttana Siri Wattanasathien^c,
Pornthip Boonsri^a, Kittipong Chainok^d, Apichart Suksamrarn^c, Maneekarn Namsa-aid^a,
Prasert Pattanaprateeb^a, Sunit Suksamrarn^{a,*}

^a Department of Chemistry and Center of Excellence for Innovation in Chemistry, Faculty of Science, Srinakharinwirot University, Bangkok 10110, Thailand

^b AB Sciex (Thailand) Limited, Bangkok 10400, Thailand

^c Department of Chemistry, Faculty of Science, Ramkhamhaeng University, Bangkok 10240, Thailand

^d Materials and Textile Technology, Faculty of Science and Technology, Thammasat University, Pathum Thani 12121, Thailand

ARTICLE INFO

Keywords:

Garcinia fusca
Oxygenated xanthenes
Acetylcholinesterase inhibitor
Butyrylcholinesterase inhibitor
Molecular docking

ABSTRACT

Three new oxygenated xanthenes, fuscaxanthenes L-N (1–3), and 14 known xanthenes 4–17, together with the other known metabolites 18–20 were isolated from the stem barks of *Garcinia fusca* Pierre. Their chemical structures were determined based on NMR and MS spectroscopic data analysis, as well as single X-ray crystallography. The geranylated compounds, cowanin (13), cowagarcinone E (15), norcowanin (16) and cowanol (17) exhibited potent inhibitions against acetylcholinesterase (AChE) (IC₅₀ 0.33–1.09 μM) and butyrylcholinesterase (BChE) (IC₅₀ 0.048–1.84 μM), which were more active than the reference drug, galanthamine. Compound 15 was highly potent BChE inhibitor (IC₅₀ 0.048 μM) and was 76-fold more potent than the drug. Structure-activity relationship studies indicated that the C-2 prenyl and C-8 geranyl substituents in the tetraoxygenated scaffold are important for high activity. Molecular docking studies revealed that the leads 13 and 15–17 showed similar binding orientations on both enzymes and very well-fitted at the double binding active sites of PAS and CAS with strong hydrophobic interactions from both isoprenyl side chains.

1. Introduction

The secondary metabolites xanthenes are important class of natural products isolated mainly from plants in Clusiaceae, Gentianaceae, Moraceae and Polygalaceae families, fungi, ferns and lichens [1–6] which possess rich chemistry and pharmacology including cholinesterase inhibition [7–12]. Among several frame works, oxygenated xanthenes of *Garcinia* species received much attention [13–21]. *Garcinia fusca* Pierre (Clusiaceae), a native tree distributed in the north-eastern part of Thailand and Asian countries, is used in food preparation and ethnomedicinally used for the relief of fever, improvement of blood circulation, expectorant, treatment of coughs, indigestion and laxative [22]. Previous examinations of bioactive constituents on *G. fusca* led to the identification of xanthenes with inhibitory effects on Epstein-Barr virus early antigen induction [23] and as α-glucosidase inhibitors [24]. Recently, we reported the anti-*Helicobacter pylori* activity of xanthenes and bioflavonoids isolated from the roots of *G. fusca* [25]. The present work deals with the isolation and structure elucidation of 3 new oxygenated xanthenes, fuscaxanthenes L-N (1–3), and

identification of 14 known xanthenes 4–17 and 3 known metabolites 18–20 from the stem barks of *G. fusca*. Anti-cholinesterase activities of the isolated constituents were evaluated. Molecular docking studies were also performed to examine interactions of the leads with the active sites of AChE and BChE.

2. Materials and methods

2.1. General experimental procedures

All 1D and 2D NMR experiments were measured on a Bruker AVANCE 300 FT-NMR and a Bruker ASCEND 400 NMR spectrometer. Chemical shifts were reported using residual CDCl₃ (δ_H 7.24 and δ_C 77.0 ppm) as internal standards. High resolution time-of-flight mass spectra were obtained using a Bruker micrOTOF QII spectrometer. IR spectra were recorded on a Perkin-Elmer UATR TWO spectrophotometer. UV spectra were taken on a Jasco V-750 UV-Vis spectrophotometer. Melting points were determined on a Griffin melting point apparatus and are uncorrected. Specific optical rotations were

* Corresponding author.

E-mail address: sunit@gswu.ac.th (S. Suksamrarn).

<https://doi.org/10.1016/j.fitote.2020.104637>

Received 21 April 2020; Received in revised form 23 May 2020; Accepted 23 May 2020

Available online 27 May 2020

0367-326X/ © 2020 Elsevier B.V. All rights reserved.

measured using a Jasco-1020 polarimeter. The spots were monitored using TLC sheet precoated with UV fluorescent Merck silica gel 60 F₂₅₄ and were visualized under UV light (254 and 365 nm) followed by heating after spraying with anisaldehyde-H₂SO₄ reagent. Column chromatography was carried out using Merck silica gel 60 (particle size less than 0.063 mm), Silicycle silica gel 60 (< 0.063 mm) and Sephadex LH-20 (GE Health care). Organic solvents were distilled prior to use.

2.2. Plant material

The stem barks of *G. fusca* were collected from Yangtalad District, Kalasin Province, Thailand, in January 2016 and the plant species was authenticated by Professor Nopporn Damrongsiri. A voucher specimen has been deposited under number AS001 at the Laboratory of Natural Product Research Unit, Department of Chemistry, Faculty of Science, Srinakharinwirot University, Thailand.

2.3. Extraction and isolation

The air-dried stem barks (10 kg) of *G. fusca* were powered and extracted with EtOAc (3 × 20 L) and then with MeOH (3 × 20 L) at room temperature for one week in each extraction and the filtered combined solution of each solvent extraction was evaporated to yield the EtOAc (brownish residue, 271 g) and MeOH (reddish brown sticky mass, 542 g) extracts, respectively. Unless indicated otherwise, column chromatography (CC) was carried out using silica gel as the adsorbent. The EtOAc extract (255 g) was fractionated by quick CC (150 g) eluting with a gradient system of *n*-hexane-acetone (96:4 to 0:100) and acetone-MeOH (95:5 to 0:100) to afford 13 main fractions (E1-E13) based on TLC investigations. Fraction E3 (15 g) was further chromatographed with a gradient of *n*-hexane-acetone (96:4 to 0:100) to provide 14 sub-fractions (E.3.1-E.3.14). Repeated CC of sub-fraction E.3.2 (293 mg) eluting with hexane-acetone (96:2 to 0:100) furnished gartanin (4, yellow solid, 35 mg), 8-deoxygartanin (5, yellow solid, 18 mg) and β -mangostin (6, yellow solid, 10 mg). Lakoochin A (19, 4 mg) and cowagarcinone B (7, 42 mg) were successfully yielded by repeated CC of sub-fraction E.3.3 (117 mg) using the same eluent. Repeated CC of sub-fraction E.3.4 (429 mg) eluting with hexane-acetone (96:2 to 0:100) gave 7-O-methylgarcinone E (8, yellow solid, 110 mg) and fuscaxanthone A (9, yellow solid, 10 mg) and garbogiol (10, pale yellow needles, 23 mg). Fraction E.4 (388 mg) was purified by CC eluting with hexane-acetone (95:5) to give compound 20 (2 mg) as a colorless solid. Fraction E5 (19 g) was purified by CC eluting with hexane-acetone (96:4 to 0:100) to yield 9 sub-fractions (E.5.1-E.5.9). Two successive repeated CC of sub-fraction E.5.6 (1.86 g) eluted with hexane-acetone (98:2) afforded 3-O-methylcowaxanthone (11) (8 mg) as a yellow solid and fuscaxanthone M (2) (6.4 mg). Fraction E6 (5.2 g) was separated by CC eluting with hexane-acetone (98:2 to 0:100) to give 14 sub-fractions (E.6.1-E.6.14) and rheedixanthone A (12) (5.7 mg) and fuscaxanthone L (1, 1.9 mg) were successfully obtained from sub-fraction E.6.2 (55 mg). Fraction E10 (25.6 g) was subjected to CC eluting with a gradient of *n*-hexane-acetone (96:4 to 0:100) to provide 7 sub-fractions (E.10.1-E.10.7) and the major compounds, cowanin (13, 3.2 g) and cowaxanthone (14, 723 mg) were furnished from sub-fraction E.10.1 as yellow solids. Fraction E11 (29 g) was subjected to CC eluting with a gradient of *n*-hexane-acetone (96:5 to 0:100) to obtain 12 sub-fractions (E.11.1-E.11.12). Sub-fractions E.11.6 (1.6 g) and E.11.7 (28.4 g) were combined and three successive CC eluting with *n*-hexane-acetone (90:10 to 0:100) gave cowagarcinone E (15, 967 mg), norcowanin (16, 16 mg) and cowanol (17, 2 g). Sub-fraction E.11.9 (10 mg) was separated by a Sephadex LH-20 column using MeOH to afford fuscaxanthone N (3, 1.2 mg). Fraction E12 (20.8 g) was rechromatographed eluting with *n*-hexane-acetone (65:35 to 0:100) to yield 6 sub-fractions E.12.1-E.12.6). Repeated CC of sub-fraction E.12.3 eluting with CH₂Cl₂-MeOH (93:100) yielded GB-2 (19, 256 mg) as a yellow solid.

Table 1

¹H (300 MHz) and ¹³C NMR (75 MHz) spectroscopic data of compounds 1–3 in CDCl₃.

Position	1	2	3
	δ_{H} (J in Hz)	δ_{H} (J in Hz)	δ_{H} (J in Hz)
1		160.0	159.8
2		108.3	111.5
3		162.1	163.5
4	6.42, s	94.1	6.34, s
4a		156.0	154.3
5		115.4	6.84, s
6		150.7	155.7
7		143.9	142.6
8	7.49, s	101.9	137.1
8a		112.9	112.4
9		180.3	181.9
9a		103.0	103.8
10a		149.9	155.2
11	3.49, d (7.3)	21.3	3.35, d (6.9)
12	5.31, br t (7.3)	121.2	5.26, br t (6.9)
13		139.8	131.6
14	2.10, m	39.7	1.68, s
15	2.10, m	26.3	1.80, s
16	5.06, br t (7.3)	123.6	4.10, d (6.2)
17		132.1	5.22, br t (6.2)
18	1.68, s	25.6	135.5
19	1.84, s	16.2	2.02, m
20	1.59, s	17.7	2.02, m
21	3.61, d (7.2)	22.3	5.02, br t (6.0)
22	5.27, br t (7.2)	120.8	131.2
23		132.7	1.60, s
24	1.68, s	17.9	1.83, s
25	1.88, s	25.6	1.55, s
1-OH	13.48, s		13.44, s
3-OH	6.28, s		
6-OH	6.43, s		
3-OCH ₃		3.91, s	55.8
7-OCH ₃	4.00, s	56.3	3.81, s
			62.0

Data assignments were based on HSQC, HMBC and NOESY experiments.

2.3.1. Fuscaxanthone L (1)

Yellow amorphous solid; IR: ν_{max} 3522, 2909, 1634, 1610, 1485, 1443, 1287, 1224, 1190, 1159, 773 cm⁻¹; ¹H NMR (300 MHz, CDCl₃) and ¹³C NMR (75 MHz, CDCl₃) data, see Table 1; HR-TOFMS (ESI⁺) *m/z* 501.2262 [M + Na]⁺ (calcd. For C₂₉H₃₄O₆Na, 501.2247).

2.3.2. Fuscaxanthone M (2)

Yellow gum; UV (MeOH) λ_{max} (log ϵ): 318 (3.1), 257 (3.2), 244 (3.3) nm; IR: ν_{max} 3403, 2919, 1641 1599, 1460, 1432, 1273, 1155, 1087, 838 cm⁻¹; ¹H NMR (300 MHz, CDCl₃) and ¹³C NMR (75 MHz, CDCl₃) data, see Table 1; HR-TOFMS (ESI⁺) *m/z* 491.2436 [M - H]⁻ (calcd. For C₃₀H₃₅O₆, 491.2439).

2.3.3. Fuscaxanthone N (3)

Yellow amorphous solid; UV (MeOH) λ_{max} (log ϵ): 319 (3.5), 259 (3.8), 244 (3.8) nm; IR: ν_{max} 3360, 2919, 1634, 1613, 1582, 1454, 1279, 1194, 1157, 982, 821, 773 cm⁻¹; ¹H NMR (300 MHz, CDCl₃) and ¹³C NMR (75 MHz, CDCl₃) data, see Table 1; HR-TOFMS (ESI⁺) *m/z* 503.2057 [M + Na]⁺ (calcd. For C₂₈H₃₂O₇Na, 503.2040).

2.3.4. (+)-(12S)-Garbogiol (10) and crystallography

Pale yellow needles; mp 235–237 °C; [α]_D²⁶ + 79.6 (c 0.11, MeOH)

[lit [26] $[\alpha]_D^{20}$ 0 (c 0.1, MeOH). Single crystal of **10** was mounted to the end of a hollow glass fibre. X-ray diffraction data were collected using a Bruker D8 QUEST CMOS and operating at $T = 296(2)$ K. Data were measured using ω and ϕ scans and using Mo-K α radiation ($\lambda = 0.71073$ Å). The total number of runs and images was based on the strategy calculation from the program APEX3 and unit cell indexing was refined using SAINT (V8.38A). Data reduction and scaling were performed using SAINT (V8.38A) and SADABS-2016/2 was used for absorption correction [27]. The structure was solved with the ShelXT structure solution program using combined Patterson and dual-space recycling methods [28]. The structure was refined by least squares using ShelXL [29]. All non-hydrogen atoms were refined anisotropically. The hydrogen atoms of organic ligands were placed in calculated positions and refined using a riding model on attached atoms with isotropic thermal parameters 1.2 times those of their carrier atoms. The O–H hydrogen atoms were located in difference Fourier maps but refined with O–H = 0.82 ± 0.01 Å. Crystallographic data have been deposited at the Cambridge Crystallographic Data Centre under the reference number 1938838.

2.4. Anti-ChE assay

In vitro assay was conducted using the Ellman's method as previously described [30] employing *Electrophorus electricus* AChE and equine serum BChE (Sigma Aldrich). Briefly, 140 μ L of 10 mM sodium phosphate buffer (pH 8.0), 20 μ L of AChE (0.2 unit/mL in 10 mM sodium phosphate buffer, pH 8.0) and 20 μ L of test compound in 80% MeOH were mixed and incubated at RT for 10 min. The reaction was started by adding 20 μ L of mixture solution of 5 mM DTNB in 10 mM sodium phosphate buffer (pH 8.0), containing 0.1% bovine serum albumin (BSA) and 5 mM acetylthiocholine iodide (ASCh) in 10 mM sodium phosphate buffer, pH 8.0 (5:1). The hydrolysis of ASCh was monitored by the yellow 5-thio-2-nitrobenzoate anion formation as result of the reaction with DTNB and thiocholines (SCh), catalyzed by enzymes at a wavelength of 405 nm and the absorbance was measured after 5 min of incubation at RT. Percentage of inhibition was calculated by comparing the rate of enzymatic hydrolysis of ASCh for the sample to that of the blank (80% MeOH in buffer). In the similar manner, BChE inhibition was performed as described for AChE. All the samples were run in triplicate in 96-well microplates and galanthamine was used as a positive control. Enzyme inhibitory activity assay (%)

$$= \frac{[(\text{Absorbance of control} - \text{Absorbance of sample}) / \text{Absorbance of control}] \times 100}{\text{Absorbance of control}}$$

The IC_{50} values were determined graphically from inhibition curves (inhibitor concentration vs percent of inhibition) and each concentration was performed in triplicate.

2.5. Molecular modelling

The 3D crystal structure of AChE complexed with galanthamine (code ID: 4EY6) and BChE complexed with choline (code ID: 1P0P) were obtained from the protein data bank (PDB) with a resolution of 2.4 and 2.3 Å respectively [31,32]. Before performing molecular docking, existing ligand, lipids and heteroatoms were removed from the crystal structure. Then, the crystal structure of protein was saved in separate file for input in the docking. The 3D structure of selected compounds were built and minimized at B3LYP/6-31G level of calculations by using Gaussian programme [33]. The docking studies were performed using the AutoDock 4.2 package [34]. The polar hydrogen atoms were added to the amino acid residues and Gasteiger charges were assigned to all atoms of enzyme by using AutoDock Tools 1.5.6 [35]. To determine the binding orientation of ligand, the grid box size was set to $60 \times 60 \times 60$ Å centered coordinate at the reference inhibitors for AChE and BChE, respectively with 0.375 Å spacing to cover the binding site of protein. After the grid box was centered in the protein, grid potential maps were calculated using module AutoGrid 4.0. One

hundred and fifty binding posed were generated in each docking calculation with a maximum of 2,500,000 energy evaluations and the population size 150 with a crossover rate of 0.8. Additional all docking parameters were set to default values. Finally, the docking results were then clustered on the basis of the RMSD between the coordinates of the atoms in a given ligand, and were ranked on the basis of calculated free energy of binding. The results were then analyzed to find the best clustered compounds with lowest free energy of binding for visualization of intermolecular protein-ligand interactions by using the application in Discovery Studio 2020 Client program [36].

3. Results and discussion

The stem barks extract of a medicinal plant *G. fusca* was revealed significant *in vitro* cholinesterase inhibitory activity. The EtOAc extract, which exhibited greater both AChE (IC_{50} 1.35 μ g/mL) and BChE (IC_{50} 0.50 μ g/mL) inhibitory activities than the MeOH soluble fraction (IC_{50} 11.0 and 7.5 μ g/mL, respectively), was therefore subjected to chromatographic isolation and purification for the active principles. Based on spectroscopic analysis (mainly NMR and MS) the chemical structures were characterized and determined as three new xanthenes **1–3** and 17 previously described compounds: gartanin (**4**) [37], 8-deoxygartanin (**5**) [37], β -mangostin (**6**) [28], cowa-garcinone B (**7**) [38], 7-methoxy-garcinone E (**8**) [23], fuscaxanthone A (**9**) [25], garbogiol (**10**) [24], 3-methoxycowaxanthone (**11**) [39], rheedi-xanthone A (**12**) [40], the major xanthone cowanin (**13**) [25], cowaxanthone (**14**) [25], cowa-garcinone E (**15**) [24,41], norcowanin (**16**) [23], the second major cowanol (**17**) [25], a biflavonoid of GB-2 (**18**) [42,43], an aryl 2-benzofuran lakoochin A (**19**) [30] and an oleanane triterpene lactone (**20**) [44], (Fig. 1). Compounds **4–5**, **11–12** and **18–20** are first reported from this plant species.

Compound **1** was obtained as a yellow amorphous solid and the molecular formula was deduced to be $C_{29}H_{34}O_6$ on the basis of HR-ESI-TOFMS data (m/z 501.2262 $[M + Na]^+$, calcd 501.2247) and NMR analyses. The IR absorptions indicated the presence of hydroxyl (3522 cm^{-1}) and conjugated carbonyl (1634 cm^{-1}) functionalities. The NMR, HR-MS and IR spectra of compound **1** are presented in Figs. S1–S8. The ^1H NMR data of **1** in CDCl_3 (Table 1) showed resonances for a hydrogen-bonded hydroxyl group at δ_H 13.48 (1-OH), two aromatic singlets at δ_H 7.49 (H-8) and 6.42 (H-4), two phenolic hydroxyls at δ_H 6.43 and 6.28, a methoxyl (δ_H 4.00) together with two sets of isoprenyl units (Fig. 1). The ^{13}C NMR, DEPT and HSQC data offered the presence of 29 carbons attributable to one methoxyl, five methyls, four methylenes, five methines and 13 quaternary carbons including a conjugated carbonyl carbon. Analysis of the ^1H and ^{13}C NMR spectroscopic data of **1** suggested for a tetraoxygenated xanthone skeleton in which the 6 oxygenated aromatic carbons were observed at δ_C 162.1, 160.0, 156.0, 150.7, 149.9 and 143.9 ppm [37]. HBMBC correlations from the chelated hydroxyl proton to three aromatic carbons C-1 (δ_C 160.0), C-2 (δ_C 108.3) and C-9a (δ_C 103.0), from the aromatic singlet H-4 to C-3 (δ_C 162.1) and from the comparable deshielded aromatic signal at δ_H 7.49 (H-8) to the C-7 (δ_C 143.9), C-6 (δ_C 150.7) and the C-9 carbonyl (δ_C 180.3) resonances (Fig. 2) further supported the described oxygenated pattern. In addition, the methoxyl proton displayed an NOE enhancement with H-8 signal and an interaction with C-7 in their NOESY and HMBC spectra, respectively, confirmed the placement of the methoxyl group at C-7 carbon. The presence of two isoprenyl units was evident from their characteristic resonances in the NMR data. A geranyl (or 3,7-dimethyloct-2,6-dienyl) unit was present from the following observations: the two olefinic protons at δ_H 5.31 (1H, br t, $J = 7.3$ Hz, H-12) and 5.06 (1H, br t, $J = 7.3$ Hz, H-16); three methylenes at δ_H 3.49 (2H, d, $J = 7.3$ Hz, H-11) and 2.10 (4H, m, H-14 and H-15); and three methyl singlets at δ_H 1.84 (H-19), 1.68 (H-18) and 1.59 (H-20) including a set of carbon chemical shifts at δ_C 139.8 (C-13), 132.1 (C-17), 123.6 (C-16), 121.2 (C-12), 39.7 (C-14), 26.3 (C-15), 25.6 (C-18), 21.3 (C-11), 17.7 (C-20) and 16.2 (C-19). A prenyl moiety was suggested from the

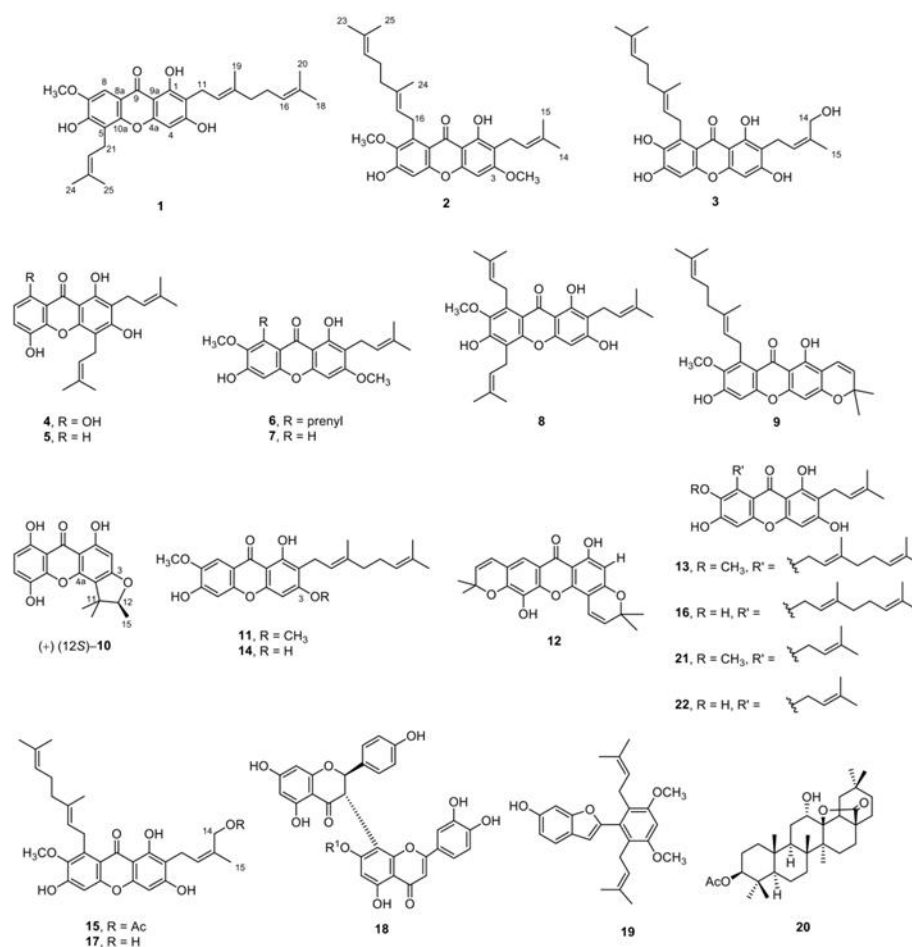


Fig. 1. Chemical structures of compounds 1–22.

resonances of a methine proton at δ_H 5.27 (1H, br t, $J = 7.2$ Hz, H-22), two methylenes at δ_H 3.61 (2H, d, $J = 7.2$ Hz, H-21) and two methyls at δ_H 1.68 (3H, s, H-24) and 1.88 (3H, s, H-25), as well as their carbon signals at δ_C 132.7 (C-23), 120.8 (C-22), 17.9 (C-24), 22.3 (C-21), 25.6 (C-25). The HMBC spectrum showed interactions from the methylene proton at δ_H 3.49 (H-11) to carbon resonances of C-2, oxygenated C-3 and C-13; from the methyl signal at δ_H 1.84 (H-19) to C-12, C-13 and C-14 and from another methyl singlet at δ_H 1.59 (H-20) to C-16, C-17 and C-18, including the consecutive NOESY connectivities from H-12 to H-18 (via H-12/H-14/H-16/H-18) were observed permitting the geranyl residue was resided at C-2 carbon. The double bond at C-12/C-13 was assigned as *E* by strong NOE enhancements observed among those pairs of H-11 / H-19 and of H-12 / H-14 in the NOESY data. Placement of the prenyl unit at C-5 was determined by the HMBC correlations from the methylene protons (δ_H 3.61, H-21) to C-5 and C-22 and from H-22 to C-24 and C-25, in addition to those of NOESY relations of those pairs of H-21/H-25 and H-22/H-24 (Fig. 2). In fact, the ^1H NMR spectral feature of 1 was similar to those of cowaxanthone (14) except for the presence of

an additional 3-methylbut-2-enyl residue in 1, which replaces aromatic proton at δ_H 6.94 (H-5) of 14. Thus, the structure of compound 1 was deduced as (*E*)-2-(3,7-dimethylocta-2,6-dien-1-yl)-1,3,6-trihydroxy-7-methoxy-5-(3-methylbut-2-en-1-yl)-9H-xanthen-9-one or 5-prenyl-cowaxanthone and was named fuscaxanthone 1.

Compound 2 was isolated as a yellow gum and its IR spectrum showed the presence of hydroxyl group at 3403 cm^{-1} and a conjugated carbonyl group at 1641 cm^{-1} . The UV spectrum exhibited absorptions of a xanthone chromophore at λ_{max} 318, 257 and 244 nm [25]. The molecular formula was found to be $\text{C}_{30}\text{H}_{36}\text{O}_6$ based on HR-ESI-TOFMS ion at m/z 491.2436 $[\text{M} - \text{H}]^-$ (calcd. For $\text{C}_{30}\text{H}_{35}\text{O}_6$, 491.2439). The NMR, HR-MS and IR spectra of 2 are included in Figs. S10–S15. The ^1H NMR spectrum (CDCl_3 , Table 1) showed signals for a chelated hydroxyl group [δ_H 13.44 (1H, s, 1-OH)], two isolated aromatic protons at δ_H 6.84 and 6.34 (each 1H, each s, H-5 and H-4), a 3-methylbut-2-enyl group, a geranyl group and two methoxyl singlets (δ_H 3.91 and 3.81, each 3H). The NMR data of 2 are quite similar to those of cowanin (13) and the only difference between them is the presence of an additional

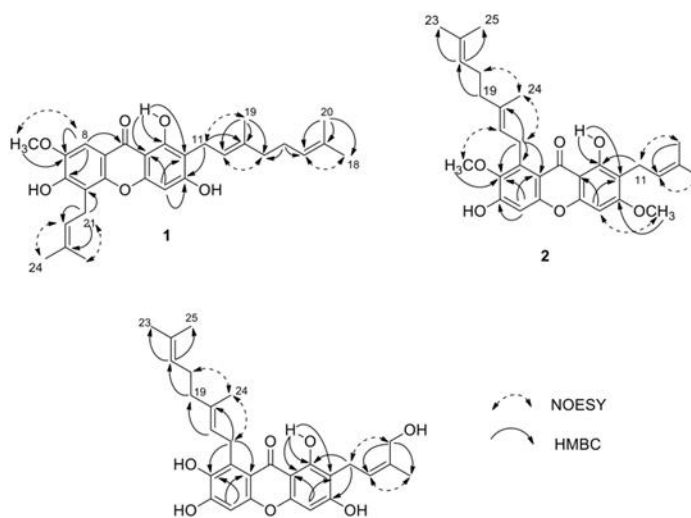


Fig. 2. Selected HMBC and NOESY correlations for compounds 1–3.

methoxyl in **2**. Careful comparison of the ^{13}C NMR data of compound **2** to those of the 6-O-methylcowanin [45], particularly the shifts of C-2, C-3, and C-4 suggested that this additional methoxyl substituent should be located at C-3. The methoxyl proton at δ_{H} 3.91 (3-OCH₃) showed connectivities to an oxyquaternary carbon at δ_{C} 163.5 (C-3) and to a lone aromatic H-4 (δ_{H} 6.34) in the respective HMBC and NOESY spectra supporting the above conclusion (Fig. 2). Correlations from another methoxyl singlet at δ_{H} 3.81 to C-7 (δ_{C} 142.6), from the proton H-4 to C-2 (δ_{C} 111.5), C-4a (δ_{C} 154.3) and C-9a (δ_{C} 103.8) and from H-5 (δ_{H} 6.84) to C-8a (δ_{C} 112.4), C-7 (δ_{C} 142.6) and C-6 (δ_{C} 155.7) were also present in its HMBC data. The structure of **2** was therefore determined to be (*E*)-1-(3,7-dimethylocta-2,6-dien-1-yl)-3,8-dihydroxy-2,6-dimethoxy-7-(3-methylbut-2-en-1-yl)-9H-xanthen-9-one and was named fuscaxanthone M.

Compound **3** was obtained as a yellow amorphous solid and its HR-ESI-TOFMS exhibited a pseudomolecular ion at m/z 503.2057 [$\text{M} + \text{Na}$]⁺ (calcd. 503.2040) suggesting the molecular formula C₂₈H₃₂O₇. Its UV absorption bands at λ_{max} 319, 259 and 244 nm also suggested for a xanthone chromophore. The NMR, HR-MS, and IR spectra of **3** are included in Figs. S16–S23. The ^1H and ^{13}C NMR data (CDCl₃, Table 1), aided by a HSQC experiment, disclosed the presence of a carbonyl, 13 quaternary carbons (six of which are oxygen bearing), five methine protons, five methylene protons, and four methyl groups. The NMR spectroscopic data indicated that the molecule also consists of a tetraoxygenated xanthone skeleton bearing a geranyl and a modified prenyl moieties. The ^1H NMR spectrum of **3** displayed the signals of a chelated phenolic hydroxyl proton at δ_{H} 13.94 (1-OH), two isolated aromatic singlets at δ_{H} 6.77 (H-5) and 6.28 (H-4) and two sets of resonances for a geranyl and a prenyl alcohol units. The characteristic resonances of 4-hydroxy-3-methyl-2-butenyl residue was appeared at δ_{H} 3.51 (2H, d, $J = 7.1$ Hz, H-11), 5.46 (1H, br t, $J = 7.1$ Hz, H-12), 4.33 (2H, s, H-14) and 1.79 (3H, s, H-15) and this unit was connected to C-2 (δ_{C} 108.0) by cross-peaks determined from the H-11 to C-1, C-2, C-3 and C-13 in its HMBC spectrum (Fig. 2). Compound **3** showed ^1H and ^{13}C NMR spectra similar to those of cowanol (**17**) except for the absence of a methoxyl resonance in **3**. The geometric isomer of the double bond at C-12/C-13 is *Z*, which was assigned by more significant NOE enhancements marked between those pairs of the CH₂OH (δ_{H} 4.33) / H-11 (δ_{H} 3.51) and of H-12 (δ_{H} 5.46) / H-15 (δ_{H} 1.79) displayed in the NOESY

spectrum. On the other hand, the geometric arrangement of the C-17/C-18 double bond is *E* as evidenced by correlations displayed between the methyl protons (δ_{H} 1.86) of C-24 and the methylene protons (δ_{H} 4.29) of C-16 in the NOESY spectrum. Thus, **3** was established as 1-((*E*)-3,7-dimethylocta-2,6-dien-1-yl)-2,3,6,8-tetrahydroxy-7-((*Z*)-4-hydroxy-3-methylbut-2-en-1-yl)-9H-xanthen-9-one and was named fuscaxanthone N.

Compound **10** was obtained as pale yellow needles and identified as (+) garbogiol by examinations of its 1D- and 2D-NMR and MS spectroscopic data along with its positive specific rotation [$\alpha_{\text{D}}^{26} + 79.6$ (c 0.11, MeOH)] and by comparison with the reported values [24,26]. Previous reported garbogiol was a racemate [α_{D}^{20} 0 (c 0.1, MeOH)] [26]. The X-ray crystal structure of **10** confirmed a 1,3,5,8-oxygenated xanthone featuring with a furano group attached at C-3/C-4 position and the absolute configuration was defined as 14*S* (Fig. 3). The structure of **10** was therefore deduced as (+) (5*S*)-5,7,10-trihydroxy-1,1,2-trimethyl-1H-furo[2,3-*c*]xanthen-6(2H)-one or (+) (5*S*)-garbogiol.

3.1. Cholinesterase inhibitory activities

The *in vitro* AChE and BChE inhibitory activities of the isolated compounds, except for **1**, **3** and **20**, were assessed using the standard

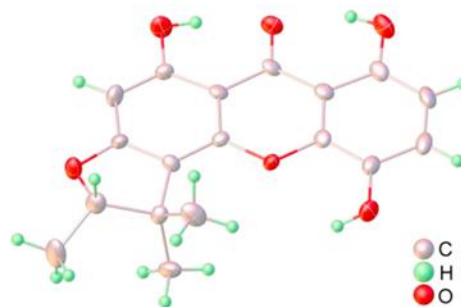


Fig. 3. ORTEP plot of the X-ray crystal structure for compound **10**.

Table 2
ChE inhibitory activity ($IC_{50} \pm SD$) of compounds **2**, **4–19** and **21–22**.

Compounds	IC_{50} (μM)		Selectivity for	
	AChE	BChE	AChE ^b	BChE ^b
1	Nr ^c	Nr ^c		
2	97.22 \pm 0.26	42.95 \pm 0.53	0.44	2.26
3	Nr ^c	Nr ^c		
4	9.35 \pm 0.0003	1.46 \pm 0.00003	0.15	6.40
5	20.41 \pm 0.14	1.23 \pm 0.00003	0.06	16.5
6	Inactive ^d	82.00 \pm 0.60		
7	Inactive ^d	Inactive ^d		
8	10.95 \pm 0.13	2.92 \pm 0.06	0.26	3.75
9	81.26 \pm 5.9	25.67 \pm 0.23	0.31	3.16
10	23.90 \pm 0.59	14.04 \pm 0.66	0.58	1.70
11	73.15 \pm 0.32	108.28 \pm 0.47	1.48	0.67
12	Inactive ^d	126.42 \pm 0.19		
13	1.09 \pm 0.09	0.51 \pm 0.006	0.46	2.13
14	3.89 \pm 0.15	4.25 \pm 1.09	1.09	0.91
15	0.79 \pm 0.05	0.048 \pm 0.003	0.06	16.45
16	0.33 \pm 0.04	0.35 \pm 0.03	1.06	0.94
17	0.72 \pm 0.05	1.84 \pm 0.29	2.55	0.39
18	Inactive ^d	16.75 \pm 0.23		
19	27.22 \pm 0.40	13.65 \pm 0.05	0.50	1.99
21	2.38 \pm 0.20	3.18 \pm 0.05	1.33	0.74
22	2.62 \pm 0.06	1.05 \pm 0.02	0.40	2.49
Gаланthamine	1.56 \pm 0.28	3.67 \pm 0.04		

Data presented as the mean \pm SD ($n = 3$).

^a Selectivity for AChE is defined as IC_{50} BChE / IC_{50} AChE.

^b Selectivity for BChE is defined as IC_{50} AChE / IC_{50} BChE.

^c Not tested.

^d Inactive at 0.1 mg/mL.

drug, galanthamine, as a reference. As shown in Table 2, cowanin (**13**) (IC_{50} 1.09 μM), cowagarcinone E (**15**) (IC_{50} 0.79 μM), norcowanin (**16**) (IC_{50} 0.33 μM) and cowanol (**17**) (IC_{50} 0.72 μM) showed, at the sub-micromolar level, more pronounced anti-AChE effects than the reference drug (IC_{50} 1.56 μM) and **16** was the most active compound which was approximately 5-fold more active than the control. The rest xanthenes, biflavonoid and arylbenzofuran compounds exhibited moderate to inactive activity. In the anti-BChE mode (Table 2), compound **15** exerted the highest inhibition with the IC_{50} value of 0.048 μM and was 76-fold higher activity than galanthamine (IC_{50} 3.67 μM), when compared with the lower activity of **14** (IC_{50} 3.89 μM) which followed by the strong activity of xanthenes **16**, **13**, **5**, **4**, **17** and **8** (IC_{50} 0.35, 0.51, 1.23, 1.46, 1.84 and 2.92 μM , respectively), while compound **14** (IC_{50} 4.25 μM) was moderately active. The biflavonoid **18**, aryl benzofuran **19** and other xanthenes displayed weak to inactive action under the same test.

Based on the observed activity, for the high anti-AChE effect, the xanthone scaffold should obviously bear a 1,3,6,7-tetraoxygenated function carrying two isoprenyl substituents at both positions of C-2 and C-8, as observed in compounds **13** and **15–17** (IC_{50} 0.33–1.09 μM), when compared with the lower activity of **14** (IC_{50} 3.89 μM) which have only a geranyl group at C-2 position. The weak action was suggested from the 1,3,5,8-tetraoxygenated (**4** and **10**) and 1,3,5-trioxygenated (**5**, IC_{50} 20.41 μM) or the inactivity of the 1,3,5,6-tetraoxygenated (**12**) systems. The inhibitory activity was further reduced depending on the number and position of isoprenyl substituents or their modifications in the frame work, as marked in **8** (which bears three prenyls at C-2, C-5 and C-8 with the IC_{50} of 10.95 μM), **9** (a modified prenyl, IC_{50} 81.26 μM) and **12** (inactive). The higher inhibitory potency was shown for the preference of free hydroxyl groups in the core structure as shown in the series of **16** (IC_{50} 0.33 μM) / **13** (IC_{50} 1.09 μM) / **2** (IC_{50} 97.22 μM), in addition to those pair of **14** (IC_{50} 3.89 μM) / **11** (IC_{50} 73.15 μM). A terminal hydroxyl and its acetate derivative of the prenyl side chain in **17** and **15** seemed to display a slightly better inhibitory activity than **13**.

Similar trend was observed in the BChE inhibitory activity, for the most pronounced effect, the 1,3,6,7-tetraoxygenated xanthone possessing two hydrophobic isoprenyl substituents at C-2 and C-8 is also important. Therefore, **15** was at least 76-fold more active than that of the drug, followed by norcowanin (**16**) (IC_{50} 0.35 μM), **13** (IC_{50} 0.51 μM) and **17** (IC_{50} 1.84 μM), in which a terminal acetate group in **15** was obviously associated for a remarkable inhibition enhancement. Whereas an additional prenyl group in **8** (IC_{50} 2.92 μM) or a lesser isoprenyl unit content in **14** (IC_{50} 4.25 μM) lowered the activity. Modified prenyl group in **10** (IC_{50} 14.04 μM), **9** (IC_{50} 25.67 μM), and **12** (IC_{50} 126.42 μM) gradually decline the effect.

Oxygenated xanthenes and the synthetic compounds have been shown to be ChE inhibitors [7–12,46], in particular those of α - and γ -mangostins (**21** and **22**) [9,47] which have the same oxygenated pattern comprising two prenyl groups oriented at the same positions as those of the geranylated ones in **13** and **15–17**. In order to further gain more insight into structural requirements that favor ChE inhibition, compounds **21** and **22** were also taken into consideration. The mangostins **21** and **22** were previously isolated as major constituents from the well-known tropical fruits *G. mangostana* by our group [37,48,49] and exhibited approximately the same anti-AChE potency (IC_{50} 2.38–2.62 μM), while γ -mangostin (**22**, IC_{50} 1.05 μM) was about 3-fold more active than α -mangostin (**21**, IC_{50} 3.18 μM) towards BChE in our test (Table 2). Our results were comparable to the previous study by Khaw et al. [9]. In comparative ChE inhibitory measurements, the IC_{50} values of **13** and **16** were about 2–8 times superior to those of the respective **21** and **22** in both enzymatic inhibitions further substantiate the preference of the C-8 geranyl moiety in the structural feature.

From the results, it could be concluded that the oxygenated xanthone core of the lead **15** was highly potent and selective BChE inhibitor (selectivity for BChE of 16.45, Table 2), while those of the geranylated **13**, **16** and **17** as well as the prenylated compounds **21** and **22** were considerably potential dual AChE/BChE inhibitors (selectivity for BChE 0.39–2.49 and selectivity for AChE 0.40–2.55, Table 2). Inhibition of AChE and BChE enzymes which breakdown acetylcholine, are considered as a promising strategy for the treatment of Alzheimer's disease (AD). Recent evidences suggested that in advanced AD the BChE levels were unchanged or progressively increased while AChE activity decreases, hence management of both AChE and BChE levels may be beneficial for AD therapy [50]. Furthermore, inhibition of BChE can promote ACh level was also indicated and dual AChE/BChE inhibitor has also shown to lower the toxic effect of the amyloid- β (A β) peptide production [51]. Naturally-occurring compounds from plants with diverse structure are considered to be a potential source of new inhibitors, including our findings on geranylated xanthenes as lead dual/selective anti-ChE candidate with the aim of effective AD therapeutics.

3.2. Molecular docking study

In order to investigate the binding affinities which related to the inhibitory activity, docking simulations were performed on the leads of geranylated **13** and **15–17**, as well as the prenylated compounds: α -mangostin (**21**) and γ -mangostin (**22**) against AChE and BChE. The docking results revealed that all compounds were posed into the active pockets of both enzymes with good binding affinities as shown in Fig. 4 and Table S1, and apparently exhibited a dual inhibition of AChE/BChE. The superimposition of the compounds to AChE and BChE are displayed in Fig. 4A and Fig. 4B, respectively.

Regarding AChE, **13** and **15–17** strongly formed the π - π Stacking, π - σ , and π -Anion interactions between the xanthone core and key residues Tyr124, Trp286, Tyr341, Asp74 in the peripheral active site (PAS). Furthermore, the C-8 geranyl moiety could generate the hydrophobic interaction to His447 in the catalytic active site (CAS) which can be clearly explained in Fig. 4A and Table S1. In the case of prenylated compounds, **21–22** could also bind to both the PAS and the CAS regions with negligible different binding mode from the

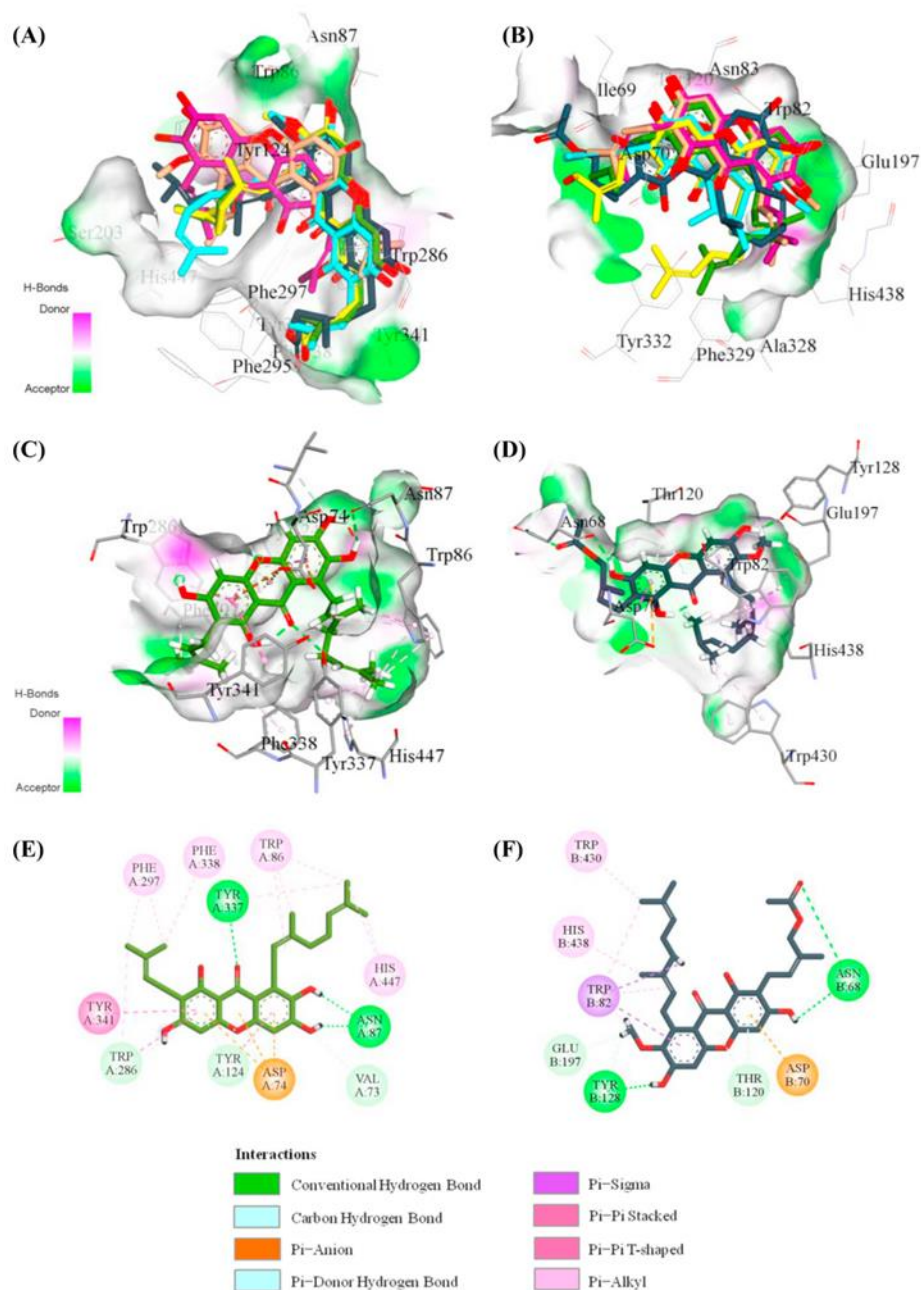


Fig. 4. Superimpositions of **13** (cyan), **15** (dark grey), **16** (green), **17** (light yellow), **21** (orange) and **22** (magenta) in the AChE (A) and BChE (B) active pockets. The 3D diagram from docking poses of **16** (green) and **15** (dark grey) interacted to AChE (C) and BChE (D) active pockets, respectively. Atom colors: dark blue-nitrogen atoms, red-oxygen atoms, white-hydrogen atoms. The figure was prepared using the application in Discovery Studio 2020 Client program [36]. (For interpretation of the references to colour in this figure legend, the reader is referred to the web version of this article.)

geranylated ones. It is noteworthy that even the binding pose was slightly changed thought all the leads highlights the dual binding site AChE inhibitors which agree well to the previous studies [47,52].

Norcowanin (**16**) showed the highest AChE inhibition, resulted from the more tight binding to keys residues in both the CAS and the PAS established the strong hydrogen bonding to the Asn87, then to the Tyr337 which located at the anionic subsite. The 3D and 2D protein-ligand interactions of **16** interacted to AChE binding pocket are clearly explained in Fig. 4C and E, respectively. Interestingly, the hydroxyl group at C-7 formed hydrogen bonding to Asn87 (not found in other compounds), which played a vital role for anti-AChE activity. Additionally, the hydrophobic interactions were observed between **16** interacted to the aromatic residues located at the anionic site (Trp86, Tyr337, Phe338), acyl pocket (Phe297), the PAS cavity (Tyr124, Trp286, Tyr341), and at the CAS (His447), and via electrostatic interactions with Asp74.

For BChE binding, the superimpositions of all compounds to the BChE active pocket are obtained in Figs. 4B and Table S1. All compounds also exhibited similar mode of binding to BChE when compared to AChE, except for prenylated xanthenes **21** and **22** which lack of the interactions in the PAS cavity. This indicated that the geranyl side-chain plays a significant role in supporting the dual site binding BChE inhibitors. The binding mode and conformation of **15** interacted to the amino acids in the BChE active pocket is clearly displayed from the 3D and 2D protein-ligand interactions as shown in Fig. 4D and F, respectively. The two hydrogen bonds were formed between the xanthone core of **15** to Tyr128 (1.83 Å) and Asn68 (2.19 Å) of BChE active pocket. Surprisingly, the acetate group at C-14 position of a prenyl moiety formed the strong hydrogen bonding to Asn68 (1.86 Å) which effected selectivity and enhanced inhibitory activity on BChE. Then, the tight hydrophobic interactions were obtained between the geranyl part of **15** to interact with residues in the choline binding site (Trp82), the CAS (His438), and Trp430. Furthermore, the core ring of **15** formed the Pi-Sigma and Pi-Anion interactions to the residue Asp70 in the PAS cavity.

4. Conclusion

In this work, we discovered that geranylated xanthenes of *G. fusca* are good sources of anti-ChE agents in Alzheimers' disorder. Compounds **13**, **16** and **17** demonstrated a comparable level of dual ChE inhibition and more potent than the reference drug galanthamine. Compound **15** showed a remarkable BChE inhibitory property, which was 76-fold superior to that of the reference drug. The presence of a geranyl unit at C-8 in the xanthone nucleus exhibited superior inhibition to the prenylated xanthenes, α -mangostin (**21**) and γ -mangostin (**22**), which were obtained from mangosteen fruits. The results of this study represent the discovery of geranylated xanthenes from *G. fusca* as an additional potential new class of the multi-target ChE inhibitors.

Acknowledgements

This work was supported by the Center of Excellence for Innovation in Chemistry (PERCH-CIC), Ministry of Higher Education, Science, Research and Innovation and the Faculty of Science, Srinakharinwirot University (Grant number 662/2559). Support from The Thailand Research Fund (Grant number DBG6180030) was gratefully acknowledged. SS and PB are grateful to Faculty of Science, Srinakharinwirot University (Grant number 484/2562) for partial financial support. The authors are thankful to National e-Science Infrastructure Consortium for providing computing resources that have partly contributed to the paper.

Conflict of interest

The authors declare that there is no conflict of interest.

Appendix A. Supplementary data

Supplementary data to this article can be found online at <https://doi.org/10.1016/j.fitote.2020.104637>.

References

- [1] S. Genovesi, S. Florito, V.A. Taddeo, F. Epifano, Recent development in the pharmacology of prenylated xanthenes, *Drug Discov. Today* 21 (2016) 1814–1819.
- [2] A. Singh, N. Kaur, S. Sharma, P.M.S. Bedi, Recent progress in biologically active xanthenes, *J. Chem. Pharm. Res.* 8 (2016) 75–131.
- [3] T. Wezeman, S. Brase, K.-S. Masters, Xanthone dimers: a compound family which is both common and privileged, *Nat. Prod. Rep.* 32 (2015) 6–28.
- [4] D.K. Winter, D.L. Sloman, J.A. Porco Jr., Polycyclic xanthone natural products: structure, biological activity and chemical synthesis, *Nat. Prod. Rep.* 30 (2013) 382–391.
- [5] O. Chantarasriwong, A. Batova, W. Chavasiri, E.A. Theodorakis, Chemistry and biology of the caged *Garcinia xanthenes*, *Chem. Eur. J.* 16 (2010) 9944–9962.
- [6] H.R. El-Seedi, M.A. El-Barbary, D.M.H. El-Ghorab, L. Bohlin, A.-K. Borg-Karlson, U. Göransson, R. Verpoorte, Recent insights into the biosynthesis and biological activities of natural xanthenes, *Curr. Med. Chem.* 17 (2010) 854–901.
- [7] M.I. Cruz, H. Cidade, M. Pinto, Dual/multitargeted xanthone derivatives for Alzheimer's disease: where do we stand? *Future Med. Chem.* 9 (2017) 1611–1630.
- [8] N. Jamila, K.K. Yeong, V. Murugaiyah, A. Atlas, I. Khan, N. Khan, S.N. Khan, M. Khairuddean, H. Osman, Molecular docking studies and in vitro cholinesterase enzyme inhibitory activities of chemical constituents of *Garcinia hombroniana*, *Nat. Prod. Res.* 29 (2015) 86–90.
- [9] K.Y. Khaw, S.B. Choi, S.C. Tan, H.A. Wahab, K.L. Chan, V. Murugaiyah, Prenylated xanthenes from mangosteen as promising cholinesterase inhibitors and their molecular docking studies, *Phytomedicine* 21 (2014) 1303–1309.
- [10] C. Sabphon, T. Sermboonpaisarn, P. Sawasdee, Cholinesterase inhibitory activities of xanthenes from *Anaxagorea luzonensis* A. Gray, *J. Med. Plants Res.* 6 (2012) 3781–3785.
- [11] A.S. Darvesh, R.T. Carroll, A. Bishayee, W.J. Geldenhuys, C.J.V. Schyf, Oxidative stress and Alzheimer's disease: dietary polyphenols as potential therapeutic agents, *Expert Rev. Neurother.* 10 (2010) 729–745.
- [12] A. Urbain, A. Marston, L.S. Grilo, J. Bravo, O. Purev, B. Purevsuren, D. Batsuren, M. Reist, P.-A. Garrup, K. Hostettmann, Xanthenes from *Gentianaella amarella* ssp. *acuta* with acetylcholinesterase and monoamine oxidase inhibitory activities, *J. Nat. Prod.* 71 (2008) 895–897.
- [13] W. M. Aizat, I. N. Jamil, F. H. Ahmad-Hashim, N. M. Noor, Recent updates on metabolite composition and medicinal benefits of mangosteen plant, *Peer J.* 7, e6324.
- [14] C. Chen, Y. Li, W. Wang, L. Deng, Bioactivity and pharmacological properties of γ -mangostin from the mangosteen fruit: a review, *Expert Opin. Ther. Pat.* 28 (2018) 415–427.
- [15] B. Choudhury, R. Kandimala, R. Elancheran, R. Bharali, J. Kotoky, *Garcinia morella* fruit, a promising source of antioxidant and anti-inflammatory agents induces breast cancer cell death via triggering apoptotic pathway, *Biomed. Pharmacother.* 103 (2018) 562–573.
- [16] N.T.M. Phuong, N.V. Quang, T.T. Mai, N.V. Anh, C. Kuhnarn, V. Reutrakul, A. Bolhuis, Antibiofilm activity of γ -mangostin extracted from *Garcinia mangostana* L. against *Staphylococcus aureus*, *Asian Pac. J. Trop. Med.* 10 (2017) 1154–1160.
- [17] C.I. Buba, S.E. Okhale, I. Muazzam, *Garcinia kola*: The phytochemistry, pharmacology and therapeutic applications, *Int. J. Pharmacogn.* 3 (2016) 67–81.
- [18] S. Kaennakam, P. Siripong, S. Tip-pyang, Kaennacowanols A–C, three new xanthenes and their cytotoxicity from the roots of *Garcinia cowa*, *Fitoterapia* 102 (2015) 171–176.
- [19] T. Okoko, D. Ere, Some bioactive potentials of two biflavonols isolated from *Garcinia kola* on cadmium-induced alterations of raw U937 cells and U937-derived macrophages, *Asian Pac. J. Trop. Med.* (2013) 43–48.
- [20] T. Ritthiwitrom, S. Laphookhieo, S.G. Pyne, Chemical constituents and biological activities of *Garcinia cowa* Roxb., *Maejo. Int. J. Sci. Tech.* 72 (2013) 212–213.
- [21] M. Hemshekar, K. Sunitha, M.S. Santhosh, S. Devaraja, K. Kemparaju, B.S. Vishwanath, S.R. Niranjana, K.S. Girish, An overview on genus *Garcinia*: phytochemical and therapeutic aspects, *Phytochem. Rev.* 10 (2011) 325–351.
- [22] S. Poomiparn, A. Kumkong, Edible Multipurpose Tree Species, Faung Fa Printing, Bangkok, 1997.
- [23] C. Ito, M. Itoigawa, T. Takakura, N. Ruangrunsi, F. Enjo, F. Tokuda, H. Nishino, H. Furukawa, Chemical constituents of *Garcinia fusca*: structure elucidation of eight new xanthenes and their cancer chemopreventive activity, *J. Nat. Prod.* 66 (2003) 200–205.
- [24] N. K. Nguyen, X. A. Truong, T. Q. Bui, D. N. Bui, H. X. Nguyen, P. T. Tran, L.-H. D. Nguyen, Glucosidase inhibitory xanthenes from the roots of *Garcinia fusca*, *Chem. Biodivers.* 14, 1700232. doi:<https://doi.org/10.1002/cbdv.201700232>.
- [25] J. Nontakham, N. Charoenram, W. Upamai, M. Taweechotipatr, S. Suksamarn, Anti-helicobacter pylori xanthenes of *Garcinia fusca*, *Arch. Pharm. Res.* 377 (2014) 972–977.
- [26] M. Iinuma, T. Ito, R. Miyake, H. Tosa, T. Tanaka, V. Chelladurai, A xanthone from *Garcinia cambogia*, *Phytochemistry* 47 (1998) 1169–1170.
- [27] APEX3, SADABS and SAINT, Bruker AXS Inc., Madison, Wisconsin, USA (2016).
- [28] G.M. Sheldrick, SHELXT-integrated space-group and crystal-structure determination, *Acta Cryst. A* 71 (2015) 3–8.
- [29] G.M. Sheldrick, Crystal structure refinement with SHELXL, *Acta Cryst. C* 71

- (2015) 3–8.
- [30] U. Namdaung, A. Aithipornchai, T. Khamee, M. Kuno, S. Suksamrarn, 2-Arylbenzofurans from *Artocarpus lakoocha* and methyl ether analogs with potent cholinesterase inhibitory activity, *Eur. J. Med. Chem.* 143 (2018) 1301–1311.
 - [31] J. Cheung, M.J. Rudolph, F. Burshteyn, M.S. Cassidy, E.N. Gary, J. Love, M.C. Franklin, J.J. Height, Structures of human acetylcholinesterase in complex with pharmacologically important ligands, *J. Med. Chem.* 55 (2012) 10282–10286.
 - [32] Y. Nicolet, O. Lockridge, P. Masson, J.C. Fontecilla-Camps, F. Nachon, Crystal structure of human butyrylcholinesterase and of its complexes with substrate and products, *J. Biol. Chem.* 278 (2003) 41141–41147.
 - [33] M.J. Frisch, G.W. Trucks, H.B. Schlegel, G.E. Scuseria, M.A. Robb, J.R. Cheeseman, G. Scalmani, V. Barone, B. Mennucci, G.A. Petersson, H. Nakatsuji, M. Caricato, X. Li, H.P. Hratchian, A.F. Izmaylov, J. Bloino, G. Zheng, J.L. Sonnenberg, M. Hada, M. Ehara, K. Toyota, R. Fukuda, J. Hasegawa, M. Ishida, T. Nakajima, Y. Honda, O. Kitao, H. Nakai, T. Vreven, J.A. Montgomery, J.E. Peralta, F. Ogliaro, M. Bearpark, J.J. Heyd, E. Brothers, K.N. Kudin, V.N. Staroverov, R. Kobayashi, J. Normand, K. Raghavachari, A. Rendell, J.C. Burant, S.S. Iyengar, J. Tomasi, M. Cossi, N. Rega, J.M. Millam, M. Klene, J.E. Knox, J.B. Cross, V. Bakken, C. Adamo, J. Jaramillo, R. Gomperts, R.E. Stratmann, O. Yazyev, A.J. Austin, R. Cammi, C. Pomelli, J.W. Ochterski, R.L. Martin, K. Morokuma, V.G. Zakrzewski, G.A. Voth, P. Salvador, J.J. Dannenberg, S. Dapprich, A.D. Daniels, J.B. Foresman, J.V. Ortiz, J.J. Cioslowski, D.J. Fox, Gaussian 09, Revision B.01, Gaussian, Inc., Wallingford CT, 2009.
 - [34] G.M. Morris, R. Huey, W. Lindstrom, M.F. Sanner, R.K. Belew, D.S. Goodsell, A.J. Olson, AutoDock4 and AutoDockTools4: automated docking with selective receptor flexibility, *J. Comput. Chem.* 30 (2009) 2785–2791.
 - [35] M.F. Sanner, Python: A programming language for software integration and development, *J. Mol. Graphics Mod.* 17 (1999) 57–61.
 - [36] Dassault systèmes BIOVIA, discovery studio visualizer, discovery studio 2020 client, Dassault Systèmes, San Diego, 2020.
 - [37] S. Suksamrarn, O. Komutiban, P. Ratananukul, N. Chimnoi, N. Lartpornmatulee, A. Suksamrarn, Cytotoxic prenylated xanthenes from the young fruit of *Garcinia mangostana*, *Chem. Pharm. Bull.* 54 (2003) 301–305.
 - [38] W. Mahabusarakam, P. Chairerk, W. C. Taylor, Xanthenes from *Garcinia cowa* Roxb. latex, *Phytochemistry* 66 (2005) 1148–1153.
 - [39] Z. Na, R. Song, H. Hu, A new prenylated xanthone from the latex of *Garcinia cowa* Roxb, *Rec. Nat. Prod.* 7 (2013) 220–224.
 - [40] P.G. Waterman, R.A. Hussain, Major xanthenes from *Garcinia staudtii* stem barks, *Phytochemistry* 21 (1982) 2099–2101.
 - [41] B.T.D. Trinh, T.T.T. Quach, D.N. Bui, D. Staerk, L.-H.D. Nguyen, A.K. Jäger, Xanthenes from the twigs of *Garcinia oblongifolia* and their antidiabetic activity, *Fitoterapia* 118 (2017) 126–131.
 - [42] B.B. Mesi, K. Ndjoko-Isoet, B. Hertlein-Amslinger, A.M. Lannang, A.E. Nkengfack, J.-L. Wolfender, K. Hostettmann, G. Bringmann, Preussanone, a new flavanone-chromone biflavonoid from *Garcinia preussii* Engl, *Molecules* 17 (2012) 6114–6125.
 - [43] V. Kumar, V. Brecht, A.W. Frahm, Conformation analysis of the biflavonoid GB2 and a polyhydroxylated flavanone-chromone of *Cratogeomys neriifolium*, *Planta Med.* 70 (2004) 646–651.
 - [44] B. Siewert, J. Wiemann, A. Köwitsch, R. Csuk, The chemical and biological potential of C ring modified triterpenoids, *Eur. J. Med. Chem.* 72 (2014) 84–101.
 - [45] L.D. Ha, P.E. Hansen, O. Vang, F. Duus, H.D. Pham, L.-H.D. Nguyen, Cytotoxic geranylated xanthenes and O-alkylated derivatives of a-mangostin, *Chem. Pharm. Bull.* 57 (2009) 830–834.
 - [46] Shagufta I. Ahmad, Recent insight into the biological activities of synthetic xanthone derivatives, *Eur. J. Med. Chem.* 116 (2016) 267–280.
 - [47] X.-Q. Chi, B. Hou, L. Yang, C.-T. Zi, Y.-F. Lv, J.-Y. Li, F.-C. Ren, M.-Y. Yuan, J.-M. Hu, J. Zhou, Design, synthesis and cholinesterase inhibitory activity of α -mangostin derivatives, *Nat. Prod. Res.* doi:https://doi.org/10.1080/14786419.2018.1510925.
 - [48] S. Suksamrarn, N. Suwannapoch, W. Phakhodee, J. Thanuhiranlert, P. Ratananukul, N. Chimnoi, A. Suksamrarn, Antimicrobial activity of prenylated xanthenes from the fruits of *Garcinia mangostana*, *Chem. Pharm. Bull.* 51 (2003) 857–859.
 - [49] S. Suksamrarn, N. Suwannapoch, P. Ratananukul, N. Aroonlerk, A. Suksamrarn, Xanthenes from the green fruit hulls of *Garcinia mangostana*, *J. Nat. Prod.* 65 (2002) 761–763.
 - [50] Z. Luo, J. Sheng, Y. Sun, C. Lu, J. Yan, A. Liu, H.B. Luo, L. Huang, X. Li, Synthesis and evaluation of multi-target-directed ligands against Alzheimer's disease based on the fusion of donepezil and ebselen, *J. Med. Chem.* 56 (2013) 9089–9099.
 - [51] M.F. Eskander, N.G. Nagykeri, E.Y. Leung, B. Khelghati, C. Geula, Rivastigmine is a potent inhibitor of acetyl- and butyrylcholinesterase in Alzheimer's plaques and tangles, *Brain Res.* 1060 (2005) 144–152.
 - [52] P. Munoz-Ruiz, L. Rubio, E. García-Palomero, I. Dorronsoro, M. del Monte-Millán, R. Valenzuela, P. Usan, C. de Austria, M. Bartolini, V. Andrisano, A. Bidon-Chanal, M. Orozco, F.J. Luque, M. Medina, A. Martínez, Design, synthesis, and biological evaluation of dual binding site acetylcholinesterase inhibitors: new disease-modifying agents for Alzheimer's disease, *J. Med. Chem.* 48 (2005) 7223–7233.

VITA

NAME Audchara Saenkham

DATE OF BIRTH 9 January 1989

PLACE OF BIRTH Kalasin

INSTITUTIONS ATTENDED 2012 Bachelor of Science Degree in Chemistry
Mahasarakham University, Mahasarakham, Thailand
2015 Master of Science Degree in Chemistry
Srinakharinwirot University, Bangkok, Thailand

HOME ADDRESS 166 Tumbol Yangtalad, Yangtalad District, Kalasin, Thailand

PUBLICATION
Lupane- and ceanothane-type triterpenes of *Ziziphus cambodiana* Pierre stem barks with anti-*Helicobacter pylori* activity.
Potent α -glucosidase inhibitory activity of some *Ziziphus* plants.
Highly potent cholinesterase inhibition of geranylated xanthones from *Garcinia fusca* and molecular docking studies.
In silico and in vitro analysis of the role of cowaxanthone as a histone deacetylase inhibitor and apoptosis inducer in human leukemic T-cells.